ABSTRACT

NIEROBISZ, LIDIA SYLWIA. Molecular Mechanisms Characterizing Skeletal Muscle Phenotype and Function. (Under the direction of Dr. Paul Mozdziak).

Skeletal muscle is composed of metabolically heterogeneous myofibers that exhibit high plasticity in response to the external environment. Because of its high plasticity and rapid growth rate, turkey skeletal muscle is an exciting model for studying the mechanisms that govern vertebrate skeletal muscle development and function. Cellular energy sources and muscle fiber types are associated with incidence of muscular disorders and with histological alterations in muscle fibers that have detrimental effects on muscle growth. The focus of this dissertation is to determine the effect of nutrition, age, and physical location of a muscle on muscle metabolism and transcription of genes governing muscle phenotype.

The objective of the first set of experiments was to histochemically determine the association of apoptosis and/or macrophage infiltration with changes in muscle satellite cell mitotic activity in glycolytic Pectoralis thoracicus muscle of young turkeys. Feed-deprived birds and birds provided with three different levels of crude protein and amino acids (0.88 NRC, 1.00 NRC, and 1.12 NRC) were used in this model. The number of apoptotic nuclei was significantly elevated ($P<0.05$) and presence of macrophage infiltration was readily detectable in feed-deprived and 0.88 NRC treatment groups 72 h and 96 h post-hatch suggesting potential muscle injury and/or muscle remodeling.

The goal of the second study was to establish the relationship among whole tissue CoQ_{10} content, mitochondrial CoQ_{10} content, amount of mitochondrial protein, and muscle phenotype. Four functionally different muscles (Anterior latissimus dorsi-ALD, Posterior

latissimus dorsi-PLD, Pectoralis major-PM, and Biceps femoris-BF) were evaluated in 9- and 20-week old turkey males. The study revealed age-related reduction in mitochondrial CoQ_{10} content in muscles with fast/glycolytic profile (PLD and PM), and demonstrated that muscles with a slow/oxidative (ALD) phenotypic profile contain a higher proportion of CoQ_{10} than muscles with a fast/glycolytic phenotypic profile.

The third set of experiments focused on the effect of Coenzyme Q analog ($MitoQ_{10}$) on oxidative phenotype and adipogenesis in myotubes derived from ALD and PM muscles. The results of the study indicate differential PM and ALD myotube response to $MitoQ_{10}$ treatment. $MitoQ_{10}$ up-regulated genes controlling oxidative mitochondrial biogenesis and adipogenesis in fast-glycolytic PM myotube cultures. $MitoQ_{10}$ likely controls a range of metabolic pathways through its differential regulation of gene expression levels in myotubes derived from fast-glycolytic and slow-oxidative muscles.

The final study employed microarray analysis to reveal differentially expressed genes among ALD, PLD, and BF muscles in 1-week and 19-week old male turkeys.
The highest number of differentially expressed genes was observed between ALD and PLD muscles. The most prevalent genes over-expressed in ALD muscles, as compared to other muscles, code for extracellular matrix proteins such as dystroglycan and collagen. Moreover, several genes coding for proteins involved in glycolytic metabolism were under-expressed in ALD muscles as compared to BF and PLD muscles. Muscle-specific differences were observed in expression levels of genes coding for proteins involved in mRNA processing and translation regulation, proteosomal degradation, apoptosis, and insulin resistance.

Molecular Mechanisms Characterizing Skeletal Muscle Phenotype and Function

by
Lidia Sylwia Nierobisz

A dissertation submitted to the Graduate Faculty of
North Carolina State University
in partial fulfillment of the
requirements for the degree of
Doctor of Philosophy

Comparative Biomedical Sciences

Raleigh, North Carolina

2010

APPROVED BY:

_____	_____
Dr. Paul Mozdziak Committee Chair	Dr. Vernon Felts
_____	_____
Dr. Jack Odle	Dr. Anthony Blikslager

DEDICATION

To my family- the ones that I can always count on

BIOGRAPHY

Lidia Sylwia Nierobisz was born April 28, 1980, in Warsaw, Poland. In 1998, she arrived to the United States as an international exchange student. She completed her high school education in Johnsburg Central School, North Creek, New York in 1999. She received a Bachelor of Science degree in Biochemistry from University of Massachusetts in Boston in December 2003. In August 2007, Lidia received a M.S. degree in Nutrition with a minor in Biotechnology at North Carolina State University in Raleigh, North Carolina. Subsequent to obtaining her M.S. degree, Lidia has been compiling the requirements for a PhD degree in Comparative Biomedical Sciences at North Carolina State University. Lidia is scheduled to receive her PhD degree in December, 2010.

The author currently lives in Fuquay Varina NC with her husband, Chris and son, Oben.

ACKNOWLEDGMENTS

I could have never come this far without the scientific assistance, friendship, and encouragement of many people. Thank you all for your support and inspiration!

First and foremost, I would like to express my gratitude to my mentor Dr. Paul Mozdziak for his guidance and many invaluable teachable moments. As my advisor, he helped me to further expand my reasoning skills, make independent decisions, and prepared me for dealing with future obstacles.

I wish to extent my sincerest appreciation to the members of my graduate committee; Dr. Vernon Felts, Dr. Jack Odle, and Dr. Anthony Blikslager for their kindness and scientific feedback. I have been very fortunate to have had the opportunity to learn from and discuss my research with several faculty members. I am thankful to Dr. Felts for his great contribution to the nutritional aspects of this project and to his thorough evaluation of publications included in this dissertation. I greatly appreciate the kindness and scientific assistance of Dr. Chris Ashwell and Dr. Nathaniel Hentz. In addition, I would like to express my gratitude to Dr. Gale Strasburg, Dr. Kelly Sporer, Dr. Douglas McFarland, Dr. Kent Reed, and Dr. Sandra Velleman for their contribution to the manuscripts incorporated into this dissertation.

I earnestly thank Goldsboro Milling Company, Goldsboro, NC for providing me with animals employed in this study.

I acknowledge friendship and technical support of my colleagues, Dee Hodgson, Sun Hye Kim, Ganokon Urkasemsin (Ping Pong), Shelly Nolin, and Audrey O'Nan.

I am forever grateful to my parents, Maria and Andrzej Nierobisz, for their constant belief in me, encouragement to move forward, and for teaching me the significance of education. Many thanks to my sister, Ksenia (Xena) Nierobisz, for her friendship, emotional support, and assistance with artwork included in my manuscripts. I also would like to thank my cousin, Jola Nierobisz, for her great help and support during the last year of my PhD work.

The completion of this journey was made possible thank to unconditional love, patience, and strong encouragement of my husband, Chris Dunlap. Arrival of our son, Oben during my PhD work allowed me to fully appreciate the importance of family and inspired me to put more effort towards a better tomorrow. Oben and Chris: you boys rock my world. Thank you for being the most important part of my life!

TABLE OF CONTENTS

LIST OF TABLES

LIST OF FIGURES

CHAPTER 1

Literature Review:

Factors Governing Skeletal Muscle Growth, Phenotype, and Health

Skeletal Muscle Growth - Overview

The biochemical and biophysical characteristics of muscle fibers are typically delineated by fiber number, fiber size, and fiber phenotype (Chang, 2007). Diverse distribution of skeletal muscle fibers within each muscle type is responsible for skeletal muscle's remarkable ability to adjust to external stimuli. At birth, vertebrate skeletal muscles contain approximately the same muscle fiber number as in adulthood (Wigmore and Stickland, 1983). An increase in muscle fiber number (hyperplasia) is determined by mitotically active satellite cells that donate nuclei to pre-existing muscle fibers (Schultz and McCormick, 1994). During adult life, hyperplasic activity may only occur due to periodic repair of damaged muscle fibers. Some of the major factors that contribute to hyperplasic muscle fiber growth include myostatin, insulin-like growth factors I and II, and nutrition (Kocamis and Killefer, 2002; Lynch et al., 2001; Wood et al., 1999). While most of the hyperplasic growth of the muscle is completed at birth, muscle growth during adulthood occurs predominately due to muscle fiber hypertrophy, which is defined as enlargement and elongation of preexisting muscle fibers. Hypertrophy is a result of stimulation of biochemical pathways leading to protein synthesis. External factors, such as nutrition, exercise, and integrin signaling lead to activation of PI3K, Akt, and/or mTOR pathways that are responsible for transcription of genes required for protein accretion (Frost and Lang, 2007).

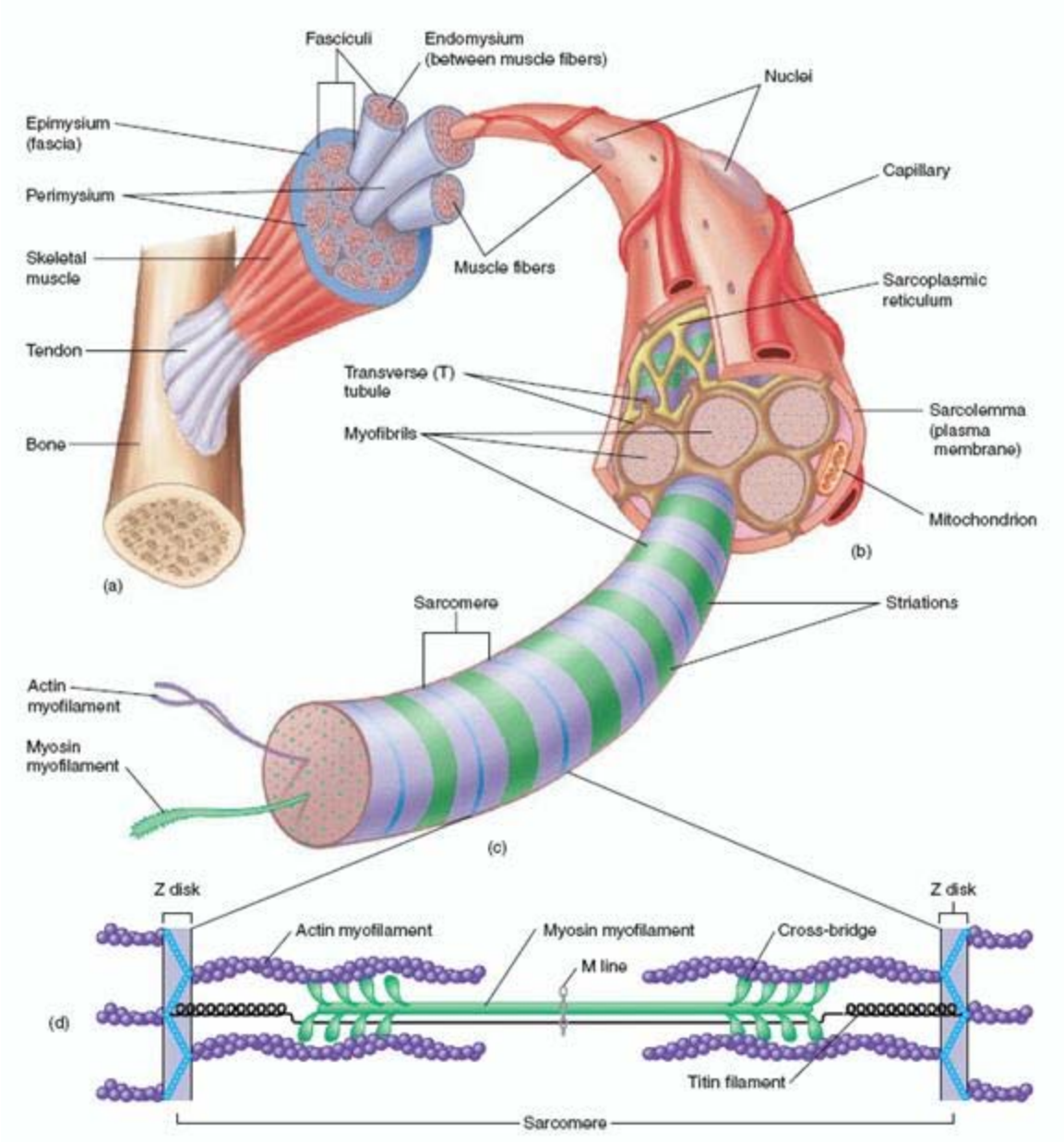

Fig. 1. Skeletal muscle structure (http://www.shoppingtrolley.net/skeletal%20muscle.shtml)

Metabolic Determination of Skeletal Muscle Phenotype

Alongside their biophysical characteristics, individual muscle fibers are categorized based on their biochemical phenotypic profile. Originally, skeletal muscles were classified based on the muscle's myoglobin content and speed of contraction (Hunt and Hedrick, 1977). Myoglobin is an oxygen carrying molecule present in muscle tissue. Myoglobin forms pigments that make the muscle appear red. Slow-contracting muscles involved in long term activities require much more oxygen for energy generation than fast-contracting muscles. Consequently, the muscles with high myoglobin content were classified as slow-red oxidative, and muscles with low myoglobin content were classified as fast-white anaerobic (or glycolytic) (Hunt and Hedrick, 1977).

Experiments performed by Wiskus et al. (1976) demonstrated that fast-white and slow-red classification of muscle fibers is not accurate and that certain muscle types (such as biceps femoris) appear red due to high myoglobin content but have enzymatic characteristics of white fibers. The histochemical fast and slow classification was based on staining for adenosine triphosphatase (ATPase), but glycolytic and oxidative fiber determination was based on succinic dehydrogenase (SDH) staining for mitochondria (Wiskus et al, 1976; Aberle et al., 1979; Smith and Fletcher, 1988). Because SDH is an important component of a TCA cycle, strong staining for this enzyme identifies muscle fibers with high oxidative potential. Wiskus et al. (1976) demonstrated that there are three main types of muscle fibers in turkey muscles. These fiber types were defined as αR (fast-oxidative), αW (fast-glycolytic), and βR (slow-oxidative) based on their differential response to ATPase and SDH staining. Wiskus et al. (1976) demonstrated that while pectoralis muscle was extremely

scarce in βR fibers, previously considered as oxidative, biceps femoris muscle was composed of both oxidative and glycolytic fast-twitch fibers (Table 1).

The fast-twitch (α also called type II) muscle fibers predominantly use glycolysis as a source of energy and contain very few mitochondria. The fast-twitch fibers can be divided into two major groups: IIA (also called αR) - fibers that use both oxidative phosphorylation and glycolysis for ATP production, and IIB (also called αW)- fibers that rely primarily on glycolysis for ATP production. The IIA fibers are commonly referred to as "intermediate" fibers because they exhibit intermediate intensities of SDH staining and their contraction speed is comparable to glycolytic fibers. Type II fibers have high levels of myosin ATPase and high levels of calcium release from sarcoplasmic reticulum during contraction. Conversely, the oxidative slow-twitch fibers (βR also called type I) use oxidative phosphorylation for ATP production and contain more mitochondria. The slow-twitch fibers also have lower levels of myosin ATPase and less calcium release from sarcoplasmic reticulum during contraction than fast-twitch fibers (Pette and Staron, 2000) (Table 1).

Various fiber types can also be characterized by expression of specific myosin isoforms. Myosin is a major protein of the muscle fiber's contractile unit, sarcomere. The myosin ATPase enzymatic activity takes place in the myosin heavy chain region (MyHC). Myosin heavy chain isoforms are encoded by a large gene family of proteins (Schiaffino and Reggiani, 1994). Myosin heavy chain gene expression can be identified based on immunohistochemical staining and in situ hybridization. Muscles expressing differential myosin isoforms vary in their fiber size, color, lipid and glycogen content, and by overall energy metabolism. Fibers with fast MyHC isoforms have larger fiber diameters, low

amount of mitochondria, high glycogen stores, and low lipid profile. These types of muscle are more prone to rapid pH drop post mortem, which has a large effect on meat quality (Chang et al., 2003). On the contrary, muscles abundant in slow MyHC isoforms have smaller fiber diameter, high amount of mitochondria, low glycogen stores, and high lipid profile. Because of its lipid content, meat plentiful in oxidative fibers is more tender than meat composed of mostly glycolytic fibers (Klont et al., 1998).

Table 1. Summary of fiber types.

Fiber Type	I	IIA	IIB
Metabolic Classification	**βR: slow-oxidative**	**αR: fast-oxidative**	**αW: fast-glycolytic**
Myoglobin Content	High	High	Low
Contraction Time	Slow	Moderately Fast	Fast
Force of Contraction	Low	Medium	High
Oxidative Capacity	High	High	Low
Mitochondrial Density	High	High	Low
Glycolytic Capacity	Low	High	High
Major Storage Fuel	Triglycerides	Glycogen, Creatine Phosphate	Glycogen, Creatine Phosphate

Skeletal Muscle Phenotype and External Environment

In general, fiber type composition of individual muscle types varies based on the functionality of the muscle. Due to great plasticity of the muscle fiber biochemical and biophysical phenotype, muscle is able to adjust to the external environment. Previous experiments demonstrated that change in functional load, nutrition, and in vitro manipulations result in transformation in muscle fiber phenotype. Physical exercise-based

trials revealed that type of physical activity has a direct effect on expression of MyHC isoforms (Baldwin and Haddad, 2001). Endurance exercise results in increase in oxidative fiber types and decrease in glycolytic fiber types in mammalian species. In contrast, long periods of inactivity causes decrease in oxidative fiber types and increase in glycolytic fiber types (Spangenburg and Booth, 2003). Experiments utilizing skeletal muscle unloading demonstrated that inactivity results in decrease of type I (slow) myosin isoforms and increase in type II (fast) myosin isoforms in soleus muscle (Fitts et al., 2001). Additionally, muscle unloading results in increased expression of calcium channel in sarcolemma, proving that inactivity results in higher muscle twitch potential (Schulte et al., 1993).

Skeletal Muscle Phenotype and Nutrition

Nutritional studies utilizing acetyl-L-carnitine supplementation revealed that Acetyl-L-Carnitine prevents muscle fiber conversion into fast-twith, increases expression of slow oxidative genes, and counteracts the loss of mitochondrial mass caused by muscle inactivity. Furthermore, Acetyl-L-Carnitine supplementation results in larger cross sectional area in both slow and fast-twitch muscle fibers (Cassano et al., 2006). Carnitine is responsible for transport of fatty acids from cytosol to mitochondria for breakdown via TCA cycle.

Dietary calcium plays a principal signaling and regulatory function in skeletal muscle (Berchtold et al., 2000). Trials utilizing C2C12 myotube cells demonstrated that addition of calcium sensitive phosphatase, calcineurin to muscle cell lines increased expression of slow troponin isoform (Chin et al., 1998). Because calcium sensitive phosphatases are needed for dephosphorylation of TCA cycle dehydrogenases, increased activity of mitochondrial TCA

cycle is responsible for an increase of more oxidative muscle fiber phenotype. Aforementioned experiments demonstrated that the muscle phenotype switching is not only possible, but it is also reversible and that biochemical reactions taking place in mitochondria have a direct effect on muscle fiber phenotype (Chin et al., 1998; Cassano et al., 2006).

Skeletal Muscle Phenotype and Mitochondrial Dysfunction

Skeletal muscle oxidative capacity and resistance to fatigue is determined by catalytic activity of mitochondrial enzymes involved in TCA cycle and/or electron transport chain enzymes (Wu et al., 2002). Fast-glycolytic fiber types are characterized by low volume density of mitochondria, high myosin ATPase activity, high glycolytic enzyme activity, and low fatigue resistance. In contrast, slow oxidative muscle fiber types, contain high volume of mitochondria, high level of oxidative enzyme activity, high number of capillaries, and are very resistant to fatigue (Spangenburg and Booth, 2003). Because of skeletal muscle's ability to adjust to external stimuli, the metabolic processes determining muscle fiber energy utilization can be altered by manipulating components of oxidative phosphorylation.

Muscle fiber phenotype was correlated with mitochondrial respiratory dysfunction and diabetes (Whittaker et al., 2007). Skeletal muscles of individuals suffering from type II diabetes mellitus exhibit an array of defects in complex I and complex IV of electron transport chain (Anderson, 1999). Furthermore, increased production of reactive oxygen species and decreased ATP synthase activity was observed in skeletal muscle mitochondria of patients suffering from type II diabetes mellitus (Anderson, 1999).

High energy-requiring organs such as heart, brain, liver, and skeletal muscle, are greatly affected by free radical-induced mitochondrial dysfunction. Type IIB muscle fibers have unique mechanisms that stimulate mitochondrial superoxide generation (Anderson and Neufer, 2005). Mitochondrial free radical generation takes place almost exclusively in IIB fibers (Anderson and Neufer, 2005; Whittaker et al., 2007). Many myopathies and age-related muscle atrophy are associated with a loss of type IIB (fast-twitch, glycolytic) muscle fibers. Aging skeletal muscles are prone to atrophy and extensive wasting of muscle mass, referred to as sarcopenia, which occurs predominately in type II muscle fibers (Bua et al., 2002). Mitochondrial free radical release is mainly associated with complex I and III of electron transport chain. Although, the exact mechanisms responsible for disproportionate mitochondrial free radical release in oxidative and glycolytic fiber types have not yet been elucidated, the differences in mitochondrial function within fiber types may be related to type and efficiency of energy utilization.

Coenzyme Q_{10}

Coenzyme Q_{10} (CoQ_{10}), commonly referred to as ubiquinone (2, 3-dimethoxy-5-methyl-6-multiprenyl-1, 4-benzoquinone), is a bioactive vitamin-like molecule present in all eukaryotic cells containing mitochondria. CoQ_{10} resides in the hydrophobic middle region of the phospholipid bilayer of mitochondrial membrane and participates in electron transport chain process, where the energy from fats and carbohydrates is converted to adenosine triphosphate (ATP) (Bliznakov and Bhagavan, 2003). CoQ_{10} exists in three alternating states in the mitochondrial membrane: the fully oxidized form: ubiquinone (Q_{10}), the partially

reduced form: ubisemiquinone ($Q_{10}H.$), and in fully reduced form: ubiquinol ($Q_{10}H2$) (Kamzalov et al., 2003). CoQ_{10} accepts electrons from reducing equivalents produced from fatty acid and glucose oxidation and delivers them to electron acceptors. Specific role of CoQ_{10} in electron transport chain is to transfer electrons from NADH-Q oxidoreductase (complex I) and from succinate-Q oxidoreductase (complex II) to cytochrome c oxidoreductase (complex III) (Kamzalov at al., 2003). While passing on the electrons, CoQ_{10} also transfers protons to the outskirts of the inner mitochondrial membrane, generating proton gradient. The energy released when protons move back to mitochondria is used to generate ATP. Elevated concentration of CoQ_{10} has been found in organs with high energy requirements. The highest concentrations of CoQ_{10} have been found in heart, brain, and skeletal muscle. Former studies have demonstrated that 95% of human energy requirements are produced with help of CoQ_{10} (Bliznakov and Bhagavan, 2003). Aside from its function in electron transport chain, CoQ_{10} in its reduced form (ubiquinol) acts as a principal fat-soluble cellular antioxidant. Ubiquinol inhibits oxidation reactions by directly neutralizing free radicals, inhibiting lipid peroxidation of membranes, and protecting mitochondrial membrane proteins and DNA. In addition, ubiquinol is capable of salvaging and regenerating other antioxidants including ascorbate and tocopherol (Kamzalov et al., 2003).

Armstrong et al. (2003) revealed that CoQ_{10} analog, decyl-CoQ_{10}, inhibits mitochondrial permeability transition in HL60 (human leukemia) cells. Mitochondrial permeability transition is a change in mitochondrial transmembrane potential resulting in membrane swelling and rupture leading to necrotic and apoptotic cell death. Cytochrome c release from ruptured mitochondria leads to activation of the caspase cascade and apoptosis. Additionally,

significant decrease in cellular ATP production can lead to necrosis. The mitochondrial permeability transition is mainly regulated by cellular redox state. When a cell is depleted of antioxidants (for example glutathione depletion), the cellular environment becomes more oxidized, causing increased production of reactive oxygen species by mitochondrial cytochrome bc1 complex. Overproduction of reactive oxygen species leads to mitochondrial toxicity, which contributes to mitochondrial swelling and rupture (Armstrong et al., 2003). Therefore, deciphering mechanisms responsible for optimal mitochondrial function may provide means to improve skeletal muscle health and meat quality and quantity.

Muscle Quality in Domestic Turkeys

Over the lifespan, commercially raised turkeys are exposed to many environmental and physiological stressors that greatly alter the skeletal muscle health, size, and quality. During early post-hatch period, turkey poults are normally held for 48 to 72 hours without access to feed. Early post-hatch birds exclusively rely on the lipid-rich yolk sac to satisfy their nutrient and energy needs. Newly hatched birds need to be supplemented with dietary carbohydrates to maintain normal growth and metabolic function (Noy and Sklan, 1998; Geyra et al., 2001). Delayed access to feed results in increased satellite cell mitotic activity and increased apoptosis in turkey muscle fibers (Mozdziak et al., 2002). For many years, poultry industry has concentrated on increase of muscle yield and growth rate in turkeys. The rapid growth velocity has been directly correlated to an increased incidence of degenerative pectoral myopathies, edema, and leg weakness (Sosnicki at al., 1991; Dransfield and Sosnicki, 1999). Increased growth rate results in higher number of fast-twitch muscle fibers that mostly rely

on glycolytic metabolism as their main energy source. Cellular energy sources and muscle fiber types have been correlated with occurrence of muscular disorders and histological alterations in muscle fibers that have detrimental effects on muscle growth. Occurrence of myopathies in commercially raised birds increases with age. Sosnicki et al. (1991) revealed that muscle fibers derived from 18-week old turkeys are characterized by histopathological abnormalities such as muscular lesions and necrosis.

Research Objectives

The main objective of the current dissertation was to determine the effect of nutrition, age, and physical location of the muscle on molecular mechanisms characterizing skeletal muscle phenotype. Studies utilizing hind-limb unloading in rodents demonstrated that along with reduced oxidative capacity, up-regulated glycolytic metabolism, and reduced fatigue resistance. The unloaded muscles were characterized by increased caspase-3 activity and increased oxidative stress (Leeuwenburgh et al., 2005). Caspase-3 is a cysteine peptidase that plays a crucial role in execution of caspase-dependent apoptotic pathways. Therefore, there is evidence that stress/inactivity-induced changes in muscle fiber phenotype are associated with up-regulation of apoptotic pathways. The initial study (chapter 2) was based on the hypothesis that the function of the glycolytic PM muscle is compromised in early post-hatch turkeys due to early feed deficiency and stress. The objective of the first experiment was to histochemically determine the association of apoptosis and/or macrophage infiltration with changes in muscle satellite cell mitotic activity in the PM muscle of young turkeys. Subsequent experiments (chapter 3 and 4) were based on the hypothesis that

functionally distinct muscles vary based on their cellular energy utilization and mitochondrial redox state. The HPLC analysis was performed to determine levels of redox active molecule, CoQ_{10}, in mitochondria and whole tissue extracts of four distinct muscle types. Because CoQ_{10} levels varied among distinct muscles, subsequent experiments were based on hypothesis that administration of CoQ_{10} analog ($MitoQ_{10}$) to PM and ALD cultures will affect cellular redox state and stimulate oxidative metabolism in myotubes derived from glycolytic PM muscles. The findings indicated that myotubes derived from PM and ALD muscles respond differently to $MitoQ_{10}$ treatment suggesting that these two muscles vary based on their cellular redox state. Concluding experiments (chapter 5) utilized microarray analysis of three phenotypically distinct muscles to provide a tool for future evaluation of metabolic pathways characterizing specific muscle phenotype.

References

Aberle, E.D., Addis, P.B., Shoffner, R.N., 1979. Fiber types in skeletal muscles of broiler and layer-type chickens. Poult. Sci. 58, 1210-1212.

Anderson, E.J., Neufer, P.D., 2005. Type II skeletal myofibers possess unique properties that potentiate mitochondrial H_20_2 generation.

Anderson, C.M., 1999. Mitochondrial dysfunction in diabetes mellitus. Drug Dev. Res. 46, 67-79.

Armstrong, J.S., Whiteman, M., Rose, P., Jones, D.P., 2003. The coenzyme Q_{10} analog decylCoQ10 inhibits the redox-activated mitochondrial permeability transition. J. Biol. Chem. 278, 49079-49084.

Baldwin, K.M., Haddad, F., 2001. Plasticity in skeletal, cardiac, and smooth muscle invited review: effects of different activity and inactivity paradigms on myosin heavy chain gene expression in striated muscle. J. Appl. Physiol. 90, 345-357.

Berchtold M.W., Brinkmeier H., Müntener M., 2000. Calcium ion in skeletal muscle: Its crucial role for muscle function, plasticity, and disease. Physiol. Rev. 80:1215-1265.

Bliznakov, E.G., Bhagavan, H.N., 2003. Deficient energy metabolism and disease: role of

coenzyme Q10. FASEB 17, 694.

Bua, E.A., McKiernan, S.H., Wanagat, J., McKenzie, D., Aiken, J.M., 2002. Mitochondrial abnormalities are more frequent in muscles undergoing sarcopenia. J. Appl. Physiol. 92, 2617-2624.

Cassano, P., Sciancalepore, A.G., Pesce, V., Flück, M., Hoppeler, H., Calvani, M., Mosconi, L., Cantatore, P., Gadaleta, M.N., 2006. Acetyl-L-carnitine feeding to unloaded rats triggers in soleus muscle the coordinated expression of genes involved in mitochondrial biogenesis. Biochem. Biophys. Acta 1757, 1421-1428.

Chang, K.C., 2007. Key signaling factors and pathways in the molecular determination of skeletal muscle phenotype. Animal 1, 681-698.

Chang, K.C., Da Costa, N., Blackley, R., Southwood, O., Evans, G., Plastow, G., Wood, J.D., Richardson, R.I., 2003. Relationships of myosin heavy chain fibre types to meat quality traits in traditional and modern pigs. Meat Sci. 64, 93-103.

Chin, E.R., Olson, E.N., Richardson, J.A., Yang, Q., Humphries, C., Shelton, J.M., 1998. A calcineurin-dependent transcriptional pathway controls skeletal muscle fibre type. Genes Dev. 12, 2499-2509.

Dransfield, E., Sosnicki, A.A., 1999. Relationship between muscle growth and poultry meat quality. Poult. Sci. 78, 743-746.

Fitts, R.H., Riley, D.R., Widrick, J.J., 2001. Functional and structural adaptations of skeletal muscle to microgravity. J. Exp. Biol. 204, 3201-3208.

Frost, R.A., Lang, C.H., 2007. Protein kinase B/Akt: a nexus of growth factor and cytokine signaling I determining muscle mass. J. Appl. Physiol. 103, 378-387.

Geyra, A., Uni, Z., Sklan, D., 2001. The effect of fasting at different ages on growth and tissue dynamics in the small intestine of the young chick. B. J. Nutr. 86, 53-61.

Hunt, M.C., Hedrick, H.B., 1977. Profile of fiber types and related properties of 5 bovine muscles. J. Food Sci. 42, 513-517.

Kamzalov, S., Sumien, N., Forster, M.J., Sohal, R.S., 2003. Coenzyme Q intake elevates the mitochondrial and tissue levels of coenzyme Q and α-tocopherol in young mice. J. Nutr. 133, 3175-3180.

Klont, R.E., Brocks, L., Eikelenboom, G., 1998. Muscle fibre type and meat quality. Meat Sci. 49, S219-S229.

Kocamis, H., Killefer, J., 2002. Myostatin expression and possible functions in animal muscle growth. Dom. Anim. Endocrin. 23, 447-454.

Leeuwenburgh, C., Gurley, C.M., Strotman, B.A., Dupont-Versteegden, E.E., 2005. Age-related differences in apoptosis with disuse atrophy in soleus muscle. Am. J. Physiol. Regul. Integr. Comp. Physiol. 288, R1288-R1296.

Lynch, G.S., Cuffe, S.A., Plant, D.R., Gregorevic, P., 2001. IGF-1 treatment improves the functional properties of fast- and slow-twitch skeletal muscles from dystrophic mice. Neuromusc. Disord. 11, 260-268.

Mozdziak, P.E., Evans, J.J., McCoy, D.W., 2002. Early posthatch starvation induces myonuclear apoptosis in chickens. J. Nutr. 132, 901-903.
61-65.

Noy, Y., Sklan, D., 1998. Metabolic responses to early nutrition. J. Appl. Poult. Res. 7, 437-451

Pette, D., Staron, R.S., 2000, Myosin isoforms, muscle fiber types, and transitions. Microsc. Res. Tech. 50, 500-509.

Schiaffino, S., Reggiani, C., 1994. Myosin isoforms in mammalian skeletal muscle. J. Appl. Physiol. 77, 493-501.

Schulte, L.M., Navarro, J. Kandarian, S.C., 1993. Regulation of sarcoplasmic-reticulum calcium pump gene expression by hindlimb unweighting. Am. J. Physiol. 264, C1308-C1315.

Schultz, E., McCormick, K.M., 1994. Skeletal muscle satellite cells. Rev. Physiol. Biochem. Pharmacol. 123, 213-257.

Smith, R.A.J., Porteous, C.M., Gane, A.M., Murphy, M.P., 2003. Delivery of bioactive molecules to mitochondria in vivo. PNAS 100, 5407-5412.

Sosnicki, A.A., Cassens, R.G., Vimini, R.J., Greaser, M.L., 1991. Histopathological and ultrastructural alterations in turkey skeletal muscle. Poult. Sci. 70, 349-357.

Spangengburg, E.E., Booth, F.W. 2003. Molecular regulation of individual skeletal muscle fibre types. Acta Physiol. Scandyn. 178, 413-424.

Whittaker, R.G., Schaefer, A.M., McFarland, R., Taylor, R.W., Walker, M., Turnbull, D.M., 2007. Prevalence and progression of diabetes in mitochondrial disease. Diabetologia 50, 2085-2089.

Wigmore, P.M.C., Sickland, N.C., 1983. Muscle development in large and small pig tissues. J. Anat. 2, 235-245.

Wiskus, K.J., Addis, P.B., Ma, R.T-I., 1976. Distribution of βR, αR and αW fibers in turkey muscles. Poult. Sci. 55, 562-572.

Wood, J.D., Enser, M., Fisher, A.V., Nute, G.R., Richardson, R.I., Sheard, P.R., 1999 Manipulating meat quality and composition. Proced. Nutr. Soc. 58, 363-370.

Wu, H., Kanatous, S.B., Thumond, F.A., Gallardo, T., Isotani, E., Bassel-Duby, R., Williams, R.S., 2002. Regulation of mitochondrial biogenesis in skeletal muscle by CaMK. Science 296, 349-352.

CHAPTER 2

Apoptosis and Macrophage Infiltration Occur Simultaneously and Present a Potential Sign of Muscle Injury in Skeletal Muscle of Nutritionally Compromised, Early Post-hatch Turkeys

Abstract

Physical stress and malnutrition may cause elimination of myonuclei and produce inflammatory response in muscle. The objective of this study was to histochemically determine the association of apoptosis and/or macrophage infiltration with changes in muscle satellite cell mitotic activity in *Pectoralis thoracicus* muscle of early post-hatch turkey toms. Feed-deprived birds and birds provided with three different levels of crude protein and amino acids (0.88 NRC, 1.00 NRC, and 1.12 NRC) were used in this study. The number of apoptotic nuclei was significantly elevated ($P<0.05$) and presence of macrophage infiltration was readily detectable in feed-deprived and 0.88 NRC treatment groups 72 h and 96 h post-hatch suggesting potential muscle injury and/or muscle remodeling. The number of apoptotic nuclei was the same ($P>0.05$), and there was no detectable macrophage infiltration present in birds placed on 1.00 NRC and 1.12 NRC diet 72 h, 96 h, and 120 h post-hatch. At 120 h post-hatch, feed-deprived and 0.88 NRC birds were characterized by no detectable levels of macrophage infiltration and a significant drop ($P<0.05$) in apoptotic nuclei. Understanding mechanisms that correlate early nutrition with skeletal muscle growth and development may present a useful tool in optimizing muscle health and improving meat quality and yield.

Keywords: Amino acids, Apoptosis, Feed deprivation, Macrophages, Muscle, Satellite cells, Turkey

1. Introduction

Early post-hatch turkey poults are often subjected to a number of physiological and nutritional stressors that may potentially impact muscle growth and meat quality later in life. Under typical commercial conditions, newly hatched birds are subjected to several processing requirements that usually take up to two days. During the early post-hatch period, poults mostly rely on nutrients derived from the yolk sac and use endogenous protein to satisfy nutritional needs (Vieira and Moran, 1999; Uni and Ferket, 2004). Vieira and Moran (1999) have demonstrated that chicks with delayed placement on feed experience a decline in protein deposition in *Pectoralis thoracicus*, which results in lower muscle mass later in life. Moreover, feed-deprived, early post-hatch birds are more prone to decreased body weight and increased mortality (Pinchasov and Noy, 1993; Halevy et al., 2000).

Embryonic muscle growth occurs through an increase in myofiber number; however, post-natal muscle growth occurs with a corollary increase in myofiber DNA content (Stockdale and Holtzer, 1961; Mozdziak et al., 1997). In young animals, new myonuclei are derived from mitotically active satellite cells that fuse with pre-existing growing myofibers (Moss and Leblond, 1971; Kawano et al., 2008). Early myonuclear accretion of satellite cells is a determining factor of mature muscle size (Mozdziak et al., 1997). Furthermore, it has been demonstrated that broiler chicks denied feed early post-hatch exhibited decreased satellite cell mitotic activity and decline in body and skeletal mass in adulthood (Halevy et al., 2000; Mozdziak et al., 2002b; Halevy et al., 2003).

Satellite cells not only contribute to muscle growth, but they are also an important factor in muscle regeneration. Following muscle injury, satellite cells proliferate and fuse to

repair injured myofibers. Previous research studies have demonstrated that satellite cell activation following muscle injury is supported by a number of growth factors released from injured myofibers (Bischoff, 1990; Chen and Quinn, 1992; Jimena et al., 1993; Malm et al., 2004; Smith et al., 2008). Furthermore, it has been shown that inflammatory cells, such as macrophages activate satellite cells and delay their differentiation by releasing a variety of growth factors and chemoattractants (Merly et al., 1999). More recently, a study performed by Chazaud et al. (2003) suggested that satellite cells are able to attract macrophages that secrete factors to prevent apoptosis and enhance muscle growth. In injured muscle, newly recruited macrophages also participate in removal of necrotic debris to facilitate successive muscle repair (Honda et al., 1990; McLennan, 1996; Pimorady-Esfahani, 1997, McCroskery et al., 2005).

Aside from their role in muscle repair, macrophages have been shown to contribute to muscle damage (Tidball, 2005). Macrophages are able to secrete growth factors and cytokines, as well as free radicals. During the process of inflammation, macrophages lyse target muscle cells through a nitric oxide-dependent mechanism (Nguyen and Tidball, 2003). It is likely that nutritionally-compromised animals are more prone to muscle injury and inflammation, which results in increased muscle damage.

The process of apoptosis also adversely affects muscle growth by elimination of pre-existing myonuclei (Sandri and Carraro, 1999; Leeuwenburgh et. al, 2005). Apoptosis is characterized by chromatin compaction and segregation, rapid cellular condensation, membrane blebbing, and nuclear fragmentation (Sandri and Carraro, 1999). Apoptosis plays an important role in myofiber remodeling and it is part of a normal process involved in

shaping of tissues. Additionally, apoptosis has been correlated to muscular atrophy resulting from skeletal muscle unloading (Allen, et al., 1997; Adams, et al., 1999). Growth factor deprivation in nutritionally compromised myoblasts has been shown to contribute to increased rate of myonuclear apoptosis (Dee et al., 2002). Recent studies have demonstrated that early post-hatch starvation induces myonuclear apoptosis in chick skeletal muscle (Mozdziak et al., 2002a; Pophal et al., 2003). Nierobisz et al. (2007) suggests that feed-deprived, early-post hatch turkey poults also exhibit significantly lower satellite cell mitotic activity as compared to poults fed nutritionally adequate diets. In contrast, poults provided with a diet that was 88% of the NRC requirement exhibited significantly higher satellite cell mitotic activity than other treatment groups (Nierobisz et al., 2007). The objective of this study was to determine if apoptosis and/or macrophage infiltration are associated with changes in muscle satellite cell mitotic activity in nutritionally compromised, early post-hatch turkey toms.

2. Materials and methods

2.1. Birds and Dietary Treatments

Nicholas male turkey poults (*Meleagris gallopavo*) were randomly selected at hatch from a single breeding flock. Selected turkeys were placed at commercial breeding facility at 48 hours post-hatch, divided into four groups and assigned to one of four dietary treatments described in detail in Nierobisz et al. (2007). In brief, the treatments consisted of one of the following:

1) 0.88 NRC diet formulated based on 88% of the values for crude protein (cp), lysine (lys), methionine and cysteine (met+cys), and threonine (thr) determined by National Research Council for male turkeys from 0-4 weeks of age (NRC, 1994).

2) 1.00 NRC diet formulated based on 100% of the values for cp, lys, met+cys, and thr determined by NRC.

3) 1.12 NRC diet formulated based on 112% of the values for cp, lys, met+cys, and thr determined by NRC.

4) Feed-deprived: diet formulated based on 100% of the values for cp, lys, met+cys, and thr determined by NRC given to poults at 72 h post-hatch.

2.2. Data Collection

At 72, 96, and 120 h post-hatch, ten birds per treatment were weighed and euthanized by intra-abdominal injection of Euthasol® (Delmarva Laboratories, Midlothian, VA, USA) at a dose of 0.25 mL/kg body mass. Left *Pectoralis thoracicus* muscle was excised and weighed immediately post-mortem. Muscle samples were snap frozen using isopentane and dry ice and stored at -80°C until further use.

2.3. Apoptosis Detection

Muscle samples from five random birds per treatment were utilized to perform histochemical analysis of the muscle tissue. Transverse muscle sections, 15µm thick were placed on pre-cleaned glass slides coated with poly-L-lysine. The sections were allowed to dry and were subsequently fixed using 2% paraformaldehyde. The number of apoptotic

nuclei was identified using a histochemical assay for staining double-stranded DNA breaks. This method uses terminal deoxynucleotidyl transferase (TUNEL) enzyme to incorporate fluorescein isothiocyanate (FITC)-labeled dUTP at 3'-OH side of fragmented DNA ends. In previous studies, the amount DNA-fragmentation measured using the TUNEL assay was directly associated with the amount of apoptotic protein expression such as ICE and Bax (Tews and Goebel, 1997). Therefore, TUNEL assay was regarded as an appropriate way to measure the level of apoptosis in the present experiment. An apoptosis detection kit (Promega, Madison, WI, catalog #G3250) was utilized to account for the apoptotic myonuclei. Paraformaldehyde fixed sections were rinsed, permeabilized using Proteinase K, washed in PBS buffer, and incubated with equilibration buffer (200 mmol/L potassium cacodylate, 25 mmol/LTris-HCl, 0.2mmol/L dithiothreitol, 0.25 g/L bovine serum albumin, and 2.5 mmol/L cobalt chloride). Following incubation in the equilibration buffer, the DNA strand breaks were labeled with fluorescein-12-dUTP utilizing the terminal deoxynucleotidyl transferase (TDT) enzyme, and the tissue sections were counterstained with propidium iodide (50 mg/L) to account for all nuclei present.

Lastly, the sections were covered with mounting media (75% vol/vol glycerol, 75mM KCl, 10 mM tris(hydroxymethyl) aminomethane, 2 mM $MgCl_2$, 2mM ethylene glycol-bis(β-aminoethyl ether)-N,N,N',N'-tetraacetic acid, 1 mM NaN_3, pH 8.5, 1 mg/mL p-phenylenddiamine), and a glass cover slip was sealed to the slide using clear enamel.

2.4. Macrophage Infiltration Detection

Frozen sections from the same muscle samples (5 birds per treatment) utilized in the apoptosis detection procedure were employed to detect macrophage infiltration into the muscle tissue. Transverse muscle sections, 15 μm thick were placed on pre-cleaned glass slides coated with poly-L-lysine. The sections were allowed to dry followed by fixation in 2% paraformaldehyde. Fixed muscle sections were stained with Harris hematoxylin to identify basophilic structures (such as nuclei) and counterstained with eosin, which was employed to identify cytoplasmic structures.

2.5 Image Analysis

2.5.1. Apoptosis Detection

TUNEL-labeled *Pectoralis thoracicus* muscle sections were examined using a Leica DMR microscope (Leica Microsystems, Bannockburn IL, USA) equipped with epi-fluorescence illumination. The TUNEL-labeled apoptotic nuclei, stained with fluorescein, were visualized using a fluorescein isothiocyanate filter set (Omega Optical, Brattleboro VT, USA). Propidium iodide (PI) nuclei were evaluated using a PI filter set (Omega Optical, Brattleboro VT, USA). A Retiga 4000R Fast camera was utilized to capture the images of *Pectoralis thoracicus*. All images of TUNEL-labeled tissues were captured and analyzed at 40x magnification. Image-Pro Plus software (Media Cybernetics, Version 6, 2006) was used to quantify the results. The criterion for establishing accurate quantification of myonuclei was counting all PI-stained nuclei from each tissue section analyzed. The apoptotic labeling

was established by calculating the percent index of TUNEL stained nuclei relative to PI stained nuclei.

2.5.2. Macrophage Infiltration Detection

A Leica DMR light microscope (Leica Microsystems, Bannockburn IL, USA) was utilized to observe Harris hematoxylin and eosin-stained *Pectoralis thoracicus* muscle sections. All images were taken at 100x oil magnification using a Retiga 4000R fast camera (Q Imaging, Surrey BC, Canada). Image-Pro Plus software (Media Cybernetics, Version 6, 2006) was utilized to identify macrophages infiltrating from the blood into the muscle tissue. The macrophages were identified based on their morphological characteristics. The criterion for accurate detection of macrophage infiltration was to evaluate at least 50 serial *Pectoralis thoracicus* muscle sections per bird (5 birds per treatment).

2.6 Statistical Analysis

The General Linear Models (GLM) procedure of SAS (SAS Institute, 1985) was performed to analyze the effect of four dietary treatments (0.88 NRC, 1.00 NRC, 1.12 NRC, and feed deprived) on the amount of apoptotic nuclei present in *Pectoralis thoracicus* muscle tissue. A two-way analysis of variance (ANOVA) was performed to evaluate the effect of treatment and time (72 h, 96h, and 120h) on each parameter (Fig. 1). Means of each treatment were separated using Fisher's least significant differences. All calculated values were considered as statistically significant at $P<0.05$.

3. Results

3.1. Apoptosis Detection

The index of apoptotic nuclei was significantly higher ($P<0.05$) in both feed-deprived and 0.88 NRC treatment groups, 72 h and 96 h post-hatch compared to 1.00 NRC and 1.12 NRC treatment groups (Fig. 1). Additionally, the percent index of apoptotic nuclei was the same ($P>0.05$) in feed-deprived and 0.88 NRC birds at 72 h post-hatch birds. The amount of apoptotic staining was also the same ($P>0.05$) in feed-deprived 72 h post-hatch birds and both feed-deprived and 0.88 NRC 96 h post-hatch birds. While the amount of apoptotic nuclei remained the same in 1.00 NRC and 1.12 NRC birds on each day analyzed, a significant drop ($P<0.05$) in apoptotic nuclei in feed-deprived and 0.88 NRC treatment groups was observed 120h post-hatch (Fig.1).

3.2. Macrophage Infiltration Detection

Macrophage infiltration was readily detectable in feed-deprived and 0.88 NRC treatment groups at 72 h and 96 h post-hatch (Fig.2). However, the presence of inflammatory cells were not observed in 1.00 NRC, 1.12 NRC groups at 72 and 96 h and in all treatment groups at 120 h post-hatch. Readily detectable presence of intramuscular inflammatory cells (macrophages) was closely correlated to increased number of apoptotic nuclei.

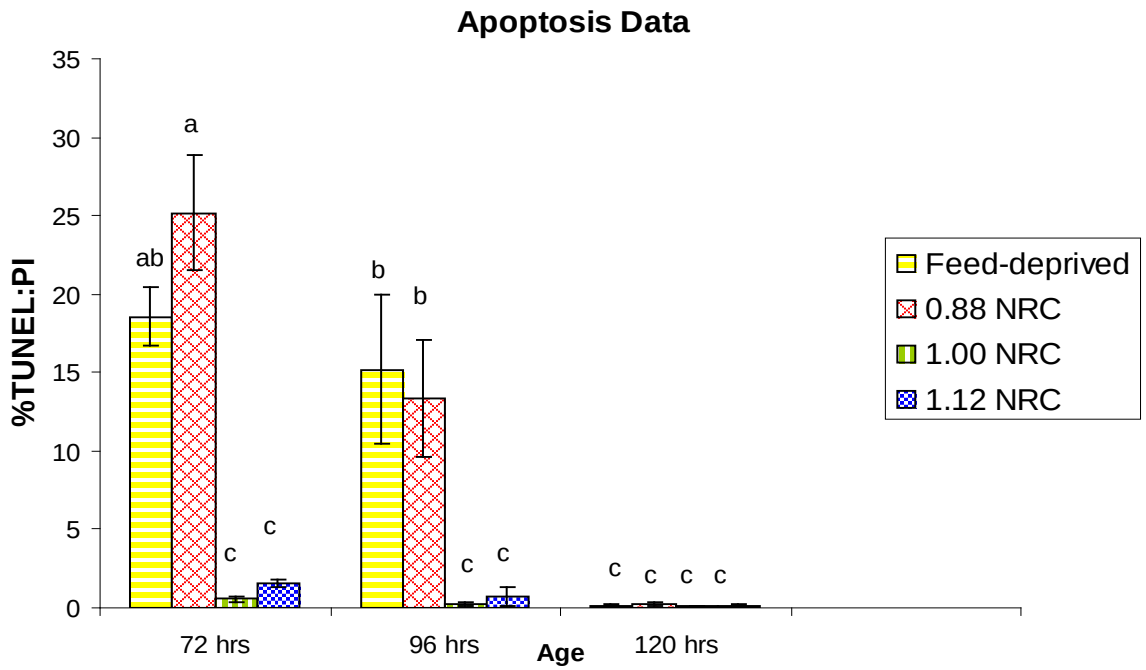

Fig. 1. Two-way ANOVA analysis of the percent ratio of TUNEL-labeled nuclei to the total number of nuclei present in four experimental treatment groups: feed deprived for 72 h post-hatch and then given a diet containing adequate amount of essential nutrients (1.00 NRC); the other treatment groups were given diets containing either 0.88 NRC, 1.00 NRC, or 1.12 NRC requirement for essential nutrients. Increased level of apoptotic cells was noted in feed-deprived and 0.88 NRC treatment groups at 72 h and 96 h post-hatch.

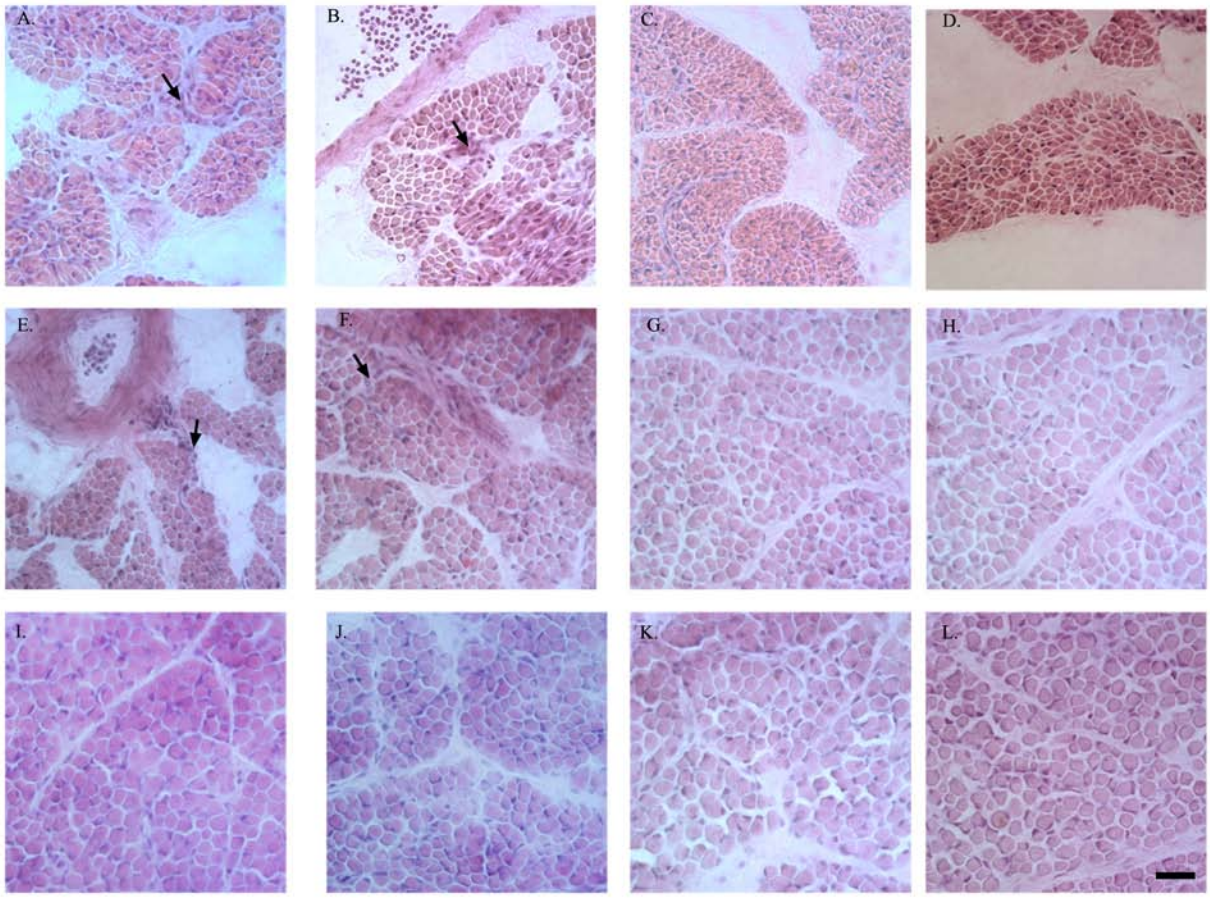

Fig. 2. Presence of inflammatory cells in *Pectoralis thoracicus* muscle in early post-hatch turkey poults. A.-D.: 72 h post-hatch; E.-H.: 96 h post-hatch; I.-L.: 120 h post-hatch; where A., E., and I. represent feed-deprived birds; B., F., and J. represent 0.88 NRC group; C., G., and K. represent 1.00 NRC group; and D., H., and L. represent 1.12 NRC group. Macrophages infiltrating between fasicles and muscle fibers (indicated by arrows) are visible in feed-deprived and 0.88 NRC birds at 72 h and 96 h post-hatch. Magnification: 100x oil. Scale bar 50µm.

4. Discussion

A variety of exogenous and endogenous factors are involved in maintenance of muscle development and metabolism. Growth and regeneration of muscular tissue requires a sequence of cellular events involving growth factors that play an important role in the regulation of proliferation, differentiation, and motility of satellite cells. The response of quiescent satellite cell activation to growth factors varies depending on overall health and nutritional status. Factors such as malnutrition, hind limb unloading, and denervation negatively affect satellite cell proliferation and result in atrophy of skeletal muscle that is characterized by a decrease in the number of myonuclei (Carlson and Faulkner 1988; Dedkov et al. 2001).

Recent experiments utilizing *Pectoralis thoracicus* muscle of the same group of turkeys as the ones employed in the current study, demonstrated that early post-hatch nutritional perturbations (feed-deprivation, 0.88 NRC, 1.00 NRC, and 1.12 NRC requirements for crude protein and amino acids) have a significant impact on myofiber satellite cell mitotic activity (Nierobisz et al., 2007). Specifically, turkeys provided a diet slightly deficient in crude protein and amino acids (0.88 NRC) exhibited significantly higher ($P<0.05$) satellite cell mitotic activity 72 h post-hatch as compared to feed-deprived, 1.00 NRC, and 1.12 NRC treatment groups. However, 96 h post-hatch satellite cell mitotic activity in 0.88 NRC group remained the same ($P>0.05$). Additionally, 96 h post-hatch satellite cell mitotic activity of the group provided with 1.00 NRC diet was the same ($P>0.05$) as the satellite cell mitotic activity in birds fed 0.88 NRC diet. Moreover, at 120 h post-hatch, the satellite cell mitotic activity was very similar in all treatment groups

(Nierobisz et al., 2007). Although satellite cell mitotic activity of 0.88 NRC treatment group was significantly higher at 72 hours post-hatch ($P<0.05$) compared to the other treatment groups, at 96 h post-hatch feed-deprived birds exhibited notably lower satellite cell mitotic activity than other treatment groups (Nierobisz, et al., 2007). The present study demonstrates that both feed-deprived and 0.88 NRC birds exhibit a significantly higher ($P<0.05$) number of apoptotic nuclei and prominent macrophage infiltration at 72 h and 96 h post-hatch. In contrast, 1.00 NRC, and 1.12 NRC treatment groups had low levels of myonuclear apoptosis and macrophage infiltration at both 72 and 96 h post-hatch. Additionally, the apoptotic nuclei count was significantly lower ($p<0.05$) and levels of macrophage infiltration were not detectable at 120 h post-hatch. It is likely that increase in apoptotic nuclei and influx of macrophages into the muscle in 0.88 NRC and feed-deprived turkeys may be associated with increased incidence of myofiber injury.

Since both feed-deprived birds and birds provided with 0.88 NRC diet were in a nutritionally compromised state, the amount of exogenous factors required to maintain normal muscle homeostasis early post-hatch was limited. In feed-deprived birds, the carbohydrates derived from the yolk sac provided minimal energy source to sustain life. However, with no exogenous supply of feed, total oxidative metabolism and overall metabolic rate appreciably decrease, leading to loss of myonuclei and atrophy of a muscle (Hikida et al., 1997; Edgerton et al., 2002). Feed-deprivation results in low levels of insulin-like growth factor I (IGF-I) and high levels of glucocorticoids that activate proteolysis (Jagoe et al., 2002). IGF-I has been shown to contribute to muscle growth and hypertrophy through its impact on satellite cell mitotic activity (Adams and McCue, 1998; Barton-Davis et al.,

1999). Halevy et al. (2003) demonstrated that a high level of IGF-I in the muscle was correlated with increase in satellite cell proliferation in turkeys provided with feed immediately post-hatch. In contrast, the IGF-I and satellite cell proliferation levels were noticeably lower in turkeys denied feed immediately post-hatch (Halevy et al., 2003). Consequently, the lack of early nutrition can be directly correlated with low levels of factors stimulating muscle growth and resulting from it myonuclear apoptosis. Loss of unused or injured myofibers resulting from feed-deprivation may also present a way of conserving energy essential to maintain metabolic processes required to sustain life.

Loss of myonuclei and low levels of satellite cells needed for myofiber regeneration may result in muscle weakness and make the muscle more prone to injury in feed-deprived birds. Macrophage infiltration into the feed-deprived muscle may potentially lead to even more muscle damage. Macrophages have been shown to increase muscle damage both in vivo and in vitro (Nguyen and Tidball, 2003). Experiments utilizing cytotoxicity assays have demonstrated that macrophages cause lysis of myofiber membrane through a nitric oxide-dependent mechanism. Nitric oxide-induced damage to the myofiber may also result in increased incidence of myonuclear apoptosis. Additionally, it has been shown that the presence of injured muscle cells stimulates macrophage infiltration into the muscle and increases the rate of nitric oxide-mediated macrophage cytotoxicity (Nguyen and Tidball, 2003). Studies utilizing dystrophic mice have revealed that dystrophic muscles are characterized by increased susceptibility to damage and increased rate of inflammation and membrane lysis (Petrof et al., 1993). Conversely, depletion of macrophages by macrophage-

specific antibody resulted in significant decrease in membrane lysis in dystrophic muscle (Wehling et al., 2001).

During the inflammatory response skeletal muscle requirement for nutrients is much higher than during normal conditions. Activation of immune cells results in generation of reactive oxygen species and antioxidants derived from external nutrients are necessary to prevent damage caused by free radicals (Webel et al., 1998; Yoshida et al., 1999). Activation of immune cells is also a nutrient requiring process. Activated immune cells have been shown to repartition nutrients from skeletal muscle to support immune function, which even further compromises muscle function in feed-deprived birds (Klasing, 1998).

Although both early post-hatch feed-deprived birds and birds provided with 0.88 NRC diet had a notable increase in apoptotic nuclei and readily detectable macrophage infiltration in the *Pectoralis thoracicus* muscle, the feed-deprived birds had significantly lower ($P<0.05$) satellite cell mitotic activity than other treatment groups, and 0.88 NRC group had significantly higher ($P<0.05$) satellite cell mitotic activity as compared to the rest of the experimental treatments (Nierobisz et al., 2007). The higher level of apoptotic nuclei in 0.88 NRC turkeys compared to the 1.0 NRC group may have resulted from inadequate amount of nutrients required to maintain and stimulate muscle growth during transition from feed deprivation to receipt of feed. Additionally, it is possible that in contrast to feed-deprived birds where macrophages most likely played a role in muscle injury, macrophages in 0.88 NRC treatment group participated in the muscle repair process, hence the increase in the satellite cell mitotic activity in the 0.88 NRC group (Nierobisz, et al., 2007). The main reason for macrophage infiltration in 0.88 NRC group was most likely phagocytosis of

muscle debris and additional activation of satellite cells to begin muscle remodeling and growth (Merly et al., 1999). Several studies have demonstrated that satellite cell activation following muscle injury is supported by a number of growth factors released from injured myofibers (Bischoff, 1990; Chen and Quinn, 1992; Jimena et al., 1993, Malm et al., 2004, Smith et al., 2008). Furthermore, macrophages have been shown to activate satellite cells and delay their differentiation by releasing a variety of growth factors and chemoattractants (Merly et al., 1999).

This study suggests that the process of apoptosis and inflammation play an important role in early post-hatch skeletal muscle growth and regeneration. Furthermore, the data suggests that early post-hatch nutritional perturbations affect muscle metabolism and health. Understanding nutrient requirements needed to maintain immune function and organ development will provide beneficial information that will aid in cost optimization, meat quality, and welfare of domestic animals.

Acknowledgements

The authors express their appreciation to Goldsboro Milling Company, Goldsboro NC, USA for the animals employed in this study. Additional thanks are given to Pam Jenkins for assistance in statistical analysis of data.

Support provided in part by funds under project number NC06590 (PEM) of North Carolina State University. Supported in part by National Research Initiative Competitive Grant no. 2005-35206-15241 from the USDA Cooperative State Research, Education, and Extension Service (PEM). Supported in part by the North Carolina Agricultural Foundation.

References

Adams, G.R., Haddad, F., Baldwin, K. M., 1999. Time course of changes in markers of myogenesis in overloaded rat skeletal muscles. J. Appl. Physiol. 87, 1705-1712.

Adams, G.R., McCue, S.A., 1998. Localized infusion of IGF-I results in skeletal muscle hypertrophy in rats. J. Appl. Physiol. 84, 1716-1722.

Allen, D.L., Linderman, J.K., Roy, R.R., Bigbee, A.J., Grindeland, R.E., Mukku, V., Edgerton, V.R., 1997. Apoptosis: a mechanism contributing to remodeling of skeletal muscle in response to hindlimb unweighting. Am. J. Physiol. 273, C579-C587.

Barton-Davis, E.R., Shoturma, D. I., Sweeney, H. L., 1999. Contribution of satellite cells to IGF-I induced hypertrophy of skeletal muscle. Acta Physiol. Scand. 167, 301-305.

Bischoff, R., 1990. Control of satellite cell proliferation. Adv. Exp. Med. Biol. 280, 147-157.

Carlson, B.M., Faulkner, J.A., 1988. Reinnervation of long-term denervated muscle freely grafted into an innervated limb. Exp. Neurol., 102, 50-56.

Chazaud, B., Sonnet, C. Lafuste, P., Bassez, G., Rimaniol, A.-C., Poron, F., Authier, F.-J., Dreyfus, P.A., Gheradi, R.K., 2003. Satellite cells attract monocytes and use macrophages as a support to escape apoptosis and enhance muscle growth. J. Cell Bio. 163, 1133-1143.

Chen, G., Quinn, L.S., 1992. Partial characterization of skeletal myoblast mitogens in mouse crushed muscle extract. J. Cell. Physiol. 153, 563-574.

Dedkov, E.L., Kostrominova, T.Y., Borisov, A.B., Carlson, B.M., 2001. Reparative myogenesis in long-term denervated skeletal muscles of adult rats results in a reduction of the satellite cell population. Anat. Rec., 263, 139-154.

Dee, K., Freer, M., Weyman, C.M., 2002. Apoptosis coincident with the differentiation of skeletal myoblasts is delayed by caspase 3 inhibition and abrogated by MEK-independent constitutive Ras signaling. Cell Death Differ. 9, 209-218.

Edgerton, V.R., Roy, R.R., Allen, D.L., Monti, R.J., 2002. Adaptations in skeletal muscle disuse or decreased-use atrophy. Am. J. Phys. Med. Rehabil. 81, s127-s147.

Halevy, O., Geyra, A., Barak, M., Uni, Z., Sklan, D., 2000. Early posthatch starvation decreases satellite cell proliferation and skeletal muscle growth in chicks. J. Nutr. 130, 858-864.

Halevy, O., Nadel, Y., Barak, M., Rozenboim, I., Sklan, D., 2003. Early posthatch feeding stimulates satellite cell proliferation and skeletal muscle growth in turkey poults. J. Nutr. 133, 1376-1382.

Hikida, R.S., VanNostran, S., Murray, J.D., Staron, R.S., Gordon, S.E., Kraemer, W.J., 1997. Anat. Rec. 247, 350-354.

Honda, H., Kimura, H., Rostami, A., 1990. Demonstration and phenotypic characterization of resident macrophages in rat skeletal muscle. Immunol. 70-272-277.

Jagoe, R.T., Lecker, S.H., Gomes, M., Golengerg, A.I., 2002. Patterns of gene expression in atrophying skeletal muscle: response to food deprivation. FASEB J. 16, 1697-1712.

Jimena, I., Pena, J., Luque, E., Vaamonde, R., 1993. Muscle hypertrophy experimentally-induced by administration of denervated muscle extract. J. Neuropathol. Exp. Neurol. 52, 379-386.

Kawano, F., Takeno, Y., Nakai, N., Higo, Y., Terada, M., Ohira, T., Nonaka, I., Ohira., Y., 2008. Essential role of satellite cells in the growth of rat soleus muscle. Am. J. Physiol.- Cell Physiol. 296, 458-467.

Klasing, K.C., 1998. Nutritional modulation of resistance to infectious diseases. Poult. Sci. 77, 1119-1125.

Leeuwenburgh, C., Gurley, C.M., Strotman, B.A., Dupont-Versteegden, E.E., 2005. Age-related differences in apoptosis with disuse atrophy in soleus. J. Physiol.-Regul. Integr. Comp. Physiol. 288, 1288-1296.

Malm, C., Sjodin, B., Sjoberg, B., Lenkei, R., Renstrom, P., Ludberg, I.E., 2004. Leukocytes, cytokines, growth factors and hormones in human skeletal muscle and blood after uphill or downhill running. J. Physiol.-London 556, 983-1000.

McCroskery, S., Thomas, M., Platt, L., Hennebry, A., Nishimura, T., McLeay, L., Shamra, M., Kambadur, R., 2005. Improved muscle healing through enhanced regeneration and reduced fibrosis in myostatin-null mice. J. Cell Sci. 118, 3531- 3541.

McLennan, I.S., 1996. Degenerating and regenerating skeletal muscles contain several subpopulations of macrophages with distinct spatial and temporal distributions. J. Anat. 188, 17-28.

Merly, F., Lescaudron, L., Rouaud, T., Crossin, F., Gardahaut, M.F., 1999. Macrophages enhance muscle satellite cell proliferation and delay their differentiation. Muscle Nerve 22, 724-732.

Moss, F.P., Leblond, C.P., 1971. Satellite cells as the source of nuclei in muscles of growing rats. Anat. Rec. 170, 421-436.

Mozdziak, P.E., Schultz, E., Cassens, R. G., 1997. Myonuclear accretion is a major determinant of avian skeletal muscle growth. Am. J. Physiol. 272, C565-571.

Mozdziak, P.E., Evans, J.J. McCoy, D.W., 2002a. Early posthatch starvation induces myonuclear apoptosis in chickens. J. Nutr. 132, 901-903.

Mozdziak, P.E., Walsh, T. J., McCoy, D. W., 2002b. The effect of early posthatch nutrition on satellite cell mitotic activity. Poult. Sci. 81, 1703-1708.

National Research Council 1994. Nutrient requirements of poultry, Ninth Revised Edition.

Nguyen, H.X., Tidball, J.G., 2003. Interactions between neutrophils and macrophages promote macrophage killing of muscle cells in vivo. J. Physiol. 547, 125-132.

Nierobisz, L.S., Felts, V., Mozdziak, P.E., 2007. The effect of early dietary amino acid levels on muscle satellite cell dynamics in turkeys. Comp. Biochem. Physiol. B 148, 286-294.

Petrof, B.J., Shrager, J.B., Stedman, H.H., Kelly, A.M., Sweeney, H.L., 1993. Dystrophin protects the sarcolemma from stresses developed during muscle contraction. Proc. Natl. Acad. Sci. USA 90, 3710-3714.

Pimorady-Esfahani, A., 1997. Macrophages and dendritic cells in normal and regenerating murine skeletal muscle. Muscle Nerve 20, 158-166.

Pinchasov, Y.,Noy, Y., 1993. Comparison of post-hatch holding time and subsequent early performance of broiler chicks and turkey poults. Br. Poult. Sci. 34, 111-120.

Pophal, S., Evans, J., Mozdziak, P.E., 2003. Myonuclear apoptosis occurs during early posthatch starvation. Comp. Biochem. Physiol. B. 135, 677-681.

Sandri, M., Carraro, U., 1999. Apoptosis of skeletal muscles during development and disease. Int. J. Biochem. Cell Biol. 31, 1373-1390.

SAS Institute 1985. User's guide: Statistics. Version 5 ed. SAS Institute Inc., Cary, NC.

Smith, C., Kruger, M.J., Smith, R.M., Myburgh, K.H., 2008. The inflammatory response to skeletal muscle injury illuminating complexities. Sports Med. 38, 947-969.

Stockdale, F.E., Holtzer, H., 1961. DNA synthesis and myogenesis. Exp. Cell Res. 24, 508-520.

Tews, D.S., Goebel, H.H., 1997. DNA-fragmentation and expression of apoptosis- related proteins in muscular dystrophies. 23, 331-338.

Tidball, J.G., 2005. Inflammatory processes in muscle injury and repair. Am. J. Physiol. Regul Integr. Comp. Physiol. 288, 345-353.

Uni, Z.,Ferket, P. R., 2004. Methods of early nutrition and their potential. World's Poult. Sci. J. 60, 101-111.

Vieira, S.L.,Moran, E.T.,Jr, 1999. Effects of delayed placement and used litter on broiler yields. J. Appl. Poult. Res. 8, 75-81.

Webel, D.M., Mahan, D.C., Johnson, R.W., Baker, D.H., 1998. Pretreatment of young pigs with vitamin E attenuates the elevation in plasma interleukin-6 and cortisol caused by a challenge dose of lipopolysaccharide. J. Nutr. 128, 1657-1660.

Wehling, M., Spencer, M.J., Tidball, J.G., 2001. A nitric oxide synthase transgene ameliorates muscular dystrophy in mdx mice. J. Cell Biol. 155, 123-131.

Yoshida, N., Yoshikawa, T., Manabe, H., Terasawa, Y., Kodo, M., Noguchi, N., Niki, E., 1999. Vitamin E protects against polymorphonuclear leukocyte-dependent adhesion to endothelial cells. J. Leukocyte Bio. 65, 757-763.

Chapter 3

Fiber Phenotype and CoQ_{10} Content in Turkey Skeletal Muscles

Abstract

Phenotypical differences between muscle fibers are associated with a source of cellular energy. Coenzyme Q_{10} (CoQ_{10}) is a major component of the mitochondrial oxidative phosporylation process, and it significantly contributes to the production of cellular energy in the form of ATP. The objective of this study was to determine the relationship between whole tissue CoQ_{10} content, mitochondrial CoQ_{10} content, mitochondrial protein, and muscle phenotype in turkeys. Four specialized muscles (Anterior latissimus dorsi-ALD, Posterior latissimus dorsi-PLD, Pectoralis major-PM, and Biceps femoris-BF) were evaluated in 9- and 20-week old turkey toms. The amount of muscle mitochondrial protein was determined using the Bradford assay and CoQ_{10} content was measured using HPLC-UV. The amount of mitochondrial protein relative to total protein was significantly lower ($P<0.05$) at 9 compared to 20 weeks of age. All ALD fibers stained positive for anti-slow (S35) MyHC antibody. The PLD and PM muscle fibers revealed no staining for slow myosin heavy chain (S35 MyHC), whereas half of BF muscle fibers exhibited staining for S35 MyHC at 9 weeks and 70 percent at 20 weeks of age. The succinate dehydrogenase (SDH) staining data revealed that SDH significantly increases ($P<0.05$) in ALD and BF muscles and significantly decreases ($P<0.05$) in PLD and PM muscles with age.

The study reveals age-related decreases in mitochondrial CoQ_{10} content in muscles with fast/glycolytic profile, and demonstrates that muscles with a slow/oxidative phenotypic profile contain a higher proportion of CoQ_{10} than muscles with a fast/glycolytic phenotypic profile.

Introduction

Vertebrate skeletal muscle is composed of a heterogeneous and highly dynamic groups of muscle fibers that vary based on their biophysical and metabolic profiles. The heterogeneity of muscle fibers is determined based on muscle fiber size, differential expression of contractile proteins, and on factors involved in regulation of cellular metabolism (Williams and Neufer, 1996; Pette and Staron, 1997). The number, size, and type of a muscle fiber is primarily determined by the genetic and environmental factors that influence both pre-natal/pre-hatch and post-natal/post-hatch muscle development.

Although different subtypes of muscle fibers can be distinguished during embryonic development, the genetically pre-established pattern for muscle fiber types becomes determined during the early post-natal or post-hatch period (Moss and Leblond, 1971; Swatland and Cassens, 1973; Miller et al., 1993; Garry et al., 1996). During the early post-natal or post-hatch period, muscle fibers undergo a maturation process that results in muscle fiber distribution similar to that found in adult animals. It has been shown that myoblasts develop into myofibers with diverse metabolic, biophysical, and contractile profiles (Gibson and Schultz, 1982).

Common histological techniques used to evaluate muscle fiber phenotype include enzymatic staining for mitochondrial succinate dehydrogenase (SDH) and for myosin adenine triphosphatase (ATPase). The contractile profiles of developing and adult fiber types are determined by muscle myosin heavy chain isoform composition (Reiser et al., 1985; Page et al., 1992). Each myosin isoform is a product of a different MyHC gene (Schiaffino and

Reggiani, 1996). In classical fiber typing experiments (Wiskus et al, 1976; Aberle et al., 1979; Smith and Fletcher, 1987), muscle fibers were classified as α (fast-twitch, type II) or β (slow-twitch, type I), and as red (R) or white (W). The fast and slow classifications were based on histochemical staining for adenosine triphosphatase (ATPase). However, glycolytic and oxidative fiber determination was based on succinic dehydrogenase (SDH) staining for mitochondria (Aberle et al., 1979). Because SDH is an important component of the TCA cycle, dark SDH staining identifies muscle fibers with high oxidative potential. Wiskus et al. (1976) suggested that there are three main muscle fiber types in the turkey. Based on their differential response to ATPase and SDH staining, the three fiber types were defined as αR (fast-oxidative), αW (fast-glycolytic), and βR (slow-oxidative). Wiskus et al. (1976) demonstrated that the Pectoralis major muscle was scarce in βR fibers. However, the Biceps femoris muscle was composed of both oxidative (βR, αR) and glycolytic (αW), fast-twitch fibers.

The environmental cues, physical stresses, and genetic factors affect the activity of enzymes governing specific muscle fiber metabolism and control muscle fiber phenotype. One of the major determinants of skeletal muscle fiber phenotype in turkeys of the same genetic line is the location of the muscle and its corresponding functional load. Previous studies demonstrated that increased load on a muscle induces slower, more oxidative phenotype; and decreased load induces more glycolytic phenotype (Kasper et al., 1993; Mozdziak et al., 1998).

Factors that participate in mitochondrial respiration may also play a significant role in determining muscle fiber phenotype. One of the factors that plays an important role in

mitochondrial respiration in skeletal muscle is Coenzyme Q_{10} (CoQ_{10}) (Pastore et al., 2005), which is a bioactive, vitamin-like molecule present in all eukaryotic cells containing mitochondria. CoQ_{10} is located in the hydrophobic middle region of the phospholipid bilayer of the mitochondrial membrane and participates in the electron transport chain process, where it accepts electrons from reducing equivalents produced from fatty acid and glucose breakdown, and delivers them to electron acceptors (Bliznakov and Bhagavan, 2003). The specific role of CoQ_{10} in electron transport chain is to transfer electrons from NADH-Q oxidoreductase (complex I) and from succinate-Q oxidoreductase (complex II) to cytochrome c oxidoreductase (complex III) (Kamzalov et al., 2003). The movement of electrons from one complex to another, results in generation of a proton gradient. The energy released when protons move back to mitochondria is used to generate ATP. Elevated concentrations of CoQ_{10} have been found in organs with high energy requirements such as heart, brain and skeletal muscle (Bliznakov and Bhagavan, 2003). CoQ_{10} in its reduced form (ubiquinol) acts as a principal fat-soluble cellular antioxidant that plays an important role in neutralizing free radicals, inhibiting lipid peroxidation of membranes, and in protecting mitochondrial membrane proteins and DNA (Frei et al., 1990). Furthermore, dietary supplementation of ubiquinol has been shown to result in elevated tissue and mitochondrial levels of α-tocopherol, which is also a powerful antioxidant (Kamzalov et al., 2003).

In this study, four functionally diverse muscles (Anterior latissimus dorsi, Posterior latissimus dorsi, Pectoralis major, and Biceps femoris) were examined with consideration of their metabolic profiles. Pectoralis major and Posterior latissimus dorsi represent muscle groups composed of fast-twitch fibers that rely primarily on glycolytic metabolism for energy

generation. The Biceps femoris muscle contains a combination of metabolically diverse muscle fibers. However, the Anterior latissimus dorsi muscle is characterized by extremely low anaerobic capacity, and is composed of fibers that are entirely slow twitch (Kiessling, 1976; Wiskus et al., 1976).

Turkey performance data indicates that turkeys grow rapidly before 10 weeks of age and the difference in weight gain plateaus shortly thereafter (Anthony et al., 1990). To account for growth-related differences in selected muscles, turkeys were evaluated at 9 weeks of age (rapid growth rate) and at 20 weeks of age (slow growth rate). Commercially-raised turkeys are considered adult at 16 weeks of age and are brought to market at 20 weeks of age (Dr. Peter Ferket, personal communication). Consequently, 9 week old birds are considered to be at pre-puberty stage and 20 week old birds are considered to be adult.

Additionally, previous studies demonstrated that beyond 9 weeks of age, muscle satellite cell mitotic activity begins to diminish and muscle fiber growth occurs primarily through an increase of cytoplasmic to nuclear ratio (Mozdziak et al., 1994). Consequently, from the cellular perspective, 9 weeks of age represents an important transition point in skeletal muscle development.

The aim of this study was to determine the interconnection between muscle phenotype, metabolic profile, mitochondrial content, and CoQ_{10} content in phenotypically distinct skeletal muscles in domestic turkeys selected at two different stages of maturity.

Materials and Methods

Sample Collection

All experiments involving animals were in compliance with the North Carolina State University Institutional Animal Care and Use Committee. The two groups of turkeys selected for the study consisted of young/pre-puberty (9 weeks-old) and adult (20-weeks old) toms (Meleagris gallopavo). Five 9-week-old and five 20-week-old turkeys were randomly selected from a single flock and immediately killed by intra-venous injection of Euthasol® (Delmarva Laboratories, Midlothian, VA, USA) at a dose of 0.25mL/kg body weight. Right anterior latissimus dorsi (ALD), posterior latissimus dorsi (PLD), pectoralis major (PM), and biceps femoris (BF) muscles were excised and divided in half, in a transverse manner, for both HPLC and histochemical analysis. Half of the samples were snap frozen using isopentane cooled on dry ice, and half was fixed in 2% paraformaldehyde for further histochemical analysis.

Mitochondrial Isolation

The mitochondrial isolation was performed based on procedure described by Bhattacharya et al. (1991). Frozen muscle samples were minced with scissors until homogenous and placed in protease solution (Subtilisin A, type VIII bacterial protease from Bacillus licheniforms; 12 units/mg; Sigma Cat# 9014-01-1). Following protease treatment, samples were transferred to Ionic Medium (IM; 100 mM Sucrose, 10 mM EDTA, 100 mM Tris-HCl, 46 mM KCl) combined with 0.5% bovine serum albumin (BSA). Samples were

then homogenized in a tissue grinder, placed in conical centrifuge tubes and centrifuged for 10 minutes at 500*g* at 4 ℃. The supernatant was removed and centrifuged at 12,000*g* for 10 minutes at 4 °C. The cytoplasmic fraction was removed and the pellet was resuspended in fresh IM/BSA buffer and centrifuged again at 12,000*g* for 10 minutes at 4 °C. The remaining pellet containing the mitochondrial fraction was resuspended and stored in suspension medium (SM; 230 mM mannitol, 70 mM sucrose, 0.02 mM EDTA, 20 mM Tris-HCl, 5 mM K_2HPO_4).

Western blot analysis was performed on representative cytosolic and mitochondrial fractions to account for purity of isolated mitochondria (Carson and Robertson, 2006). Protein extracts of 20µg were loaded on 10% SDS polyacrlylamide gel. The following polyclonal primary antibodies raised in rabbit were utilized in the Western blot procedure: anti-GAPDH (Sigma-Aldrich, St. Louis, MO) at 1:1000 dilution, and anti-Cox4 (Fisher Scientific, Pittsburgh, PA) at 1:1000 dilution. The proteins were detected using anti-rabbit secondary antibody conjugated to Horseradish peroxidase at 1:2000 dilution. The anti-GAPDH antibody was utilized to evaluate the possibility of cytosolic contamination in mitochondrial fraction. The anti-Cox4 antibody was utilized to examine mitochondrial proteins in the mitochondrial fraction and to confirm that mitochondrial proteins were not present in the cytosolic fraction (Fig. 1).

Mitochondrial Protein Quantification

Bradford assay was performed on the isolated mitochondrial fractions to quantify total mitochondrial protein per gram of muscle sample. The amount of mitochondrial protein was quantified based on absorbance at 595 nm (Zor and Selinger, 1996; Bradford, 1976).

HPLC-UV

Mitochondrial and whole tissue Coenzyme Q_{10} content were quantified using high performance liquid chromatography (HPLC) (Shimadzu USA Manufacturing, Inc., Canby, Oregon), which was equipped with a model LC-20AD solvent delivery pump, a model SPD-20A UV/Vis detector, a model CTO-20A column oven, and a model SIL-20C HT auto sampler. The system was controlled and data were analyzed by LC solution version 1.23 (Shimadzu Corporation).

The HPLC method used in this study was modified from that described previously by Pastore et al., 2005. Approximately 0.1 g of frozen muscle fragments (-80°C) was excised in triplicates from the most central area of the tissue and homogenized with 1000 µl hexane and 500 µl methanol in a tissue homogenizer. The mitochondrial fraction, separated from approximately 1 g of muscle, was also mixed with 1000 µl hexane and 500 µl methanol. The whole tissue and mitochondrial fractions were centrifuged at 10,000*g* for 5 minutes at 4 °C. Starting with a stock solution of 1.6 mM, the coenzyme Q_{10} standards (Sigma-Aldrich, St. Louis, MO) were prepared by serially diluting six times in a mixture of 2/3 hexane and 1/3 methanol. The concentrations of the working standards were: 16 µM, 8 µM, 4 µM, 2 µM, 1 µM, and 0.5 µM. The standards were then centrifuged at 10,000*g* for 5 minutes at 4°C.

The hexane phase containing coenzyme Q_{10} standard, coenzyme Q_{10} extracted from tissue fragments, and coenzyme Q_{10} extracted from the mitochondrial fraction were transferred to glass HPLC vials and capped with Teflon-lined septa and injected in 10 µl aliquots onto the column. A 125- x 3-mm ODS Hypersil column (Thermo Scientific, Waltham, MA) was equilibrated with mobile phase containing 15 ml glacial acetic acid, 275 ml hexane, 15 ml sodium acetate, 695 ml methanol (Fisher Scientific, Pittsburg, PA), and 15 ml 2-propanol (Sigma-Aldrich, St. Louis, MO).

The column was equilibrated with mobile phase for at least 20 minutes before analysis. The coenzyme Q_{10} standards and muscle extract samples were eluted isocratically at a flow rate of 1.0 ml/min and detected at 275 nm. The column temperature was held constant at 30 ºC. Peak area was directly proportional to concentration of standard, thus linear regression analysis was used to calculate concentration of coenzyme Q_{10} in whole muscle and mitochondrial extract.

SDH and ATPase Histochemistry

A modified version of Wiskus et al. (1976) fiber staining protocol was utilized to determine SDH and slow myosin ATPase activity. Serial transverse sections (15 µm) from ALD, PLD, PM, and BF muscle samples were cut in a cryostat at -20 °C, air dried, and subjected to histochemical staining for succinate dehydrogenase (SDH) and myofibrillar adenosine triphosphatase (ATPase) at pH 3.9.

During ATPase staining procedure, tissue sections were preincubated in a solution of 0.2 M barbital acetate buffer (1.94 g sodium acetate, 2.94 g sodium barbital (Sigma-Aldrich,

St. Louis, MO), and 100 ml distilled water) at room temperature (19-21 ℃) for 5 minutes at pH 3.9. The acidic solution was washed in the alkali-preincubating solution (pH 9.4; 20 ml of 0.2% w/v sodium barbital, 25 ml $CaCl_2$, 55 ml distilled water) for 5 seconds followed by incubation in alkali solution (pH 9.4; 90 mg ATP, 12 ml barbital, 6 ml $CaCl_2$, 40 ml distilled water) for 45 minutes at room temperature (19-21℃). The sections were then washed in 1% $CaCl_2$, transferred to 2% $CoCl_2$, washed in 0.2% sodium barbital, and rinsed with distilled water. The reaction was developed with 1% yellow ammonium sulfide for 15 seconds. Sections were dehydrated, mounted in Permount®.

The SDH staining was performed as follows: Freshly dried cryostat sections were incubated for 5 minutes at room temperature (19-21℃) in a medium composed of 2 ml of Nitroblue tetrazolium (NBT) stock solution (100 ml PBS at pH 7.6, 6.5 mg KCN, 185 mg EDTA, 100 mg Nitroblue tetrazolium), 0.2 ml succinate stock solution (2.7 g sodium succinate, 20 ml distilled water), and 0.7 mg phenazine methosulphate. The sections were rinsed in acetone gradient, cleared, and mounted in glycerin jelly.

MyHC Immunohistochemistry

Tissues were fixed in 2% paraformaldehyde, embedded in paraffin, dewaxed and dehydrated. Serial sections, 15 microns thick, were cut on a microtome and subjected to slow (S35) and fast (F59) myosin heavy chain (MyHC) immunohistochemical analysis. A supernatant generated from S35 and F59 MyHC hybridomas (Developmental Studies Hybridoma Bank, Iowa City, IA) was utilized to detect presence of slow and fast myosin isoforms in skeletal muscle sections. Dehydrated muscle sections were blocked for 15

minutes in a solution containing 0.1% bovine serum albumin (BSA), 5 mM EDTA, 3% goat serum and 1 mM sodium azide to prevent non-specific antibody binding. Subsequently, the sections were incubated in either S35 or F59 MyHC supernatant diluted 1:10 in blocking solution at 4°C in a humidified chamber for 12 hrs. The sections were rinsed 2 times for 5 minutes with IX PBS buffer and were then blocked in a solution containing 0.1% BSA, 5 mM EDTA, 3% goat serum and 1 mM sodium azide and incubated for 2 hours at room temperature (19-21°C) in goat anti-mouse secondary antibody conjugated to horseradish peroxidase (GAM-HRP) diluted 1:50 with blocking solution. The slides were rinsed in PBS and incubated in diaminobenzane and urea for 5 minutes. Subsequently, the slides were rinsed with distilled water, dehydrated, mounted with Permount®.

Image Analysis

A Leica DMR light microscope (Leica Microsystems, Bannockburn IL, USA) was utilized to observe ALD, PLD, PM, and BF muscle sections All images were captured at either 20x or 40x magnification using a Retiga 4000R fast camera (Q Imaging, Surrey BC, Canada). Image-Pro Plus software (Media Cybernetics, Version 6, 2006) was utilized to identify muscle fiber phenotype. The criterion for accurate determination of muscle fiber phenotype was to evaluate at least five hundred fibers per muscle per bird (5 birds per treatment).

The pattern of staining for myosin ATPase and for oxidative enzyme, SDH, was determined as high, middle, or low (Figs. 6-8). In ATPase-stained slides, light staining was attributed to muscle fibers with low activity of slow myosin ATPase, medium staining was

attributed to fibers with medium activity of slow myosin ATPase , and dark staining was attributed to muscle fibers with high activity of slow myosin ATPase (Figs. 6 and 8). In the SDH-stained slides, fibers stained with high intensity appeared dense blue with a band of staining inside the sarcolemma, the fibers stained with middle intensity had a band of staining inside the sarcolemma but lighter staining in the middle of the fiber, and fibers stained with low intensity for SDH lacked the sarcolemmal band and had few mitochondria dispersed throughout the section (Figs. 7 and 8) (Anapol and Herring, 2000). The MyHC isoforms were evaluated based on presence or absence of staining (Fig 9).

Statistical Analysis

The General Linear Models (GLM) procedure of SAS (SAS Institute, 1985) was performed to analyze the effect of muscle and age on the following parameters: CoQ_{10} content in the whole muscle and mitochondrial fraction, muscle mitochondrial content, and on histochemically-defined muscle fiber phenotype. A two-way analysis of variance (ANOVA) was performed to evaluate the effect of muscle and age (9 and 20 weeks) on each parameter (Fig. 2). Means of each treatment were separated using Fisher's least significant differences. Values were considered statistically significant when $P< 0.05$. Correlation analysis was performed to identify the relationship between mitochondrial CoQ_{10} content, SDH staining, and slow myosin ATPase staining (Table 1.)

Table 1. Correlation analysis of mitochondrial CoQ_{10} content, SDH, and myosin ATPase expression levels in 9 week old muscles and 20 week old muscles.

9 week data	*Mitochondrial CoQ10*	*SDH-L*	*SDH-M*	*SDH-H*	*ATPASE-L*	*ATPASE-M*	*ATPASE-H*
Mitochondrial CoQ10	1.0000						
SDH-L	-0.9752	1.0000					
SDH-M	-0.9856	0.9953	1.0000				
SDH-H	0.9826	-0.9983	-0.9993	1.0000			
ATPASE-L	-0.9089	0.9767	0.9529	-0.9635	1.0000		
ATPASE-M	0.5147	-0.3158	-0.3891	0.3603	-0.1103	1.0000	
ATPASE-H	0.6643	-0.8099	-0.7574	0.7792	-0.9155	-0.2989	1.0000

20 week data	*Mitochondrial CoQ10*	*SDH-L*	*SDH-M*	*SDH-H*	*ATPASE-L*	*ATPASE-M*	*ATPASE-H*
Mitochondrial CoQ10	1.0000						
SDH-L	-0.8459	1.0000					
SDH-M	-0.1726	0.6047	1.0000				
SDH-H	0.7559	-0.9838	-0.7376	1.0000			
ATPASE-L	-0.7205	0.9717	0.7758	-0.9983	1.0000		
ATPASE-M	0.8738	-0.4829	0.2983	0.3422	-0.2927	1.0000	
ATPASE-H	0.1960	-0.6795	-0.9506	0.7899	-0.8212	-0.3053	1.0000

Correlation coefficient of +1 indicates that two values are perfectly related in a positive manner and coefficient of -1 indicates that two values are perfectly related in a negative linear manner.

Results

Western Blot

GAPDH and COX4 antibodies have been widely used to verify mitochondrial fraction purity (Morrish et al., 2006). In the cytosolic fraction, GAPDH tetramer was detected between 30 and 40kd with anti-GAPDH polyclonal antibody. However, there was no anti-GAPDH reactivity detected in the mitochondrial fraction, suggesting that the

mitochondrial fraction is free of contamination with cytosolic components. A 17kd band was detected when mitochondrial fraction was reacted with anti-Cox4 antibody suggesting that mitochondria were indeed present in the mitochondrial fraction. No anti-Cox4 reactivity was detected in the cytosolic fraction, confirming that this fraction did not contain any mitochondria (Fig. 1).

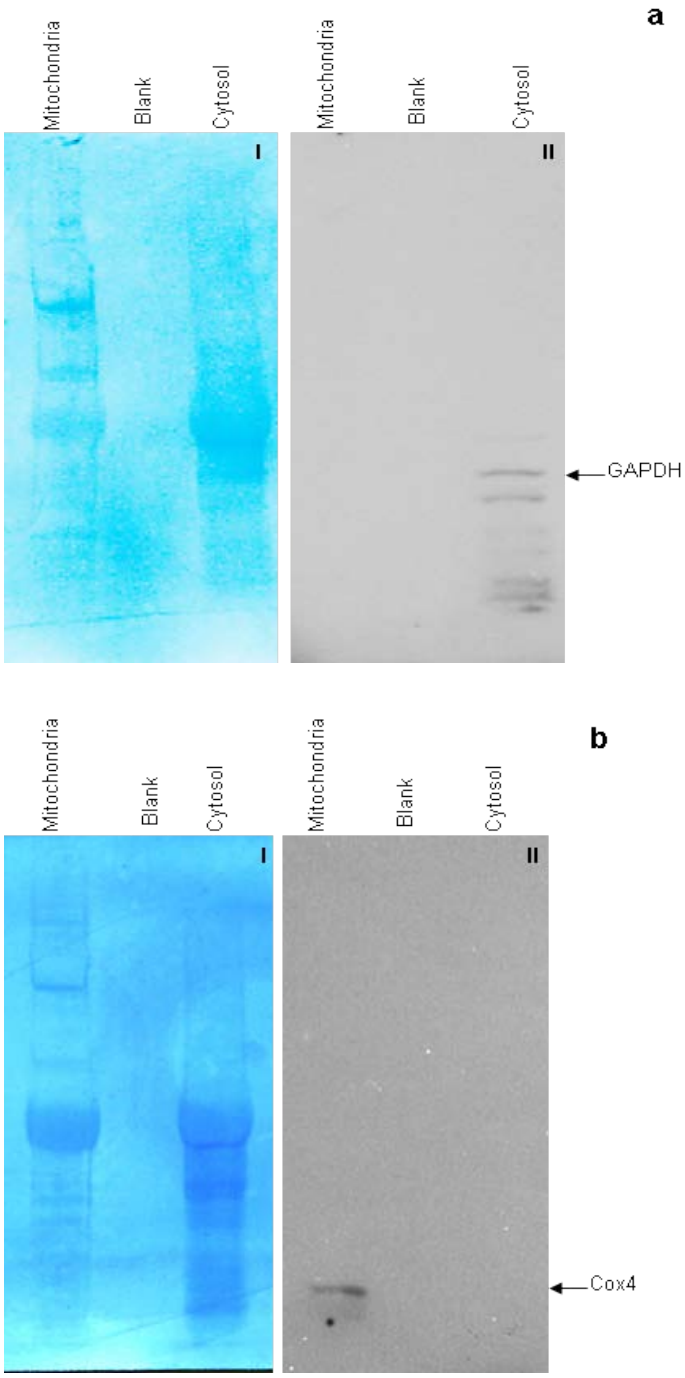

Fig. 1. Representative Western blot analysis of **a** anti-GAPDH and **b** anti-Cox4 in mitochondrial and cytosolic fractions of 9 week-od ALD muscle. The figure represents **I** coomassie blue-stained PVDF membrane and **II** Western blot scan. 20µg of protein was equally loaded to each lane.

HPLC Analysis

ALD and BF muscles exhibited significantly higher ($P<0.0001$) total CoQ_{10} content than PLD and PM muscles on week 9 and 20 (Fig. 2). Total CoQ_{10} per gram of muscle was higher ($P<0.0126$) in ALD muscles at 20 weeks of age as compared to 9 weeks of age. However, total CoQ_{10} content remained the same in PLD, BF and PM muscles at each age.

ALD and BF mitochondrial CoQ_{10} content was significantly higher ($P<0.0157$) than PLD and PM CoQ_{10} content on week 9 and 20 (Fig. 3). The mitochondrial CoQ_{10} content in ALD and BF muscles was significantly higher ($P<0.0034$) at 20 compared to 9 weeks of age. However, the mitochondrial CoQ_{10} content in PM and PLD did not change in 20 week old birds compared to 9 week old birds (Fig. 3).

Another parameter was calculated whereby a percent ratio of CoQ_{10} in mitochondria to $CoQ_{10\ in}$ total muscle (mitochondrial: total CoQ_{10}) was determined. No significant differences were revealed between the different muscles on week 9 (Fig. 4). However, on week 20, the mitochondrial: total CoQ_{10} was significantly higher ($P<0.0066$) in ALD and BF muscles than in PM and PLD muscles. Mitochondrial: total CoQ_{10} significantly decreased in PM and PLD muscles ($P<0.0160$ in PLD, $P<0.0018$ in PM), remains the same in ALD muscle, and significantly increased ($P<0.001$) in BF muscle between week 9 and 20 (Fig. 4).

Fig. 2. Total CoQ_{10} (mg) per gram of 9 wk and 20 wk-old turkey muscles determined by HPLC (**a**). Values with different superscripts represent means that are statistically different ($P<0.05$). Values with the same superscripts represent means that do not differ statistically ($P>0.05$). The superscripts represent values in ascending order. Error bars represent standard errors of individual means.
Examples of HPLC-UV chromatograms depicting total CoQ_{10} content in ALD (**b**), PLD (**c**), PM (**d**), and BF (**e**) muscles at 20 weeks.

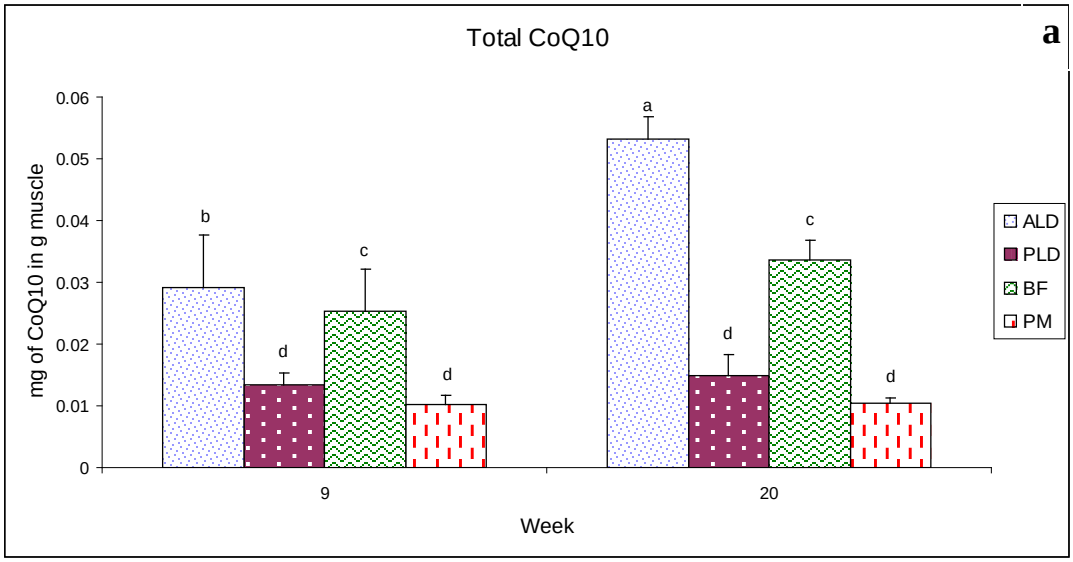
Total CoQ10
a
mg of CoQ10 in g muscle
0.06
0.05
0.04
0.03
0.02
0.01
0
b
d
c
d
a
d
c
d
9
20
Week
ALD
PLD
BF
PM

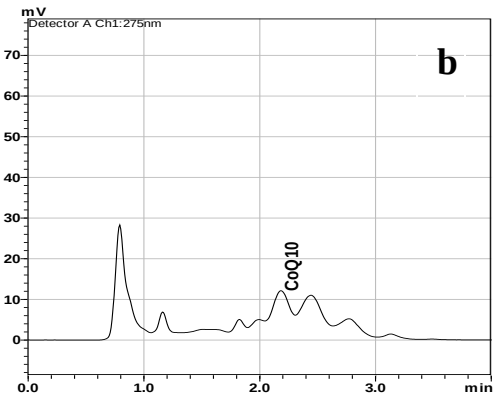
mV
Detector A Ch1:275nm
b
CoQ10
min

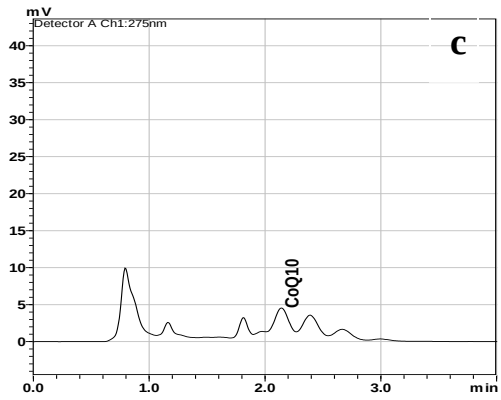
mV
Detector A Ch1:275nm
c
CoQ10
min

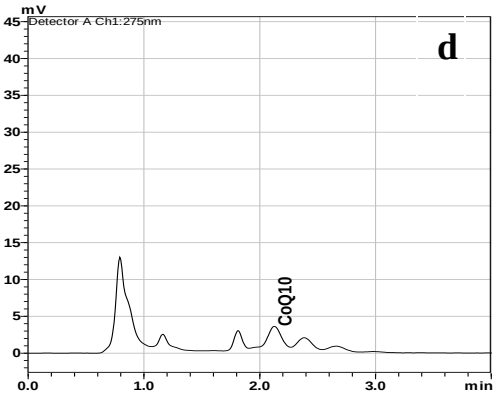
mV
Detector A Ch1:275nm
d
CoQ10
min

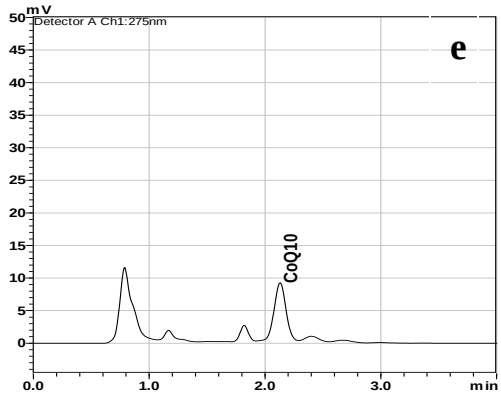
mV
Detector A Ch1:275nm
e
CoQ10
min

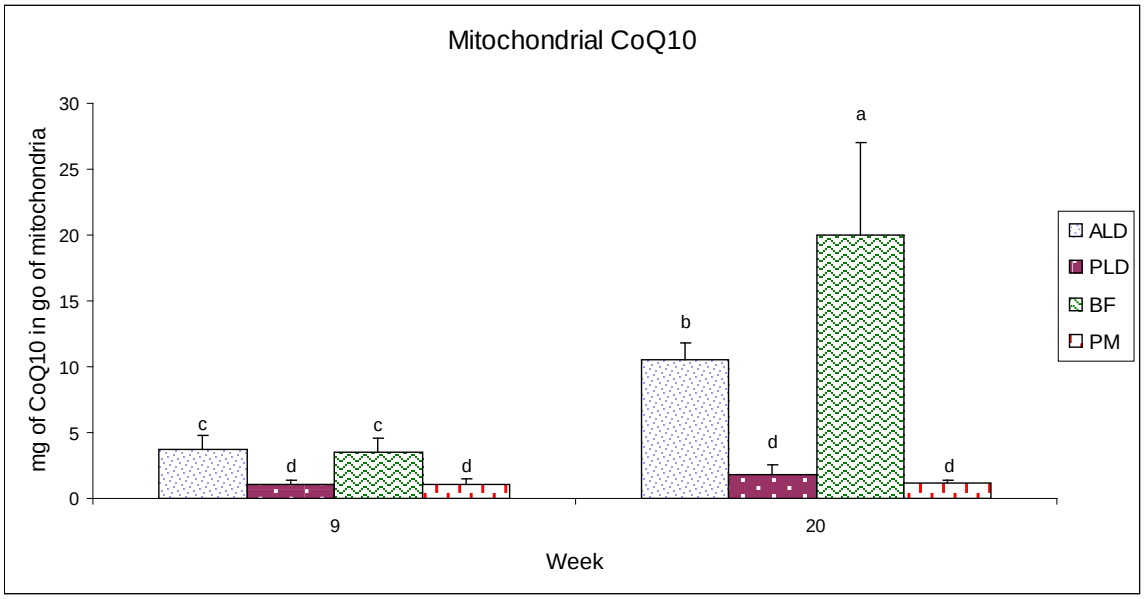

Fig. 3. CoQ_{10} (mg) per gram of mitochondria in 9 and 20 wk-old turkey muscle determined by HPLC ($P<0.0002$). The superscripts represent means that are significantly different. Error bars represent standard errors of individual means.

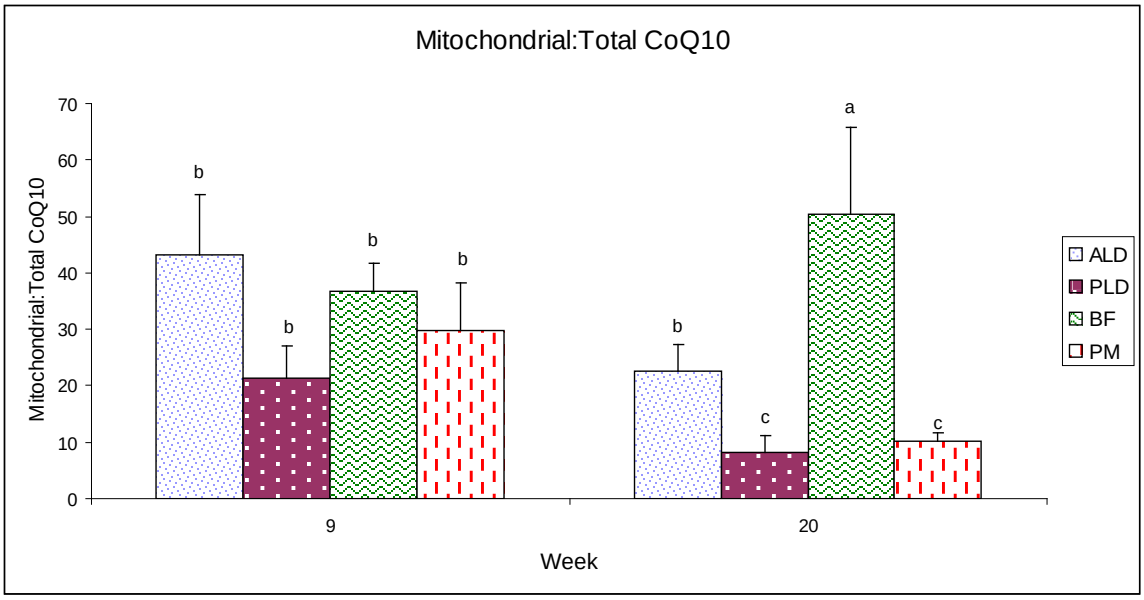

Fig. 4. Ratio of mitochondrial CoQ_{10} to total amount of CoQ_{10} in 9 and 20 wk-old turkey muscle represented in percentages and determined by HPLC ($P<0.0098$). The ratio is expressed in percentages. The superscripts represent means that are significantly different. Error bars represent standard errors of individual means.

Mitochondrial Protein Quantification

Data generated from Bradford assay reveals that the amount of mitochondrial protein relative to total protein significantly decreases ($P<0.0001$) with age in all four muscles. However, there were no significant differences in mitochondrial protein content between muscles at given time (Fig. 5).

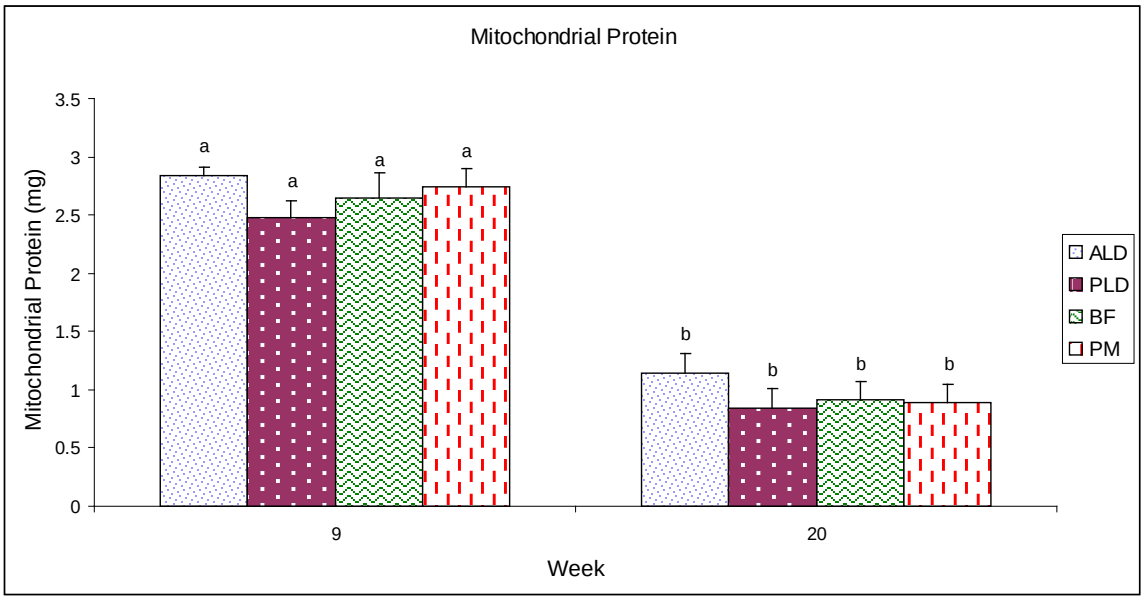

Fig. 5. Amount of mitochondrial protein (mg) relative to total protein in one g of wet muscle mass of 9 wk and 20 wk-old turkey muscle. Protein amounts were determined by the Bradford assay ($P<0.001$). The superscripts represent means that are significantly different. Error bars represent standard errors of individual means.

Fiber Typing

In the BF muscle, low, middle, and high intensity of staining for ATPase was observed, where the number of fibers stained at low intensity was significantly higher ($P<0.0001$) than the number of fibers stained and middle and high intensity (Fig. 6 and 8). The staining intensity representing activity of ATPase molecule remained statistically unchanged in ALD, PLD, BF, and PM muscles over time (Fig. 6 and 8).

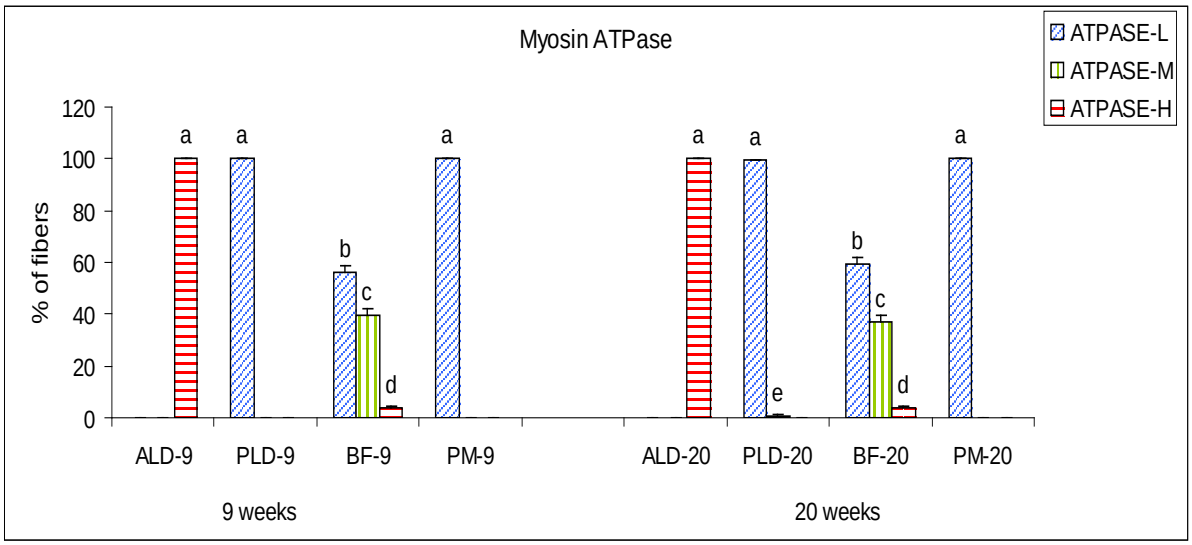

Fig. 6. Percentage of ALD, PLD, BF, and PM muscle fibers in 9 and 20-week old turkey toms with low (ATPase-L), medium (ATPase-M), and high (ATPase-H) intensity staining for myofibrillar ATPase at pH 3.9 ($P<0.0001$). The superscripts represent means that are significantly different. Error bars represent standard errors of individual means.

At 9 weeks of age, ALD muscle contained fibers stained at high and middle intensity for SDH. However, at 20 weeks of age all ALD fibers were darkly stained for SDH. The percentage of PLD fibers stained at low intensity for SDH significantly increased ($P<0.006$) over time and the percentage of PLD fibers stained at middle and high intensities for SDH were significantly lower at 20 weeks compared to 9 weeks of age (Fig. 7). In the BF muscle the percentage of fibers stained at low intensity for SDH remained the same, the percentage of fibers stained at middle intensity for SDH significantly decreased ($P<0.01$), and the percentage of fibers stained at high intensity for SDH significantly ($P<0.04$) increased with age. The percentage of PM fibers stained at low intensity for SDH significantly increased ($P<0.0001$), and the percentage of fibers stained at middle and high intensity for SDH significantly decreased ($P<0.0001$) with age (Fig. 7 and 8).

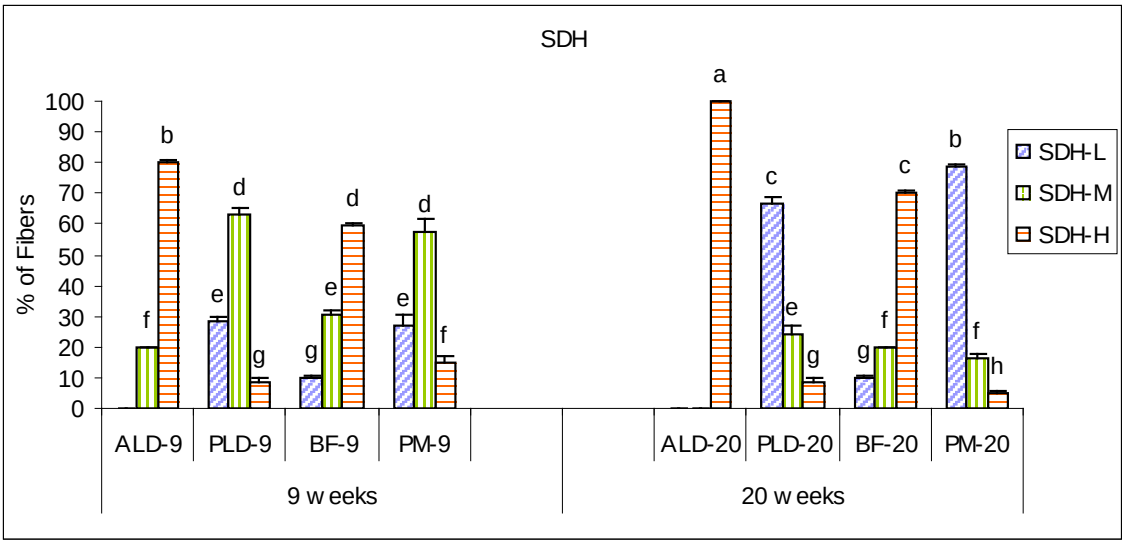

Fig. 7. Percentage of ALD, PLD, BF, and PM muscle fibers in 9 and 20-week old turkey toms with low (SDH-L), medium (SDH-M), and high (SDH-H) intensity staining for succinate dehydrogenase (SDH) ($P<0.0001$). The superscripts represent means that are significantly different. Error bars represent standard errors of individual means.

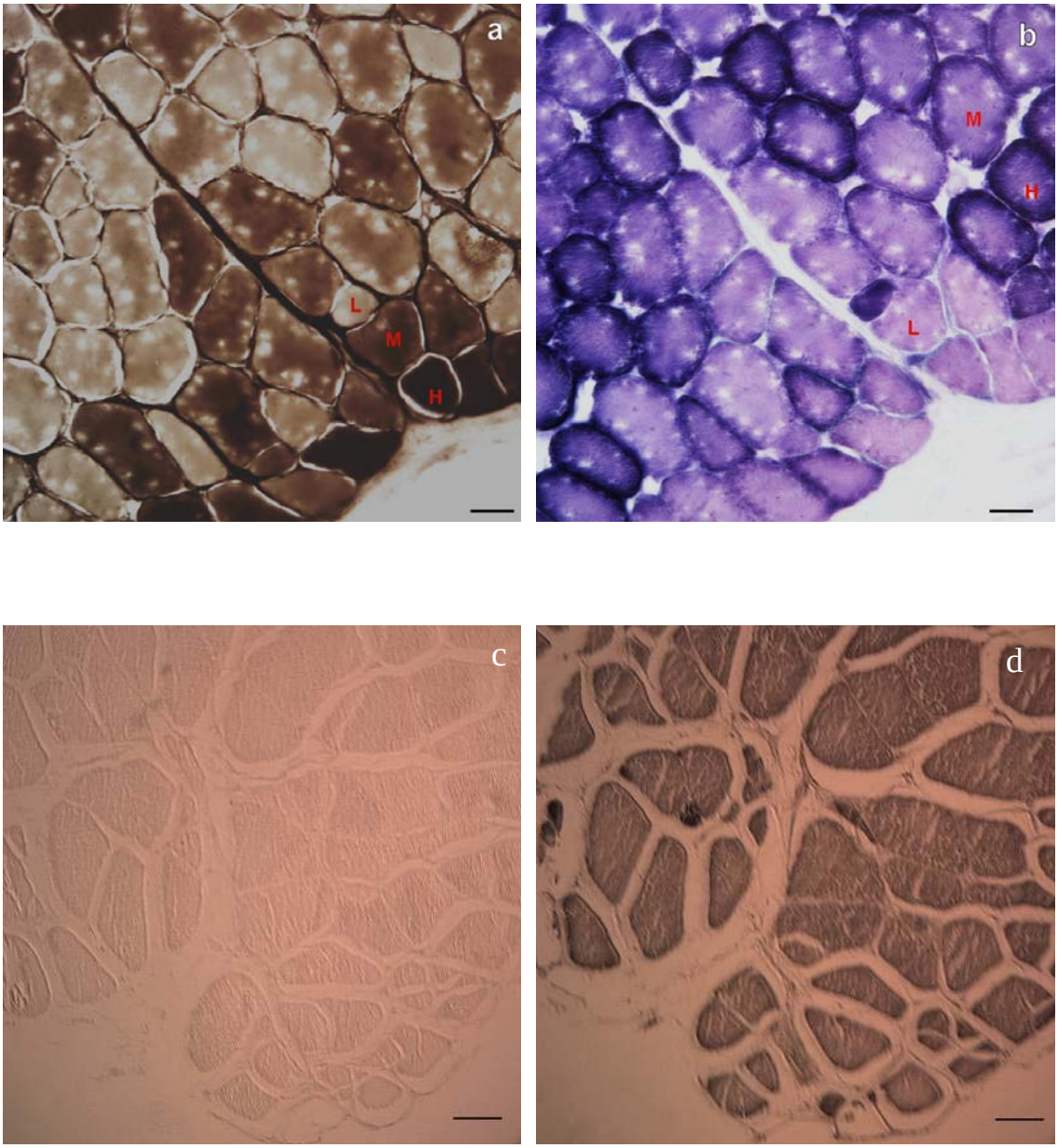

Fig. 8. An example of serial sections of 20-week-old BF muscle stained for slow myosin ATPase at pH 3.9 (**a**), and SDH (**b**); and 20-week-old ALD muscle reacted with (**c**) F59 MyHC antibody, and (**d**) S35 MyHC antibody. The figures (**a**) and (**b**) show different intensities of staining for slow myosin ATPase and SDH (L- low intensity, M- middle intensity, and H- high intensity staining). Images were captured at 20x magnification and the scale bars represent 50 microns.

All of the ALD fibers at 9 and 20 weeks of age exhibited positive staining for S35 MyHC. PLD muscle fibers showed a complete absence of S35 MyHC staining at 9 and 20 weeks of age. Half of BF muscle fibers exhibited positive staining for S35 MyHC at 9 weeks and 70% of BF muscle fibers exhibited positive staining for S35 MyHC at 20 weeks of age. At 9 and 20 weeks of age, over 90% of PM muscle fibers did not show any staining for S35 MyHC (Fig. 9). Opposite results were observed when sequential sections from ALD, PLD, PM, and BF muscle fibers were stained for F59 MyHC (Fig. 9).

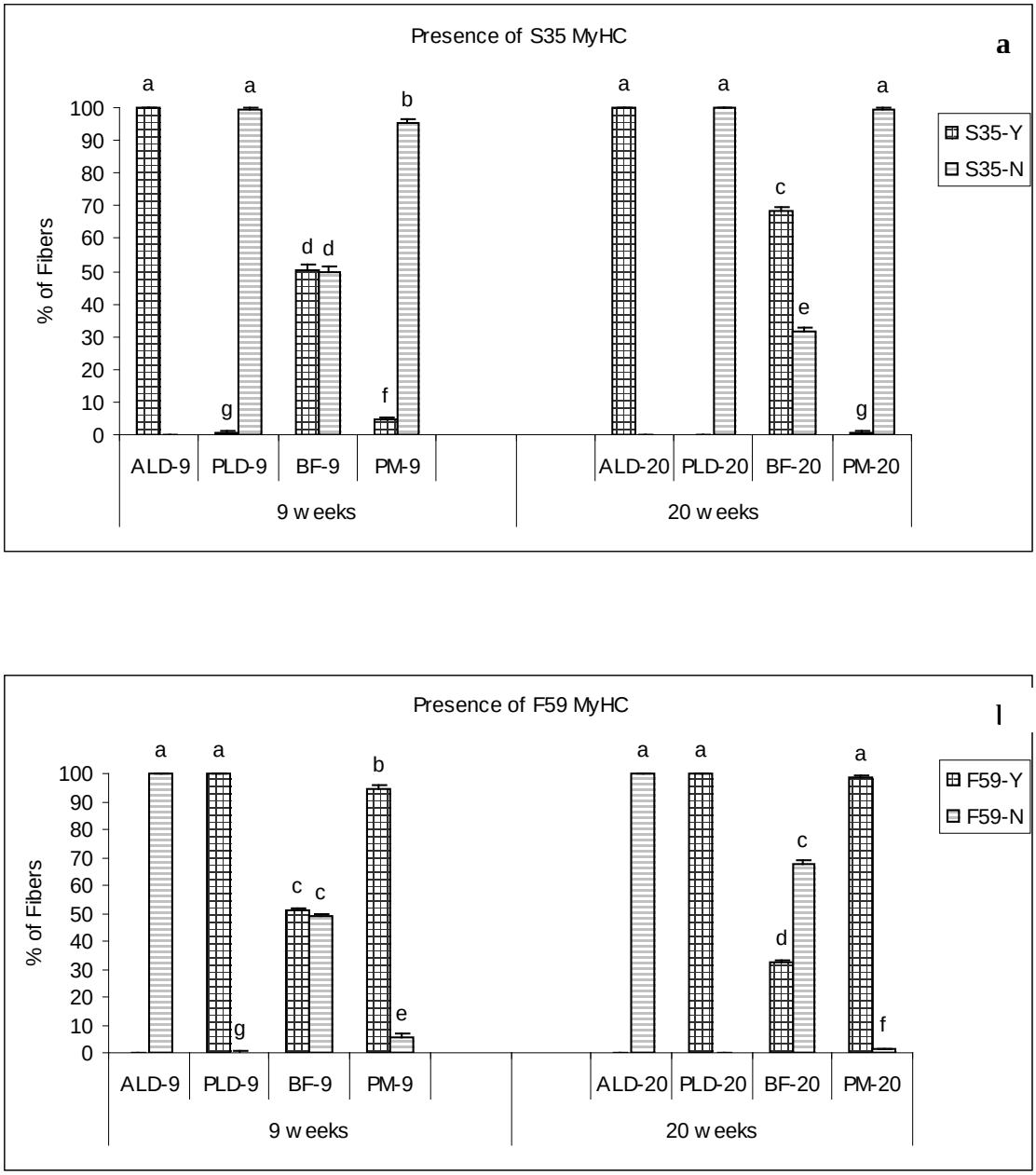

Fig. 9. Percentage of ALD, PLD, BF, and PM muscle fibers in 9 and 20-week old turkey toms with (S35-Y) or without (S35-N) pronounced staining for **a** S35 MyHC, **b** F59. The superscripts represent means that are significantly different. Error bars represent standard errors of individual means.

Correlation Analysis

Correlation analysis of mitochondrial CoQ10 content, SDH, and myosin ATPase activities revealed very strong relationship between these cellular components in 9 week-old muscles. Furthermore, strong but imperfect correlations among mitochondrial CoQ10 content, SDH, and myosin ATPase activities were observed in 20 week-old muscles (Table 1).

Discussion

Fiber Phenotype and Contractile Characteristics

Muscle fiber location, its function, and load greatly influence the metabolic and phenotypic profile of the muscle. The total number of muscle fibers, their spatial distribution, and biochemical function vary in different muscles. Understanding metabolic differences within specialized muscles presents a useful tool in deciphering mechanisms governing skeletal muscle development. The present study focused on simultaneously selected aspects of the phenotypic, and metabolic, characteristics of ALD, PLD, BF, and PM muscles. The main objective of the current work was to examine the potential relationship between muscle CoQ_{10} content, mitochondrial protein, and muscle fiber phenotype.

One of the aims of the study was to re-evaluate previously described fiber type composition in distinct muscles in adult turkey toms to further elucidate the relationship between fiber phenotype and its mitochondrial metabolism (Wiskus et al., 1976; Beermann et al., 1978; Green et al., 1982). Classic experiments assessing muscle fiber phenotype

demonstrated that there are three main types of muscle fibers in turkey muscles, which can be defined as αR (fast-oxidative), αW (fast-glycolytic), and βR (slow-oxidative). The muscle fiber characterization described in former studies was based on muscle differential response to ATPase and SDH staining (Wiskus et al., 1976). Previous data presented in Wiskus et al. (1976) has demonstrated that while pectoralis muscle is extremely scarce in βR fibers, previously considered as oxidative, biceps femoris muscle was composed of both oxidative and glycolytic fast-twitch fibers. Furthermore, Wiskus et al. (1976) demonstrated that fast-white and slow-red classification of muscle fibers may not be accurate and that certain muscles (such as biceps femoris) appear red due to high myoglobin content, but have enzymatic characteristics similar to fast muscles.

The fiber type of four muscle groups was re-evaluated and determined based on enzymatic staining for SDH and slow (acid-stable) myosin ATPase, followed by immunohistochemical labeling for slow and fast MyHC (Figs. 6-9). The data confirmed that ALD, PLD, PM, and BF muscles have different enzymatic and contractile characteristics. Concurring with Wiskus et al. (1976), the present study confirmed that despite its red appearance, BF muscle contains fibers of various metabolic profiles (Figs. 6-9). Additionally, ATPase and SDH staining profile in PM muscle was very similar to Wiskus et al. (1976) data (Table 1, Figs.6 and 7).

Staining for SDH revealed that at 9 weeks of age, approximately 60% of PM fibers contained medium activity of SDH; while at 20 weeks of age about 80% of PM fibers reveal low intensity SDH staining (Fig. 7). A similar staining pattern was observed in PLD muscle,

suggesting that there is an age-related decrease in oxidative capacity in both PM and PLD muscle groups.

Immunohistochemical analysis of S35 and F59 MyHC isoforms was utilized to further evaluate contractile profile of distinct muscles (Fig. 9). The MyHC isoforms are the main structural proteins involved in conversion of ATP to mechanical energy required for muscle contraction (Sun et al., 2003). In ALD muscles, all S35-positive fibers were negative for F59 antibody. The opposite staining pattern was observed in PLD and PM muscles, where all F59-positive fibers were negative for S35 antibody. The results demonstrated that slow myosin ATPase staining and S35 MyHC staining pattern is very similar in ALD, PLD, and PM muscles. In both age groups ALD muscles were predominantly slow, PLD muscles were predominantly fast, BF muscles contained both slow and fast fibers, and PM was primarily fast (Fig. 9). Although the BF muscle fibers were characterized by low, medium, and high intensity staining for slow myosin ATPase, the MyHC staining revealed equal amount of slow and fast MyHC in this muscle. The medium intensity staining for myosin ATPase in BF muscle could be related to the presence of S35 and F59 MyHC isoforms within individual muscle fibers (Rosser et al., 1996).

Fiber Phenotype and Energy Utilization

The capability of the muscle fibers to resist fatigue is determined by the presence and performance of mitochondria, which contain factors involved in oxidative phosporylation process (Holloszy and Coyle, 1984; Fitts, 1994). SDH is an important component of the mitochondrial TCA cycle, and strong staining for this enzyme identifies muscle fibers with

high oxidative potential. Total mitochondrial protein relative to myofibrillar protein significantly decreases between 9 and 20 weeks of age and does not differ between muscles at a given time (Fig 5). Oxidative ALD muscles contain twice as much mitochondria as the fast-twitch PLD muscles, but the ALD mitochondria are much smaller than the PLD mitochondria (Kiessling, 1976). Therefore, it is likely that total weight of mitochondrial protein in ALD and PLD muscles is not significantly different even though there is a difference in mitochondrial number. Nonetheless, data generated based on enzymatic staining for mitochondrial enzyme, SDH, shows significant difference in the activity of this enzyme between distinct muscles and between different age groups. Consequently, other mitochondrial factors in combination with SDH should be considered when quantifying tissue mitochondria. The activity of SDH increases with age in ALD and BF muscles and decreases with age in PM and PLD muscles. Therefore, it is possible that with increased size and higher functional demands, ALD and BF muscles have an increased requirement for oxidative phosphorylation (Handel and Stickland, 1986; Hoppeler and Fluck, 2003). Since PM and PLD muscles were already mostly relying on glycolytic metabolism for energy utilization, increased muscle size may have contributed to an increased demand for anaerobic respiration and decrease in mitochondrial function.

Fiber Phenotype and CoQ_{10} Content

CoQ_{10} represents one of the key components of mitochondrial oxidative metabolism, plays an indispensable role in ATP production in tissues with high energy requirements, and protects tissues from free radical damage (Crane, 2001; Dhanasekaran et al., 2008). Because

of CoQ_{10}'s role in oxidative phosphorylation and its cytoprotective properties, quantification of CoQ_{10} levels has important implications in identifying a metabolic state of the skeletal muscle HPLC-UV was utilized to determine levels of CoQ_{10} in whole muscle and in the mitochondrial fractions of four different muscle groups in 9- and 20-week-old male turkeys. The HPLC-UV analysis has revealed age-related differences in CoQ_{10} content where whole muscle homogenate CoQ_{10} content increased with age in ALD muscles and remained unchanged in PLD, BF and PM muscles (Fig. 2). Both ALD and BF muscles had significantly higher total levels of CoQ_{10} then PLD and PM muscles on week 9 and 20. Mitochondrial CoQ_{10} content in BF and ALD muscles increased with age and was significantly higher than in PLD and PM muscles. Additionally, mitochondrial CoQ_{10} content in PLD and PM muscle did not change with age (Fig 3). The differences between whole tissue homogenate and mitochondrial fraction CoQ_{10} content in distinct muscles may be related to metabolic requirements of each muscle. It appears that with increasing age mitochondrial oxidative phosphorylation process requires more CoQ_{10} in muscles that mostly rely on oxidative metabolism. Consequently, it can be concluded that older, oxidative muscles have higher energy requirements to support larger fiber size. Furthermore, higher energy requirements can be associated with increased free radical damage that has been observed in aging muscle (Lass and Sohal, 1998). Additionally, with age there is an increase in reactive oxygen species generation that corresponds to oxidative damage in mitochondria (Sohal et al., 1999). It is likely that muscle groups that rely on glycolytic metabolism possibly become more glycolytic with age; hence the lower amount of CoQ_{10} in mitochondrial fraction. Since CoQ_{10} has been shown to be a rate-limiting component of the

oxidative phosphorylation process, further depletion of CoQ_{10} may lead to reduced respiratory function of the muscle (Estronell et al., 1992; Kamzalov and Sohal, 2004).

Taken together, these results indicate the importance of CoQ_{10} in oxidative metabolism. Additionally, present study revealed strong correlation between mitochondrial CoQ_{10} content, SDH labeling, and slow ATPase labeling (Table 1). Since CoQ_{10} levels vary in different muscles and its levels are proportional to slow ATPase activity and mitochondrial SDH levels, it is reasonable to hypothesize that cellular levels of CoQ_{10} may present a potential marker of slow-oxidative skeletal muscle phenotype.

It appears that mitochondrial: total muscle CoQ_{10} ratio significantly decreases in PM and PLD muscles, remains the same in ALD muscle, and significantly increases in BF muscle between week 9 and 20 of age. Studies have demonstrated that aside from mitochondria, CoQ_{10} is located in Golgi apparatus and in lysosomes (Nyquist et al., 1970; Sun et al., 1992; Gille and Nohl, 2000). Although, mitochondria are the major sites of CoQ_{10} action, it has been recently shown that CoQ_{10} also participates in lysosomal redox chain (Gille and Nohl, 2000). Therefore, it is likely that this coenzyme exists in higher concentrations in other cellular membranes in older PLD and PM muscles (Nyquist et al., 1970; Sun et al., 1992; Gille and Nohl, 2000). Additional research needs to be performed to identify cellular pathways involving CoQ_{10} and its age-related role in the muscle.

In conclusion, the present study revealed that there is a relationship between mitochondrial and whole muscle CoQ_{10} content and muscle phenotype. Furthermore, strong correlations between mitochondrial CoQ_{10} content, SDH activity, and slow ATPase labeling in 9 week-old turkeys, and slightly weaker correlations between these metabolic components

in 20 week-old turkeys indicate increased phenotypic variation in maturing muscle fibers. These results suggest that age-related change in functional demands may have an effect on muscle phenotype.

Additionally, current experiments indicated a strong relationship between the amount of mitochondrial protein and age of the muscle. The results of this study suggest that distinct skeletal muscles are metabolically different and that there are age-related differences in internal metabolism within the same muscles.

Enzymatic staining and immunohistochemical analysis for MyHC isoforms are useful tools in fiber type characterization. However, there are many other molecular pathways involved in regulating skeletal muscle fiber phenotype. More detailed evaluation of factors participating in muscle metabolism is required for adequate identification of specific fiber phenotype. Based on the results of the present study, it can be hypothesized that CoQ_{10} may play a significant role in fiber type determination. More extensive research focusing on the impact of CoQ_{10} on signaling molecules and on genes responsible for contractile and metabolic properties of the muscle will be necessary to further define the effect of CoQ_{10} on muscle fiber phenotype.

Acknowledgements

The authors express their appreciation to Goldsboro Milling Company, Goldsboro, NC for the animals employed in this study.

Support provided in part by funds under project number NC06590 (PEM) of North Carolina State University. Supported in part by National Research Initiative. This project

was supported by National Research Initiative Competitive Grant no. 2005-35206-15241 (PEM) from the USDA Cooperative State Research, Education, and Extension Service.

The S35 and F59 hybridoma cells (developed by F. E. Stockdale) were obtained from the Developmental Studies Hybridoma Bank developed under the auspices of the NICHD and maintained by The University of Iowa, Department of Biological Sciences, Iowa City, IA 52242. Support also provided in part by the North Carolina Agricultural Foundation.

References

Aberle, E.D., P.B. Addis, R.N. Shoffner (1979) Fiber types in skeletal muscles of broiler and layer-type chickens. Poult. Sci. 58: 1210-1212

Anapol, F., S.W. Herring (2000) Ontogeny of histochemical fiber types and muscle function in the masseter muscle of miniature swine. Am J Physic Anthropol *112*: 595-613

Anthony, N.B., D.A. Emmerson, K.E. Nestor, W.L. Bacon (1990) Comparison of growth curves of weight selected populations of turkeys, quail, and chickens. Poult Sci *70*:13-19

Beermann, D.H., R.G. Cassens, G.J. Husman (1978) A second look at fiber type differentiation in porcine skeletal muscle. J Anim Sci *46*: 125-132

Bhattacharya, S.K., J.H. Thakar, P.L. Johnson, D.R. Shanklin (1991) Isolation of skeletal muscle mitochondria from hamsters using an ionic medium containing Ethylenediarninetetraacetic acid and Nagarse. Anal Biochem *192*:344-349

Bradford, M.M. (1976) A rapid and sensitive method for the quantification of microgram quantities of protein utilizing the principle of protein-dye binding. Anal Biochem *72*: 248-254

Bliznakov, E.G., H.N. Bhagavan (2003) Deficient energy metabolism and disease: role of coenzyme Q_{10}. FASEB *17*: A1114

Carson, S., D. Robertson (2006) Expression of fusion protein from positive clones and sodium dodecyl sulfate-polyacrylamide gel electrophoresis (SDS-PAGE) and immunological analysis (Western Blot): Manipulation and expression of recombinant DNA; in Elsevier Academic Press, Burlington, MA, pp 19-102

Crane, F.L. (2001) Biochemical functions of coenzyme Q_{10}. J Am Coll Nutr *20*: 591-598

Dhanasekaran, M., S.S. Karuppagounder, S. Uthayathas, L.E. Wold, K. Parameshwaran, R.J. Babu, V. Suppiramaniam, H. Brown-Borg (2008) Effect of dopaminergic neurotoxin MPTP/MPP+ on coenzyme Q content. Life Sci *83*: 92-95

Estronell, E., R. Fato, C. Castelluccio, M. Cavazzoni, C.G. Castelli, G. Lenaz (1992) Saturation kinetics of coenzyme Q in NADH and succinate oxidation in beef heart mitochondria. FEBS Lett *311* :107-109

Fitts, R.H. (1994) Cellular mechanisms of muscle fatigue. Physiol Rev *74*: 49-94

Frei, B., M.C. Kim, B.N. Ames (1990) Ubiquinol-10 is an effective lipid-soluble

antioxidant and physiological concentrations. Proc Natl Acad Sci *87*:4879-4883

Garry, D.J., R.S. Bassel-Duby, J.A. Richardson, J. Grayson, P.D. Neufer, R.S. Williams (1996) Postnatal development and plasticity of specialized muscle fiber characteristics in the hindlimb. Dev Gen *19*: 146-156

Gibson, M.C., E. Schultz (1982) The distribution of satellite cells and their relationship to specific fiber types in soleus and extensor digitorum longus muscles. Gen Hist Cyt *202*: 329-337

Gille, L., H. Nohl (2000) The existence of lysosomal redox chain and the role of ubiquinone. Arch Biochem Biophys *375*: 347-354

Green, H.J., H. Reichmann, D. Pette (1982) A comparison of 2 ATPase based schemes for histochemical muscle-fiber typing in various mammals. Histochem *76*:21-31

Handel, S.E., N.C. Stickland (1986) The growth and differentiation of porcine skeletal muscle fibre types and the influence of birth weight. J Anat *152*: 107-119

Holloszy, J.O., E.F. Coyle (1984) Adaptations of skeletal muscle to endurance exercise and their metabolic consequences. J Appl Physiol *56*:831-838

Hoppeler, H., M. Fluck (2003) Plasticity of skeletal muscle mitochondria: Structure

and function. Med Sci Sport Exer *35*: 95-104

Kamzalov, S., R.S. Sohal (2004) Effect of age and caloric restriction on coenzyme Q and α-tocopherol levels in the rat. Experiment Gerantol *39*: 1199-1205

Kamzalov, S., N. Sumien, M.J., R.S. Sohal (2003) Coenzyme Q intake elevates the mitochondrial and tissue levels of coenzyme Q and α-tocopherol in young mice. J Nutr *133*: 3175-3180

Kasper, C.E., A.L. McNulty, A.J. Otto, D.P. Thomas (1993) Alterations in skeletal muscle related to impaired physical mobility: An empirical model. Res Nurs Health *16*: 265-273

Kiessling, K. H. (1976) Metabolism of avian twitch and tonus muscle. Comp Biochem Physiol A *54*:413-417

Lass, A., R.S. Sohal (1998) Electron transport-linked ubiquinone-dependent recycling of alpha-tocopherol inhibits autooxidation of mitochondrial membranes. Arch Biochem Biophys *352*: 229-236

Morrish, F., N.E. Buroker, M. Ge, X.-H. Ning, J. Lopez-Guisa, D. Hockenbery, M.A.

Portman (2006) Thyroid hormone receptor isoforms localize to cardiac mitochondrial matrix with potential for binding to receptor elements on mtDNA. Mitoch *6*: 143-148

Miller, J.B., E.A. Everitt, T.H. Smith, N.E. Block, J.A. Dominov (1993) Cellular and molecular diversity in skeletal muscle development: news from in vitro and in vivo. Bioassays *15*: 191-196

Moss, F.P., C.P. Leblond (1971) Satellite cells as the source of nuclei in muscle of growing rats. Anat Rec *170*: 421-436

Mozdziak, P.E., E. Schultz, R.G. Cassens (1994) Satellite cell mitotic activity in post hatch turkey skeletal muscle growth. Poult Sci *73*:547-555

Mozdziak, P.E., M.L. Greaser, E. Schultz (1998) Myogenin, MyoD, and myosin expression after pharmacologically and surgically induced hypertrophy. J Appl Physiol *84*: 1359-1364

Nyquist, S.E., R. Barr, D. J. Morre (1970) Ubiquinone from rat liver Golgi apparatus fractions. Biochem et Biophys Acta *208*: 532-534

Page, S., J.B. Miller, J.X. DiMario, E.J. Hager, A. Moser, F.E. Stockdale (1992)

Developmentally regulated expression of three slow isoforms of myosin heavy chain: Diversity among the first fibers to form avian muscle. Develop Biol *154*: 118-128

Pastore, A., G. Di Giovamberardino, E. Bertini, G. Tozzi, L. M. Gaeta, G. Federici, F. Piemonte (2005) Simultaneous determination of ubiquinol and ubiquinone in s keletal muscle of pediatric patients. Anal Biochem *342*: 352-355

Pette, D., R.S. Staron (1997) Mammalian skeletal muscle fiber type transitions. Int Rev Cytol *170*:143-223.

Reiser, P.J., R.L. Moss, G.G. Giulian, M.L. Greaser (1985) Shortening velocity in single fibers from adult rabbit soleus muscles is correlted with myosin heavy chain composition. J Biol Chem *260*:9077-9080

Rosser, B.W.C., M. Wick, D. M. Waldbillig, E. Bandman (1996) Heterogeneity of myosin heavy-chain expression in fast twitch fiber types of mature avian pectoralis muscle. Biochem Cell Biol *74*: 715-728

SAS Institute 1985. User's guide: Statistics. Version 5 ed. SAS Institute Inc., Cary, NC.

Schiaffino, S., C. Reggiani (1996) Molecular diversity of Myofibrillar proteins: Gene regulation and functional significance. Physiol Rev *76*: 371-423

Smith, D.P., D.L. Fletcher (1988) Chicken breast muscle fiber type and diameter as influenced by age and intramuscular location. Poult. Sci. 67: 908-913

Sohal, R.S., A. Lass, L. J. Yan, L.K. Kwong (1999) Mitochondrial generation of reactive oxygen species and oxidative damage during aging:roles of coenzyme Q and tocopherol: . Understanding the Process of Aging; in Cadenas, E., L. Packer (eds.) Marcell Dekker, New York, NY, pp 119-142

Sun, Y.M., N. Da Costa, K.C. Chang (2003) Cluster characterization and temporal expression of porcine sarcomeric myosin heavy chain genes. J Muscle Res Cell Motil *24*: 591-570

Sun, I.L., E.E. Sun, F.L. Crane, D.J. Morré, A. Lindgren, H. Löw (1992) A requirement for coenzyme Q in plasma membrane electron transport. Proc Nat Acad Sci US *89*: 11126-11130

Swatland, H. J., R. G. Cassens (1973) Prenatal development, histochemistry and innervation of porcine muscle. J Anim Sci *36*: 343-354

Williams, R.S., P.D. Neufer (1996) Regulation of gene expression in skeletal muscle by

contractile activity:. The Handbook of Physiology: Integration of Motor, Circulatory, Respiratory and Metabolic Control During Exercise; in Rowell L.B., J.T. Shepard (eds.) American Physiology Society, Betheseda, MD, pp. 1124-1150

Wiskus, K.J., P.B. Addis, R.T-I. Ma (1976) Distribution of βR, αR and αW fibers in turkey muscles. Poult Sci *55*: 562-572

Zor, T., Z. Selinger (1996) Linearization of the Bradford protein assay increases its sensitivity: theoretical and experimental studies. Anal Biochem *226*: 302-308

Chapter 4

$MitoQ_{10}$ Influences Expression of Genes Involved in Adipogenesis and Oxidative Metabolism in Myotube Cultures

Abstract

Background. Coenzyme Q_{10} (CoQ_{10}) plays an essential role in determination of mitochondrial membrane potential and substrate utilization in all metabolically important tissues. The objective of the present study was to investigate the effect of Coenzyme Q analog ($MitoQ_{10}$) on oxidative phenotype and adipogenesis in myotubes derived from two phenotypically distinct skeletal muscles.

Methods. The myotubes were derived from 15-week-old turkeys. Fast-glycolytic Pectoralis major (PM) and slow-oxidative Anterior latissimus dorsi (ALD) myotubes were subjected to the following treatments: Fusion media alone, Fusion media+125nM $MitoQ_{10}$, and 500nM $MitoQ_{10}$. Lipid accumulation was visualized by Oil Red O staining and quantified by measuring optical density of extracted lipid at 500nm at 1, 3, and 5 days post-treatment. Quantitative Real Time PCR was utilized to quantify the expression levels of Peroxisome proliferator-activated receptor (PPARγ) and PPARγ co-activator-1α (PGC-1α).

Results. $MitoQ_{10}$ treatment resulted in the highest ($P<0.05$) lipid accumulation in PM myotubes. $MitoQ_{10}$ up-regulated genes controlling oxidative mitochondrial biogenesis and adipogenesis in PM myotube cultures. In contrast, $MitoQ_{10}$ had a limited effect on adipogenesis and down-regulated oxidative metabolism in ALD myotube cultures.

Conclusions. The PM and ALD myotubes responded differently to $MitoQ_{10}$ treatment. Differential response to $MitoQ_{10}$ treatment may be dependent on the cellular redox state.

General Significance. $MitoQ_{10}$ likely controls a range of metabolic pathways through its differential regulation of gene expression levels in myotubes derived from fast-glycolytic and

slow-oxidative muscles. Administration of $MitQ_{10}$ and its regulation of cellular redox state may be beneficial in treatment of disorders related to altered metabolic state.

Key Words: $MitoQ_{10}$, PGC-1α, PPARγ, Adipocytes, Skeletal Muscle, Avian

1. Introduction

Skeletal muscle is a diverse tissue characterized by the ability to alter its metabolic and structural properties in response to various functional demands [1, 2]. In addition, skeletal muscle considerably contributes to whole body homeostasis mainly by its regulation of glucose and fatty acid metabolism [3, 4]. Post-hatch or post-natal muscle regeneration and development of new muscle fibers is dependent on activation of muscle satellite cells located between the sarcolemma and basal lamina of the muscle fiber [5]. Satellite cells have been identified as unique multipotential stem cells that under appropriate conditions are able to differentiate into not only myotubes, but also osteocytes, chondrocytes, and adipocytes; but the primary fate of satellite cells in culture appears to be myotubes [6, 7, 8]. Satellite cell differentiation into a particular muscle phenotype or cell type is highly dependent on expression of genes coding for specific transcription factors. The determination of skeletal muscle phenotype is a complicated process that involves integration of a number of transcriptional factors, signaling pathways, and extracellular factors [9]. The current study focuses on two transcription factors, PPARγ and PGC-1α, which play important roles in determination of satellite cell fate [10].

Peroxisome proliferator-activated receptor (PPARγ) and PPARγ co-activator-1α (PGC-1α) are involved in biological processes responsible for energy homeostasis and tissue metabolism [11]. PPARγ is a nuclear hormone receptor necessary for induction of white adipocyte formation [12, 13, 14, 15]. Ectopic expression of PPARγ induces formation of white adipocytes in myotube cultures after addition of PPARγ ligand to the media [10]. Skeletal muscle cells are localized in close proximity with adipocytes *in vivo* [16, 17]. The

lipids accumulate in intramyocellular and intermuscular spaces. The degree of lipid accumulation in skeletal muscle is dependent on muscle fiber type and muscle-related insulin resistance [16, 17]. PGC-1α is highly expressed in tissues involved in thermogenesis, such as brown fat and oxidative skeletal muscle [18, 19]. Because no brown fat has been detected in avian species [20], the analysis of PGC-1α in turkey cultures likely relates only to oxidative muscle phenotype. PGC-1α is a powerful transcriptional activator that interacts with a number of nuclear hormone receptors, including PPARs, and plays an extensive role in regulation of cellular respiration, and mitochondrial biogenesis [21, 22].

Coenzyme Q_{10} (CoQ_{10}), commonly referred to as ubiquinone (2, 3-dimethoxy-5-methyl-6-multiprenyl-1, 4-benzoquinone), exists in three alternating states in the mitochondrial membrane: the fully oxidized form: ubiquinone (Q_{10}), the partially reduced form: ubisemiquinone ($Q_{10}H.$), and the fully reduced form: ubiquinol ($Q_{10}H_2$) [23]. CoQ_{10} accepts electrons from reducing equivalents produced from glycolysis and fatty acid degradation and delivers them to electron acceptors that participate in mitochondrial electron transport chain [24, 25, 26].

Because of its redox active nucleus and hydrophobic side chain, CoQ_{10} has been proposed to be an ideal candidate for neutralizing free radicals in mitochondrial phospolipid membrane and has been widely utilized as a treatment for a variety of physiological conditions [27]. Among other disorders, CoQ_{10} has been used to treat muscular dystrophy, congestive heart failure, and chronic fatigue syndrome [28, 29, 30]. Although CoQ_{10} has wide therapeutic applications, the hydrophobicity of CoQ_{10} makes it difficult to be completely absorbed by cells, limiting CoQ_{10} from fully performing its function [31]. CoQ

analogs attached to triphenylphosphohium (TPMP) cation through an alkyl linker, easily travelacross the cell membrane and to the mitochondria through non carrier-mediated process [32]. TPMP attached to a quinone will be referred to as $MitoQ_{10}$. Smith et al. (2003) [32] utilized in vivo application of $MitoQ_{10}$, where mice were orally provided with liquid diet containing $MitoQ_{10}$. Lipophilic $MitoQ_{10}$ has been shown to be accumulated 5- to 10-fold into the cytosol and 100- to 500-fold into the mitochondrial matrix in heart, brain, liver, and skeletal muscle of the treated mice. Positive charge on TPMP allows for $MitoQ_{10}$ delivery into the mitochondrial matrix to be driven by mitochondrial membrane potential.

The objective of this study was to assess the influence of $MitoQ_{10}$ supplementation to turkey myotube culture on oxidative phenotype and lipid accumulation.

2. Materials and Methods

2.1 Culture Establishment

The myotubes were derived from 15-weeks-old T24 Nicholas turkey Pectoralis major (PM) and Anterior latissimus dorsi (ALD) muscles using procedures described by McFarland et al. (1988) [33]. Frozen aliquots of cell suspension (passage 2) were thawed, and plated in T75 flasks and 35 mm 6-well culture plates coated with 0.1% gelatin (Sigma, Saint Louis MO; porcine skin 300 bloom; Cat# G-1890) at plating density of 30,000 cells per 35 mm dish and 200,000 cells per T75 flask. The plating media was composed of 84% Dulbecco's Modified Eagle's Medium (DMEM) (Sigma, Saint Louis MO; Cat# D5523), 10% Chicken Serum (CS) (Sigma, Saint Louis MO; Lot# 098K0407), 5% Horse Serum (HS) (Atlanta Biologicals, Atlanta GA; Lot# 50116), 1% Antibiotic/Antimycotic (Ab/Am) (Sigma, Saint

Louis MO; Lot# 50116), and 0.1% Gentamicin (Atlanta Biologicals, Atlanta GA; Cat# B20292). Cells were incubated at 38.5°C in a humidified 5% CO_2 incubator. After 24 hrs of attachment, the plating media was removed and cells were provided with feeding media containing 84% McCoy's 5A Medium (Sigma, Saint Louis MO; Cat# M4892), 10% CS, 5% HS, 1% Ab/Am, and 0.1% Gentamicin.

2.2 MitoQ$_{10}$ Dose Response Test

ALD and PM cells were grown to 70% confluency in feeding media (described above) in 35 mm 6-well culture plates. To assess the cell dose response to decyl-TPMP and MitoQ$_{10}$ cells were treated with 125nM, 500nM, 1μM, 2μM, and 3μM of each reagent (4 wells per treatment). After 48 hours post decyl-TPMP and MitoQ$_{10}$ treatment, cells were treated with 0.45 mL of Trypan Blue for 5 minutes at 20℃ [34]. The response to decyl-TPMP and MitoQ$_{10}$ was estimated by counting Trypan Blue-stained dead cells. The concentrations of MitoQ$_{10}$ that resulted in less than 10% cell mortality were utilized in experimental treatments.

2.3 Myotube Culture and MitoQ$_{10}$ Treatment

Cells plated in 35 mm 6-well culture plates (designated for Oil Redo O staining- 4 wells per treatment) and T75 flasks (designated for RNA isolation-3 flasks per treatment) were grown to 70% confluency under growing conditions described above. The feeding media was removed and cells were subjected to the following treatments:

1. Control treatment: fusion media alone (FM) containing DMEM, 3% HS, 1mg/mL Bovine Serum Albumin (BSA) (Sigma, Saint Louis MO; Cat# A6918), and 0.01mg/mL gelatin.
2. FM+500nM decyl-TPMP
3. FM+125nM $MitoQ_{10}$
4. FM+500nM $MitoQ_{10}$

Fresh media (treatment 1-4) were administered daily and Oil Red O and Real Time PCR data (described below) was collected on day 1, 3, and 5 post treatment.

2.4 Oil Red O Staining

Cells subjected to the above treatments were stained with Oil Red O according to modified procedure of Janderová et al. (2003) [35]. In brief, media was removed and cells were washed in 5% formalin solution in distilled water for five minutes at 21ºC. Subsequently, the formalin was removed and cells were fixed in fresh 5% formalin for one hour at 21ºC. Cells were then washed in 60% isopropanol, dried, and stained with Oil Red O working solution containing six parts of Oil Red O stock solution (0.7g Oil Red O (Sigma, Saint Louis, MO) and 200ml isopropanol) and four parts of distilled water for 10 minutes followed by repeated washes.

A Leica DMR inverted light microscope (Leica Microsystems, Bannockburn IL, USA) was utilized to observe Oil Red O-stained cells. The images of each treatment were captured using a Retiga 4000R fast camera (Q Imaging, Surrey BC, Canada) and Spot software (Sterling Heights, MI).

After image acquisition, Oil Red O was eluted by incubation in 3.6 ml/well of 100% isopropanol for 15 minutes at 21ºC. The Optical Density (OD) was measured at 500 nm with a Nanodrop spectrophotometer (NanoDrop Technologies, Wilmington, DE) using the UV-Vis function. Each sample OD was measured three times.

2.5 RNA isolation

Cells designated for RNA isolation were grown in T75 flasks (3 flasks per treatment) and treated in the same fashion as the cells grown in 6-well plates. The RNA was isolated by modified guanidinium thiocyanate-phenol-chloroform extraction method [36]. Three RNA isolations were performed per treatment. In this procedure, 7 ml of Trizol reagent (Invitrogen, Carlsbad, CA) were applied directly into T75 flasks. Cells were incubated in Trizol reagent for 10 minutes to allow for complete dissociation of nucleoprotein complexes and then moved to a 15ml centrifuge tube. The RNA was isolated from DNA and proteins by addition of 1.4 ml chloroform and centrifugation at 12,000 *g*. The upper phase containing RNA was removed and the RNA was precipitated by addition of 3.5 ml of isopropyl alcohol followed by centrifugation at 12,000 *g*. The RNA pellet was washed with 75% Ethyl alcohol, centrifuged at 7,500 *g*, and resuspended in diethylpyrocarbonate-treated water. The purity and quality of the RNA samples was evaluated by agarose gel electrophoresis. Furthermore, the quality and concentration of the isolated RNA was determined by measuring absorbance at 260 nm with a Nanodrop spectrophotometer (NanoDrop Technologies, Wilmington, DE). Samples with A260:280>1.8 were considered suitable for generating cDNA.

2.6 Quantitative Real-Time PCR

The quantitative Real-Time PCR analysis was performed to analyze gene expression levels of PPARG-γ and PGC-1α in ALD and PM myotubes after 3 days of $MitoQ_{10}$ treatment.

The reverse transcription reaction to generate cDNA was executed with a High Capacity cDNA Reverse Transcription Kit (Applied Biosystems Inc., Foster City, CA) in a 20μL volume containing 1μg of total RNA. Following the reverse transcription reaction, the cDNA samples were diluted 1:20 and analyzed by quantitative real-time PCR (qPCR) with a Bio-Rad iQ thermocycler. Each qPCR reaction contained 1 μL diluted cDNA, 1 μL primer, 10 μL Power SYBR Green PCR Master Mix (Applied Biosystems Inc., Foster City, CA), and 8 μL of diethylpyrocarbonate (DEPC)- treated water. PPARG-γ, PGC-1α, and β-actin primers (Table1) were designed according to gene sequences available through National Center for Biotechnology information (www.ncbi.nlm.nih.gov).

The qPCR reaction was executed at the following thermocycler temperature settings: 95°C for 5 min; 40 cycles of 95 °C for 30s, and primer-specific annealing temperature for 30s (Table 1), 72°C for 30s, 72°C for 5 minutes. The cDNA samples were amplified in triplicate and each gene was amplified in a separate, single thermocycler run. The efficiency of PCR reaction was established based on standard curves generated for each gene. Standards were generated by diluting pooled cDNA at 1:5, 1:25, 1:125, and 1:625. The cycle threshold (Ct) values were determined based on the cycle at which the gene amplification was the highest and the relative fluorescence was measured at each extension step (72°C). PPARG-γ, PGC-

1α gene expression was normalized against the β-actin housekeeper gene (Table 1). The fold change in gene expression level between samples was calculated using Pfaffl (2001) [37] method.

Table 1. Sequences of primers utilized in Real Time PCR amplification of genes expressed in cells derived from monolayer cultures.

Gene	Primer sequences (5'-3')	T_m [2] (ºC)	Product size (bp)
β-actin	Forward GTCCACCTTCCAGCAGATGT Reverse ATAAAGCCATGCCAATCTCG	55	129
PPARG-γ	Forward GGGCGAATGCCACAAGCGGA Reverse TGGCAAGCGCTCGCAGATC	60	100
PGC-1α	Forward AAACGGCCCAGTTTGCGGCT Reverse TGACACTGCCACCCAGGTGAA	60	146

2.7 Statistical Analysis

The statistical analysis of $MitoQ_{10}$ dose response, Oil Red O incorporation, and real time PCR data, was performed using JMP software (SAS Institute Inc., Cary, NC). A one-way analysis of variance was utilized for each of the above mentioned data sets. A one-way analysis of variance for sample gene Ct: sample housekeeper gene Ct derived from real time PCR analysis was quantified according to the following model:

$$Y = \mu+A+M+AM+e,$$

with age (A), muscle (M), and age x muscle (AM) as fixed effects.

Data were considered as significant at $P<0.05$ and fold change in expression >1.5.

The correlation analysis was performed to evaluate the relationship between PPARγ expression levels and lipid accumulation in PM and ALD myotube cultures.

3. Results

3.1 MitoQ$_{10}$ Dose Response Test

The dose response test revealed that 1 μM, 2 μM, and 3μM MitoQ$_{10}$ treatment resulted in significantly higher ($P<0.05$) cell mortality than 125nM, 500nM, and decyl-TPMP treatment after 48 hrs of MitoQ$_{10}$ treatment (Table 2). Consequently, 125nM and 500nM of MitoQ$_{10}$ were chosen to evaluate the effect of MitoQ$_{10}$ on myotube cultures.

Table 2. Results of dose response test representing % of dead cells in each treatment ± standard error of the mean. Mean values with different superscripts are significantly different ($P<0.0001$).

Treatment	**% Dead Cells**
3 μM MitoQ$_{10}$	89.75±5.02^{a}
2 μM MitoQ$_{10}$	80.00±4.80^{a}
1 μM MitoQ$_{10}$	79.25±4.85^{a}
500 nM MitoQ$_{10}$	10.00±1.29^{b}
125 nM MitoQ$_{10}$	9.75±1.20^{b}
Decyl-TPMP	8.95±0.21^{b}

3.2 Lipid Accumulation and MitoQ$_{10}$ Treatment

MitoQ$_{10}$ treatment resulted in lipid accumulation in forming myotubes. However, treatment with decyl-TPMP alone resulted in no lipid accumulation (data not shown). Sequential image acquisition revealed that accumulated lipid was most likely intratubal (Fig1) [38].

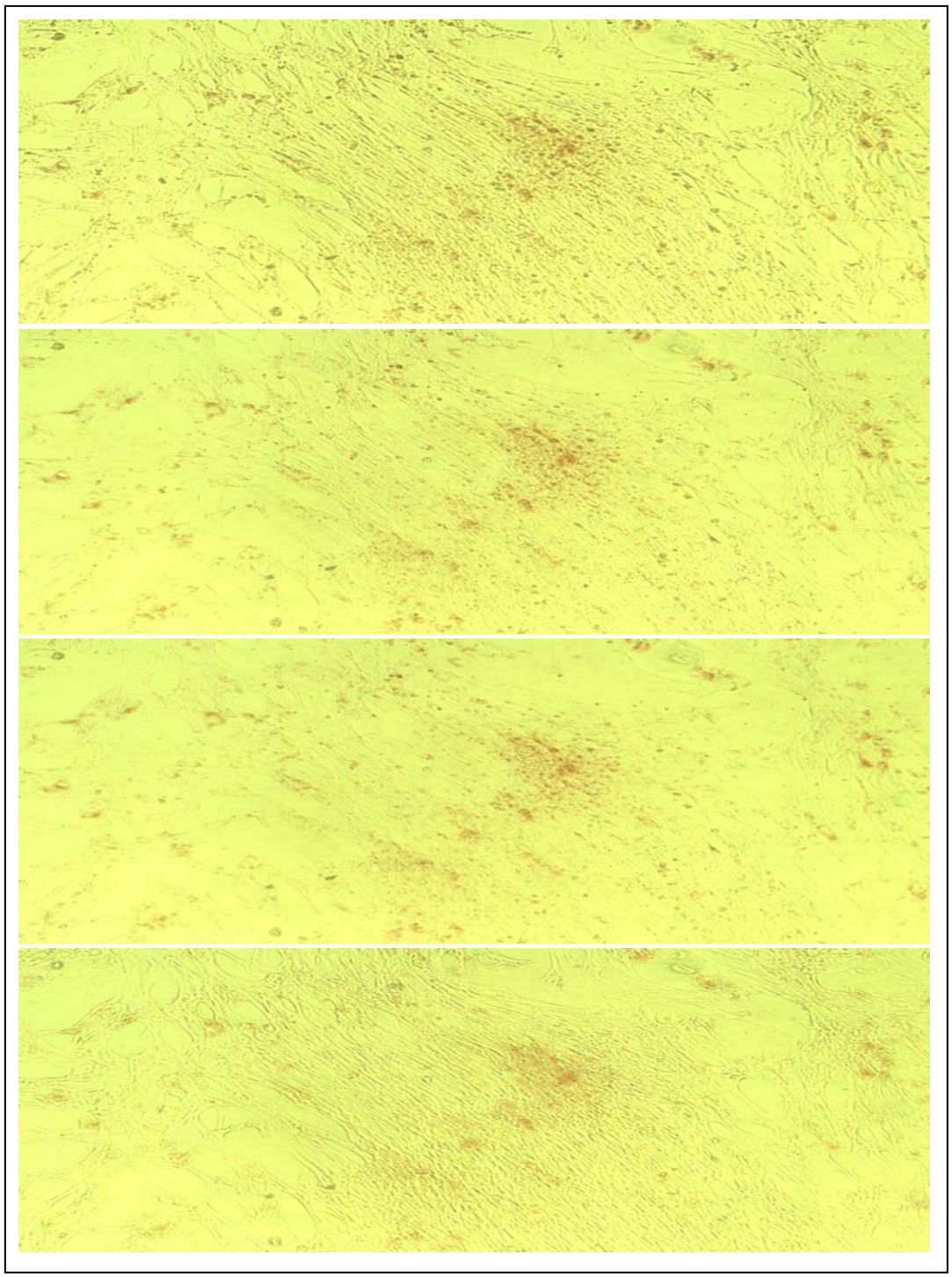

Fig 1. Sequential images representing intracellular lipid localization in myotube cultures. Images were taken at 20x magnification in four different planes of focus.

Optical density analysis of Oil Red O-stained myotubes revealed that increased concentrations of $MitoQ_{10}$ stimulated significant increase ($P<0.05$) in lipid accumulation in PM muscle culture on days 3 and 5 of treatment (Figs. 2 and 3). The lipid accumulation was the highest in PM myotube cultures treated with 500nM $MitoQ_{10}$ on day 3 and 5 of treatment, and the lowest in myotubes that were grown in Fusion Media (FM) alone. The differences in lipid accumulation were less discernable in ALD myotubes subjected to different $MitoQ_{10}$ concentrations on all treatment days, and in PM muscle on day 1 of $MitoQ_{10}$ treatment (Figs 2 and 3).

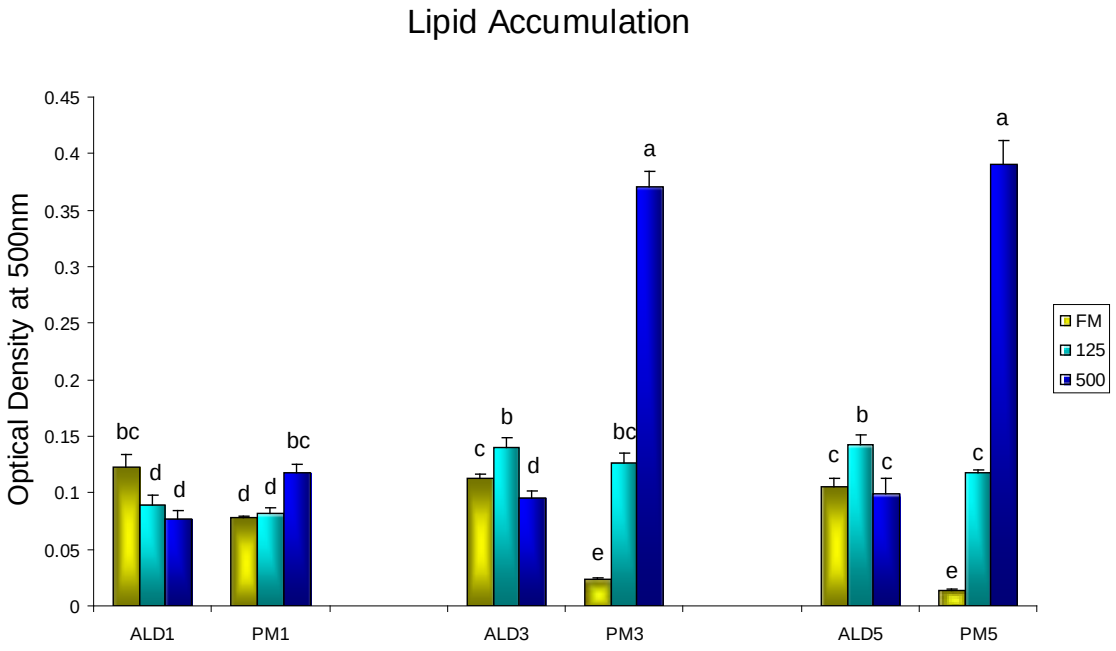

Fig 2. Lipid accumulation quantified by determining the optical density at 500nm of the Oil Red O-stained ALD and PM myotube cultures treated with feeding media alone (FM), FM+125nM MitoQ$_{10}$ (125), and FM+500nM MitoQ$_{10}$ (500). Data were acquired on day 1 (ALD1, PM1), day 3 (ALD3, PM3), and day 5 (ALD5, PM5) of treatment. Subscripts represented by different letters illustrate significantly different mean values ($P<0.05$).

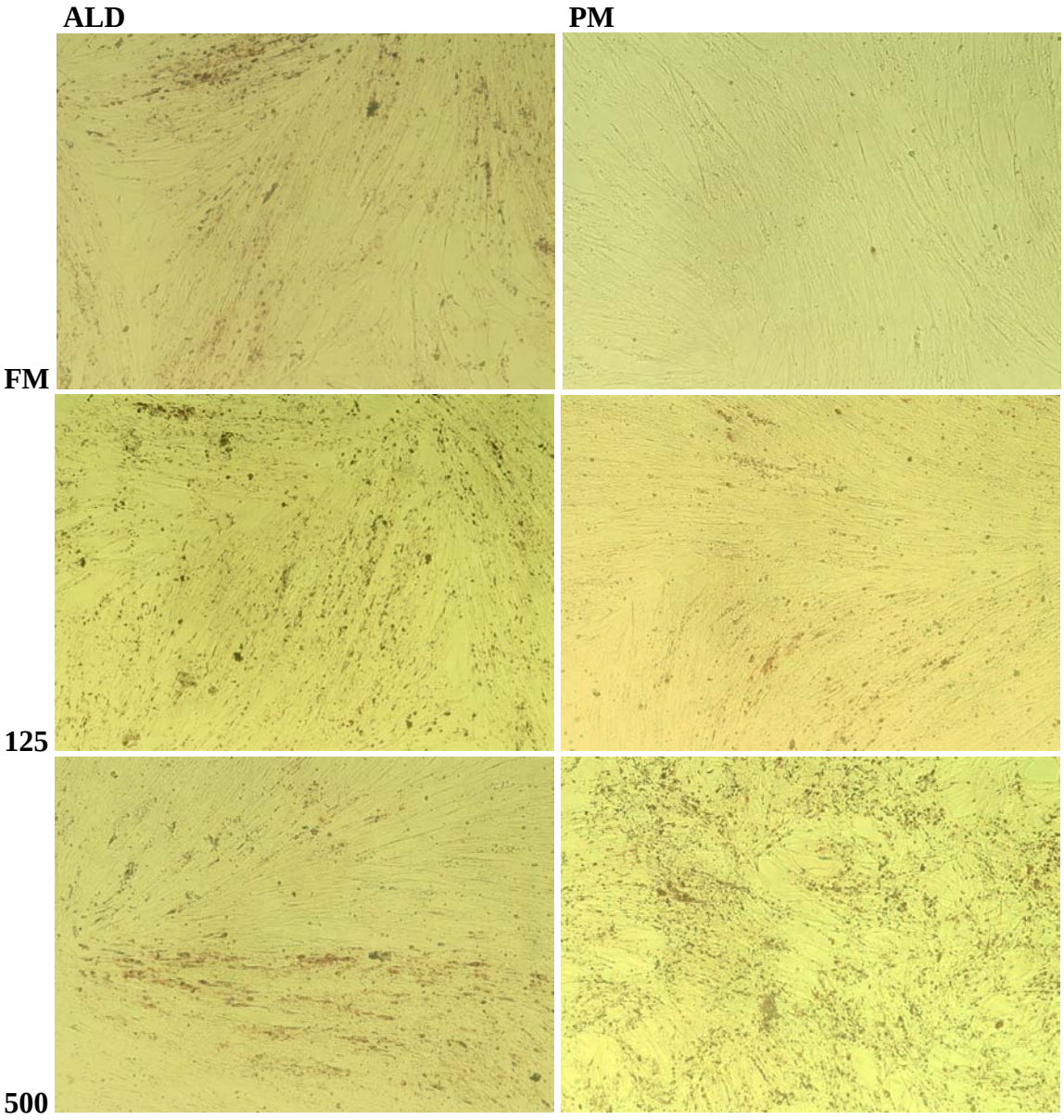

Fig 3. Lipid accumulation represented by Oil Red O staining in ALD and PM myotubes treated with feeding media alone (FM), FM+125nM MitoQ$_{10}$ (125), and FM+500nM MitoQ$_{10}$ (500). Figures represent images acquired on day 3 post-treatment. Images were acquired at 20x magnification.

3.3 PPAR-γ and PGC-1α Gene Expression

Quantitative Real Time PCR analysis was utilized to assess the *PPAR-γ* (adipogenic marker) and PGC-1α (muscle oxidative phenotype marker) gene expression levels in ALD and PM myotubes grown in Fusion Media alone (FM), FM+ 125nM $MitoQ_{10}$, and FM+ 500 nM $MitoQ_{10}$ at 3 days post $MitoQ_{10}$ treatment. Because no effect on lipid accumulation was observed with decyl-TPMP treatment, the effect of this treatment on gene expression levels was not evaluated. Each gene of interest was normalized to β-actin internal control and the gene expression data were compared to cDNA derived from PM myotubes grown in FM alone (Fig 4). The PM myotubes grown in FM alone exhibited only trace amounts of intramuscular fat. Therefore gene expression data derived from this treatment were utilized as a control to compare gene expression data derived from other treatments. Lipid accumulation and adipogenic PPAR-γ gene expression in both ALD (correlation coefficient of 0.93) and PM (correlation coefficient equal to 1.0) myotube cultures appear closely related, indicating that PPAR-γ is an appropriate marker of adipogenesis. PPAR-γ gene expression analysis confirms that 500nM $MitoQ_{10}$ treatment significantly ($P<0.05$) stimulates the adipogenic process in PM myotubes, whereas the adipogenic gene expression remains the same ($P>0.05$) in ALD myotubes in all treatment groups (Fig 4).

Expression level of oxidative phenotype marker, PGC-1α, was significantly ($P<0.05$) higher in ALD myotubes treated with FM alone and FM+125nm $MitoQ_{10}$ than in PM myotubes proving that ALD muscle maintains its native oxidative phenotype in culture. However, 500nM $MitoQ_{10}$ treatment causes decrease in PGC-1α in ALD myotube cultures. The qPCR data also indicates that $MitoQ_{10}$ treatment stimulates oxidative gene expression in glycolytic PM myotubes. The expression level of PGC-1α in 125nM and 500nM $Mitoq_{10}$-treated PM myotubes was 3-fold higher ($P<0.05$) than in the PM myotubes grown in FM alone (Fig 4).

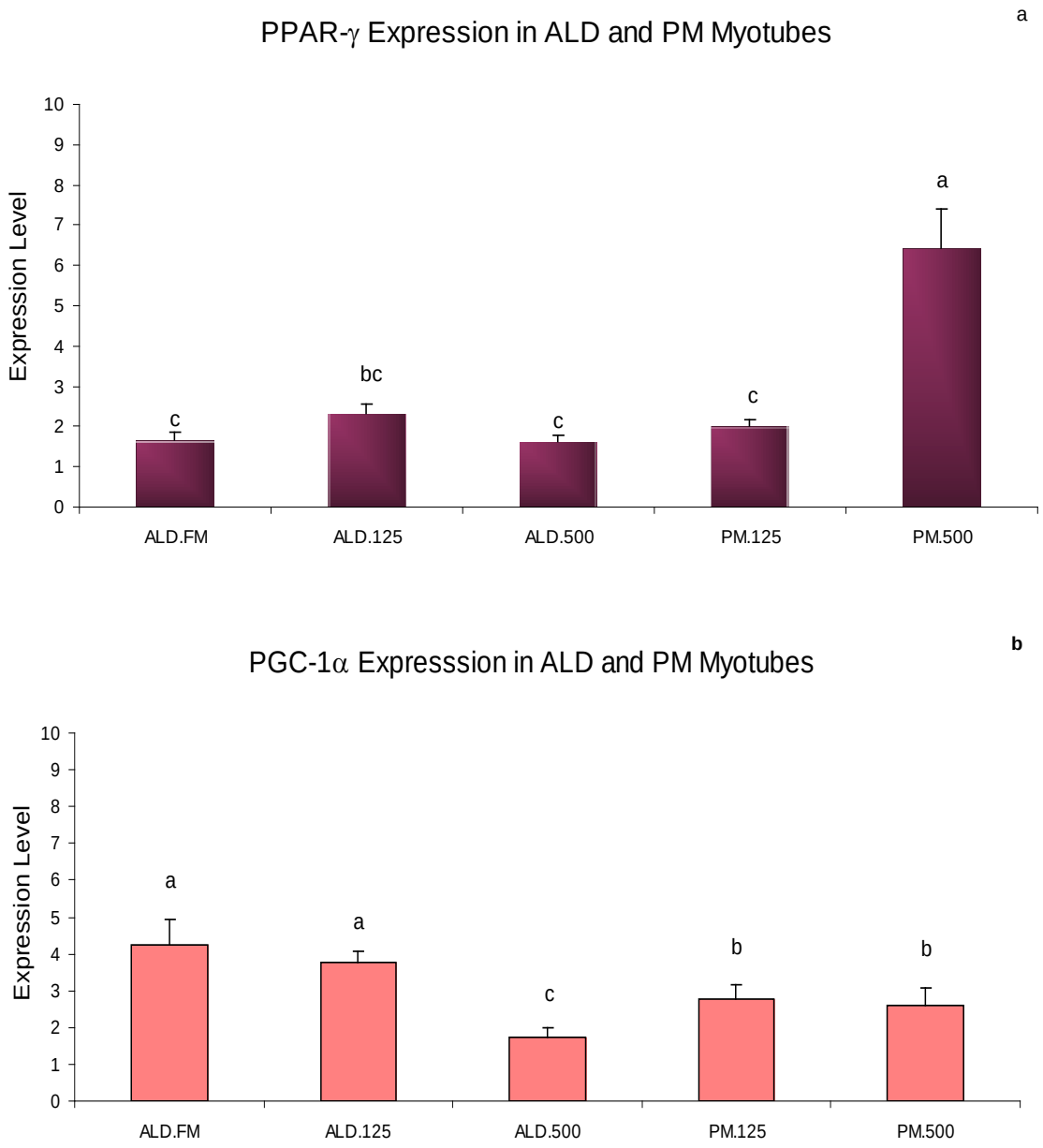

Fig 4. Expression level of **a** PPAR-γ and **b** PGC-1α gene in ALD, and PM myotube cultures treated with feeding media alone (FM), FM+125nM $MitoQ_{10}$ (125), and FM+500nM $MitoQ_{10}$ (500) as compared to gene expression data acquired from PM myotubes treated with FM alone. Subscripts represented by different letters illustrate significantly different mean values ($P<0.05$).

4. Discussion

Skeletal muscle is one of the major tissues contributing to whole body metabolic rate and energy expenditure [39]. Oxidative capacity of the muscle, intramuscular lipid composition, lipid concentration, and efficiency of muscle glucose transporters influence many biochemical pathways governing tissue metabolism [4, 40, 41]. Consequently, alterations in skeletal muscle phenotype may play a crucial role in disease development and progression. The results of the current study suggest that $MitoQ_{10}$ controls expression levels of genes regulating skeletal muscle and adipose metabolism. Interestingly, the extent of the $MitoQ_{10}$ effect on cell metabolism seems to be muscle-type dependent. The concentration of $MitoQ_{10}$ applied to the cultured myotubes also appears to play a role in regulation of phenotypic and transcriptional characteristics of analyzed myotubes. The most discernable effect of $MitoQ_{10}$ treatment was observed in PM myotube cultures, where the administration of 500nM of $MitoQ_{10}$ resulted in significant increase in lipid accumulation and caused a significant rise in the expression of the adipogenic gene, PPAR-γ. In myotube cultures, the intracellular fat is most likely derived from muscle-derived stem cells, satellite cells, or mesenchymal stem cells [42]. Although the basal level of intracellular lipid and PPAR-γ expression was higher in ALD than in PM cultures, the effect of $MitoQ_{10}$ on lipid accumulation and PPAR-γ expression in ALD was significantly lower than in PM cells. Furthermore, unlike in the PM culture, the increased concentration of $MitoQ_{10}$ did not cause increased accumulation of lipid in the ALD culture. Similarly, Horowitz et al., (2000) [43] and Campbell et al. (2001) [44] reported that genes involved in fatty acid metabolism in

mixed red muscle were over-expressed as compared to white muscles in humans. Genes regulating fatty acid metabolism that are differentially expressed in mixed-red and white muscle types are involved in transport of fatty acids (Cluster of Differentiation 36), fatty acid oxidation (acyl-CoA dehydrogenase), and regulation of genes involved in fatty acid oxidation (PPAR-α) [43, 44]. Consequently, the minimal effect of $MitoQ_{10}$ on lipid accumulation and on PPAR-γ expression in ALD cultures may be a consequence of high basal level of adipogenic gene expression in the ALD muscle. It is likely that endogenous CoQ_{10} was at a saturation level in ALD cultures and significant increase of $MitoQ_{10}$ concentration in the fusion media had no additional effect. In healthy tissues, CoQ_{10} is synthesized from phenylalanine and mevalonate [45], and it appears that CoQ_{10} reaches saturation level in cell membranes [46]. However, low levels of cellular CoQ_{10} have been reported in disease state and aging [47, 48, 49]. The autooxidation of CoQ_{10} has been shown to produce hydrogen peroxide that activates transcription factors such as NFkB [50, 51], which is associated with inflammation and has been shown to be up-regulated during fat cell differentiation [52]. Inflammation during fetal development results in elevated expression of NFkB that induces satellite cell differentiation into adipocytes [53, 54]. Accordingly, $MitoQ_{10}$-induced expression of PPAR-γ and increased adipocyte accumulation in PM cultures may be a result of NFkB action.

Notable muscle-related differences were observed in expression levels of PGC-1α gene. Over-expression of PGC-1α in vitro has been associated with an increase of oxidative mitochondrial metabolism by increasing the rate of proton leakage [55, 56]. PGC-1α may stimulate oxidative muscle phenotype through up-regulation of calcineurin and citrate

synthase [57, 21, 56]. Significantly higher basal expression levels of PGC-1α in "oxidative" ALD myotubes as compared to "glycolytic" PM myotubes confirm that the myotubes stayed true to their phenotype in culture [58]. Moreover, the 125nM of $MitoQ_{10}$ did not affect the PGC-1α expression in ALD myotubes, and 500nM of $MitoQ_{10}$ caused a significant decrease in PGC-1α expression in the ALD. In contrast, both 125nM and 500nM of $MitoQ_{10}$ stimulated PGC-1 α expression in PM muscle, and there was no significant difference in PGC-1 α expression when the $MitoQ_{10}$ concentration was elevated to 500nM. It seems that $MitoQ_{10}$ functions differently on muscles with different phenotype. Linnane et al. (2002) [59] reported that oral administration of CoQ_{10} causes an increase in fast-twitch to slow-twitch muscle fiber ratio in phenotypically mixed human vastus lateralis (quadriceps) muscles. Based on the current results, and the results of Linnane et al. (2002) [59] it can be speculated that CoQ_{10} down-regulates oxidative metabolic processes in phenotypically oxidative fiber types. Since myotubes derived from two metabolically different muscles were examined in the current study, it is likely that the differential response to $MitoQ_{10}$ may be dependent on the cellular redox state [59]. CoQ_{10} plays an imperative role in modulation of mitochondrial membrane potential though transport of protons and electrons across the mitochondrial membrane. The efficiency and rate of electron transport process regulate mitochondrial substrate utilization and energy generation [60, 61]. Since PM muscles are composed of fibers that rely mostly on glycolysis for their energy utilization, and ALD muscles are primarily composed of fibers that derive their energy from mitochondria, the cellular redox state of these two muscle types is quite different. Data demonstrating that satellite cells stay true to their original phenotype in culture [58], and reported significantly

different basal expression levels of PGC-1α in ALD and PM myotubes also indicate that redox state of ALD and PM myotubes is likely different. It is possible that in ALD myotube cultures the mitochondrial respiration was already at the optimum state and supplementation with $MitoQ_{10}$ induced production of free-radicals, hence the decrease in oxidative gene expression in 500nM $MitoQ_{10}$-treated myotubes.

Linnane et al. (2002) [59] proposed that changes in cellular redox state control anti-oxidant/pro-oxidant function of CoQ_{10} and its role in production of H_2O_2. Hydrogen peroxide likely plays a role as a second messenger and regulator of expression of genes involved in phosphorylation of various proteins [62, 59]. Hydrogen peroxide has inhibitory effects on calcineurin expression [63, 64]. Since calcineurin regulates muscle oxidative phenotype, the $MitoQ_{10}$-altered expression of PGC-1α in ALD myotubes may be in part dependent on $MitoQ_{10}$-stimulated hydrogen peroxide action.

4.1 Conclusions

In conclusion, $MitoQ_{10}$ was shown to up-regulate genes controlling oxidative mitochondrial biogenesis and adipogenesis in PM myotube cultures, with a decrease of oxidative metabolism in ALD myotube cultures. Current data indicates that $MitoQ_{10}$ likely controls a range of metabolic pathways through its regulation of gene expression levels. Therefore, administration of $MitoQ_{10}$ and its regulation of the redox state in various tissues may be beneficial in treatment of an array of physiological conditions related to altered metabolic state.

Acknowledgements

The authors express their appreciation to Dr. Chris Ashwell and Shelly Nolin for technical assistance.

$MitoQ_{10}$ and decyl-TPMP provided by Dr. Michael Murphy.

Support provided in part by funds under multi-state project number NC1131.

This project was supported by National Research Initiative Competitive Grant no. 2005-35206-15241 (PEM) from the USDA Cooperative State Research, Education, and Extension Service. Support also provided in part by the North Carolina Agricultural Foundation (PEM).

References

[1] C.E. Kasper, A.L McNulty, A.J., D.P. Otto Thomas, Alterations in skeletal muscle related to impaired physical mobility: An empirical model, Res. Nurs. Health 16 (1993) 265-273.

[2] P.E. Mozdziak, M.L Greaser, E. Schultz, Myogenin, MyoD, and myosin expression after pharmacologically and surgically induced hypertrophy, J. Appl. Physiol. 84 (1998) 1359-1364.

[3] R.A. DeFronzo, E. Jacot, E. Jequier, J. Wahren, J.P. Felber, The effect of insulin on the disposal of intravenous glucose results from indirect calorimetry and hepatic and femoral venous catherization, Diabetes 30 (1981) 1000-1007.

[4] L.J. Goodyear, M.F. Hirsham, P.M. Valyou, E.S. Horton, Glucose transporter number, function, and subcellular distribution in rat skeletal muscle after exercise training, Diabetes 41 (1992) 1091-1099.

[5] A.J. Wagers, I.M. Conboy, Cellular and molecular signatures of muscle regeneration: current concepts and controversies in adult myogenesis, Cell 122 (2005) 659-667.

[6] L. Teboul, D. Gaillard, L. Staccini, H. Inadera, E.Z. Amri, P.A. Grimaldi, Thiazolidinediones and fatty acids convert myogenic cells into adipose-like cells, J. Biol. Chem. 27 (1995) 28183-28187.

[7] B.Brand-Saberi, J. Wilting, C. Ebensperger, B. Christ, The formation of somite compartments in the avian embryo, Int. J. Dev. Biol. 40 (1996) 411-420.

[8] A. Asakura, M. Komaki, M. Rudnicki, Muscle satellite cells are multipotential stem cells that exhibit myogenic, osteogenic, and adipogenic differentiation, Differentiation 68 (2001) 245-253.

[9] K.C. Chang, Key signaling factors and pathways in the molecular determination of skeletal muscle phenotype, Animal 1 (2007) 681-698.

[10] Y.H. Yu, B.H. Liu, H.J. Mersmann, S.T. Ding, Porcine peroxisome proliferator-activated receptor γ induces transdifferentiation of myocytes into adipocytes, J. Anim. Sci. 84 (2006) 2655-2665.

[11] P. Puigserver, B.M. Spegelman, Peroxisome proliferator-activated receptor-γ coactivator 1α (PGC-1 α): Transcriptional coactivator and metabolic regulator, Endocrine Rev. 24 (2003) 78-90.

[12] P. Tontonoz, E. Hu, B.M. Spiegelman, Stimulation of adipogenesis in fibroblasts by PPARγ 2, a lipid activated transcription factor, Cell 79 (1994) 1147-1156.

[13] Y. Barak, M.C. Nelson, E.S. Ong, Y.Z. Jones, P. Ruiz-Lozano, K.R. Chien, A. Koder, R.M. Evans, PPAR γ is required for placental cardiac, and adipose tissue development, Mol. Cell 4 (1999) 585-595.

[14] E.D. Rosen, P. Sarraf, A.E Troy, K. Moore, D.S. Milstone, B.M. Spiegelman, R.M. Mortensen, PPARγ is required for the differentiation of adipose tissue in vivo and in vitro, Mol. Cell 4 (1999) 611-617.

[15] D.M. Muoio, J.M. Way, C.J. Tanner, D.A. Winegar, S.A. Kliewer, J.A. Houmard, W.E. Kraus, G.L. Dohm, Peroxisome proliferator-activated receptor-α regulates fatty acid utilization in primary human skeletal muscle cells, Diabetes 51 (2002) 901-909.

[16] B.H. Goodpaster, S. Krishnaswami, H. Resnick, D.E. Kelley, C. Haggerty, T.B. Harris, A.V. Schwartz, S. Kritchevsky, A.B. Newman, Association between regional adipose tissue distribution and both type 2 diabetes and impaired glucose tolerance in elderly men and women, Diabetes Care 26 (2003) 372-379.

[17] D. Gallagher, P. Kuznia, S. Heshka, J. Albu, S.B. Heymsfield, B. Goodpaster, M. Visser, T.B Harris, Adipose tissue in muscle: a novel depot similar in size to visceral adipose tissue, Am. J. Clin. Nutr. 81 (2005) 903-910.

[18] N.J. Rothwell, M.J.Stock, A role for brown adipose tissue in diet-induced thermogenesis, Nature 281 (1979) 31-35.

[19] B. Cannon, J. Houstek, J. Nedergaard, Brown adipose tissue. More than an effector of thermogenesis?, Ann. NY Acad. Sci. 856 (1998) 171-187.

[20] C. Duchamp, H. Barre, Skeletal muscle as the major site of nonshivering thermogenesis in cold acclimated ducklings, Am. J. Physiol. Regul. Integr. Comp. Physiol. 265 (1993) 1076-1083.

[21] J. Lin, H. Wu, P.T. Tarr, C.Y. Zhang, Z. Wu, O. Boss, L.F. Michael, P. Puigserver, F. Isotani, E.N. Olson, B.B. Lowell, R. Bassel-Duby, B.M. Spiegelman, Transcriptional co-activator PGC-1α drives the formation of slow-twitch muscle fibers, Nature 418 (2002) 797-801.

[22] H. Oberkofler, H. Esterbauer, V. Linnemayr, A.D. Strosberg, F. Krempler, W. Patsch, Peroxisome proliferator-activated receptor (PPAR) γ coactivator-1 recruitment regulates PPAR subtype specificity, J. Biol. Chem. 277 (2002) 16750-16757.

[23] S. N. Kamzalov, M.J. Sumien, R.S. Sohal, Coenzyme Q intake elevates the mitochondrial and tissue levels of coenzyme Q and α-tocopherol in young mice, J. Nutr. 133 (2003) 3175-3180.

[24] R.E. Beyer, An analysis of the role of coenzyme Q in free radical generation and as an antioxidant, Biochem. Cell. Bio. 70 (1992) 390-403.

[25] L. Ernster, G. Dallner, Biochemical, physiological and medical aspects of ubiquinone function, Biochem. Biophys. Acta 1271 (1995) 195-204.

[26] E.G. Bliznakov, H.N. Bhagavan, Deficient energy metabolism and disease: role of coenzyme Q_{10}, FASEB 17 (2003) A1114.

[27] K. Overvad, B. Diamant, L. Holm, G. Holmer, S.A. Mortensen, S. Stender, Coenzyme Q10 in health and disease, Europ. J. Clin. Nutr. 53 (1999) 764-770.

[28] H. Langsojen, P. Langsojen, R. Willis, K. Polkers, Usefulness of coenzyme Q10 in clinical cardiology: a long-term study, Mol. Asp. Med. 15 (1994) 165-175.

[29] K. Folkers, R. Simonsen, Two successful double-blind trials with coenzyme Q10 (vitamin Q10) and muscular dystrophies and neurogenic atrophies, Biochem. Biophys. Acta 1271(1995) 281-286.

[30] M.R. Werbach, Nutritional strategies for treating chronic fatigue syndrome, Altern. Med. Rev.: J. Clin. Ther. 5 (2000) 93-108.

[31] J.S. Armstrong, M. Whiteman, P. Rose, D.P. Jones, The coenzyme Q10 analog decylCoQ10 inhibits the redox-activated mitochondrial permeability transition, J. Biol. Chem. 278 (2003) 49079-49084.

[32] R.A.J. Smith, C.M. Porteous, A.M. Gane, M.P. Murphy, Delivery of bioactive molecules to mitochondria in vivo, PNAS 100 (2003) 5407-5412.

[33] D.C. McFarland, M.E. Doumit, R.D. Mishall, The turkey myogenic satellite cell: optimization of in vitro proliferation and differentiation, Tissue Cell 20 (1988) 899-908.

[34] R. Freshney, Culture of Animal Cells: A manual of basic technique, Alan R. Liss, Inc., New York, New York, 1987, p. 117.

[35] L. Janderová, M. McNeil, A.N. Murrell, R.L. Mynatt, S.R. Smith, Human mesenchymal stem cells as an in vitro model for human adipogenesis, Obes. Res. 11 (2003) 65-74.

[36] P. Chomczynski, N. Sacchi, Single-step method of RNA isolation by acid guanidinium thiocyanate-phenol chloroform extraction, Anal. Biochem. 162 (1987) 156-159.

[37] M.W. Pfaffl, A new mathematical model for relative quantification in real time PCR, Nucleic Acid Res. 29 (2001) 2002-2007.

[38] T. Yue, J.D. Yin, F.N. Li, D.F. Li, M. Du, High glucose induces differentiation and adipogenesis in porcine muscle satellite cells via mTOR, BMP Reports 43 (2010) 140-145.

[39] F. Zurlo, E. Ravussin, A low rate of fat utilization as a predictor of weight gain, in F. Belfiore, B. Jeanrenaud, D. Papalia (Eds.), Obesity: Basic Concepts and Clinical Aspects. Front Diabetes, Karger, Basel, Switzerland,1992, pp. 50-60

[40] L.H. Storlien, D.A. Pan, M. Milner, S. Lillioja, Skeletal muscle membrane lipid composition is related to adiposity in man (Abstract), Obesity Res. 2 (1993) 77.

[41] A.D. Kriketos, D.A. Pan, S. Lillioja, G.J. Cooney, L.A. Baur, MR. Milner, J.R. Sulton, A.B. Jenkins, C. Boardus, L.H. Storlein, Interrelationship between muscle morphology, insulin action, and adiposity, Am. J. Physiol-Regul. Integr. Comp. Physiol. 270 (1996)1332-1339.

[42] B. Cao, J. Huard, Muscle-derived stem cells, Cell Cycle 3 (2004) 104-107.

[43] J.F. Horowitz, T.C. Leone, W. Feng, D.P. Kelly, S. Klein, Effect of endurance training on lipid metabolism in women: a potential role for PPAR-α in the metabolic response to training, Am. J. Physiol. Endocrinol. Metab. 279 (2000) E348-E355.

[44] W.G Campbell, S.E. Gordon, C.J. Carlson, J.S. Pattison, M.T. Hamilton, F.W. Booth, Differential global gene expression in red and white skeletal muscle, Am. J. Physiol. Cell. Physiol. 280 (2001) 763-768.

[45] J.R. Schultz, C.T. Clarke, Functional roles of ubiquinone, in E. Cardenas, L. Parker, (Eds.), Mitochondria, Oxidants and Ageing, M Dekker, New York, New York, 1999, pp. 95-118

[46] M.F. Beal, Coenzyme Q administration and its potential for treatment of neurodegenerative diseases. Biofactors 9 (1999) 261-266.

[47] S. Reahal, J. Wriggleworth, Tissue concentration of coenzyme Q10 in rat following its oral and intraperitoneal administration, Drug Metabol. Dispos. 20 (1992) 423-427.

[48] F.L. Rosenfeldt, S. Pepe, R. Ou, J.A. Mariani, M.A. Rowland, P. Nagley, A.W. Linnane, Coenzyme Q10 improves the tolerance of the senescent myocardium to aerobic and ischemic stress, Biofactors 9 (1999) 291-300.

[49] R. Willis, M. Anthony, L. Sun, Y. House, G.Qiao, Clinical implications of the correlation between coenzyme Q10 and vitamin B6 status, Biofactors 9 (1999) 359-363.

[50] B. Kaltschimdt, T. Sparna, C. Kaltschmidt, Activation of NFKB by reactive oxygen intermediates in the nervous system, Antioxid. Redox. Signal. 1(1999) 129-144.

[51] H. McLennan, M. Degli Esposti, The contribution of mitochondrial respiratory complexes to the production of reactive oxygen species, J. Bioenerg. Biomemb. 32 (2000) 153-162.

[52] A.H. Berg, Y. Lin, M.P. Lisanti, P.E. Scherer, Adipocyte differentiation induces dynamic changes in NF-kappaB expression and activity, Am. J. Physiol. Endocrinol. Metab. 287 (2004) 1178-1188.

[53] S.A. Bayol, B.H. Simbi, J.A. Bertrand, N.C. Stickland, Offspring from mothers fed 'junk food' diet in pregnancy and lactation exhibit exacerbated adiposity that is more pronounced in females, J. Physiol. 586 (2008) 3219-3230.

[54] J.F. Tong, X. Yang, M.J. Zhu, S.P. Ford, P.W. Nathanielsz, M. Du, Maternal obesity downregulates myogenesis and β-catenin signaling in fetal skeletal muscle, Am. J. Physiol. Endocrinol. Metab. 296 (2009) 917-924.

[55] J. St. Pierre, J. Lin, S. Krauss, P.T. Tarr, R. Yang, C.B. Newgard, B.M. Spiegelman, Bioenergetic analysis of peroxisome proliferator-activated receptor gamma coactivators 1alpha and 1beta (PGC-1alpha and PGC-1beta) in muscle cells, J. Biol. Chem. 278 (2003) 26597-26603.

[56] O.H. Mortensen, L. Frandsen, P. Schjerling, E. Nishimura, N. Grunnet, PGC-1α and PGC-1β have both similar and distinct effects on myofiber switching toward an oxidative phenotype, Am. J. Physiol. Endocrinol. Metab. 291(2006) 807-816.

[57] J. Higginson, H. Wackerhage, N. Woods, P. Schjerling, A. Ratkevicius, N. Grunnet, B. Quistorff, Blockades of mitogen-activated protein kinase and calcineurin both change fibre-type markers in skeletal muscle culture, Pflugers Arch. 445 (2002) 437-443.

[58] S. Düsterhöft, S. Pette, Satellite cells from slow rat muscle express slow myosin under appropriate culture conditions, Differentiation 53 (1993) 25-33.

[59] A.W. Linnane, G. Kopsidas, C. Zhang, N. Yarovaya, S. Kovalenkom, P.Papakostopoulos, H. Eastwood, S. Graves, M. Richardson, Cellular redox activity of

coenzyme Q10: Effect of CoQ10 supplementation on human skeletal muscle, Free Rad. Res. 36 (2002) 445-453.

[60] F.L. Crane, I.L. Sun, R.A. Crowe, F.J. Alcain, H. Low, Coenzyme Q10 plasma membrane oxidase and growth control, Mol Asp Med 15 (1994) 1-11.

[61] R. van Belzen, A.B. Kotlyar, N. Moon, W.R. Dunham, S.P. Albracht, The iron-sulfur clusters 2 and ubisemiquinone radicals of NADH:ubiquinone oxidoreductase are involved in energy coupling in submitochondrial particles, Biochem. 36 (1997) 886-893.

[62] F. Rusnak, T. Reiter, Sensing electrons: protein phosphatase redox regulation, Trends Biochem. Sci. 25 (2000) 527-529.

[63] L. Yu, J. Golbeck, J. Yao, F. Rusnak, Spectroscopic and enzymatic characterization of the active site dinuclear metal center of calcineurin: implications for a mechanistic role, Biochem. 36 (1997) 10727-10734.

[64] T.A. Reiter, R.T. Abraham, M. Choi, F. Rusnak, Redox regulation of calcineurin in T-lymphocytes, J. Biol. Inorg. Chem. 4 (1999) 632-644.

Chapter 5

Differential Expression of Genes Characterizing Myofiber Phenotype

Abstract

Because of its high plasticity and rapid growth rate, turkey skeletal muscle is an important model for studying mechanisms responsible for vertebrate skeletal muscle development and function. Skeletal muscle is composed of metabolically heterogeneous myofibers that exhibit high plasticity at both the morphological and transcriptional levels. The objective of this study was to employ microarray analysis to elucidate the differential gene expression between the tonic- "red" anterior latissimus dorsi (ALD) muscle, the phasic- "white" posterior latissimus dorsi (PLD), and "mixed"-phenotype biceps femoris (BF) in 1-week and 19-week old male turkeys. A total of 170 differentially expressed genes were identified in the analyzed muscle samples ($P<0.05$). Gene Go analysis software was utilized to identify top gene networks and metabolic pathways involving differentially expressed genes.
The largest differences were observed between ALD and PLD muscles, where 32 genes were over-expressed and 82 genes were under-expressed in ALD1-PLD1 comparison, and 70 genes were over-expressed and 70 under-expressed in ALD19-PLD19 comparison. The largest number of genes over-expressed in ALD muscles, as compared to other muscles code for extracellular matrix proteins such as dystroglycan and collagen. FThe gene analysis revealed that phenotypically "red" BF muscle has high expression of glycolytic genes usually associated with the "white" muscle phenotype. Muscle-specific differences were observed in expression levels of genes coding for proteins involved in mRNA processing and translation regulation, proteosomal degradation, apoptosis, and insulin resistance. Current findings can have large implications in muscle-type related disorders and improvement of muscle quality in agricultural species.

Introduction

In conjunction with its function in movement and posture, skeletal muscle is an important metabolic organ that plays a major role in overall health by participating in processes regulating insulin utilization, glucose breakdown, and blood lipid profile in both mammalian and avian species [1,2,3,4]. Furthermore, skeletal muscle metabolism is closely associated with meat quality in agricultural species [5, 6]. The precise genetic mechanisms that govern differentiation, development, and function of vertebrate skeletal muscles are still not yet fully understood. There is an extensive variation in phenotype among anatomically distinct muscles. Physical location of a skeletal muscle significantly influences its metabolic, biochemical, and biophysical characteristics [7]. Slow-twitch, oxidative muscles, such as anterior latissimus dorsi (ALD), and soleus, are adapted to continuous activation under aerobic conditions. Conversely, fast-twitch, glycolytic muscles, such as pectoralis major, and posterior latissimus dorsi (PLD), are subjected to sporadic bouts of exercise and are susceptible to fatigue, as their main source of energy comes from anaerobic catabolism of glucose [8]. Based on myosin protein isoform analysis, avian ALD and PLD muscles have been utilized as models of true tonic/fatigue resistant and pure phasic/fatigue prone muscles respectively [9, 10]. Phenotypic differences between ALD and PLD muscles are associated with varying functional demands associated with physical location of these muscles [11, 12].

Knowledge of genetic basis of fiber phenotype is important to the medical and agricultural fields. The oxidative versus glycolytic metabolic profile of the muscle may indicate whether an individual is prone to disease outbreak and progression and it may be related to occurrence of myopathies in both mammalian and avian species. It has been

demonstrated that oxidative capacity of the muscle is likely related to occurrence of chronic metabolic syndromes such as obesity, type 2 diabetes, insulin resistance, and increased risk of cardiovascular disease in mammals [1, 2, 13, 14]. Furthermore, discovery of leptin gene in chickens and turkeys establishes poultry as a potential animal model for studying obesity in humans because leptin deficiency or receptor resistance results in obesity in mammals [3, 4]. Skeletal muscle of agricultural species may also be utilized as a model for growth-related myopathies. In the poultry industry, increased genetic selection for rapid growth and heavy musculature results in higher incidence of defects in meat and carcass quality, and is one of the major causes of growth-induced myopathies [15, 6, 16, 17].

The objective of this study was to utilize microarray technology to identify muscle phenotype-specific genes that may be regulating metabolic processes associated with skeletal muscle health and optimal meat quality. Microarray technology presents a useful tool to simultaneously measure gene expression levels of thousands of genes in a particular tissue. The relationship between phenotypic characteristics of the muscle and resulting variations in muscle function can be reflected by differences at the transcriptional level. Although muscle fiber-specific microarray analysis has already been performed on functionally important muscle groups in vertebrate species [18, 19, 20], this report presents the first muscle fiber-related gene expression profile analysis pertaining to two metabolically extreme muscles: the "true red" ALD "true white" PLD [10, 21]. The ALD and PLD muscles were chosen for analysis because they represent muscle groups composed of metabolically and phenotypically homogenous muscle fibers in avian species [10, 21]. In addition to differences in their energy metabolism, ALD and PLD muscles can be distinguished based on

their myofibrillar arrangement [9]. The PLD muscle is composed of equally sized myofilaments that are organized into distinct myofibrils separated by abundant sarcoplasmic reticula; however, the ALD muscle myofilaments are less organized and contain less sarcoplasmic reticulum than PLD muscles [9]. The structural differences between ALD and PLD muscles are reflected in differences in tension resistance and speed of contraction. Biceps femoris (BF) was selected for this study because of its unique phenotypic and metabolic characteristics. Wiskus et al. (1976) [22] demonstrated that based on histochemical staining for succinic dehydrogenase, the BF muscle is composed of both oxidative and glycolytic fibers. However, histochemical staining for adenosine triphosphatase (ATPase) revealed that BF muscle is composed mostly of fast-twitch fibers [22]. Skeletal muscle enlargement of post-hatch fast growing turkeys is accompanied by both hypertrophy and hyperplasia of the muscle fibers [21]. Due to its high plasticity and accelerated growth, the heavy weight turkey is an exciting model for studying mechanisms governing muscle development [9, 10, 21, 23].

The goal of this study was to identify the genetic basis of phenotypically distinct muscles at 1 and 19 weeks of age. These ages were selected to account for growth-related differences in selected turkey muscles. Skeletal muscles in early-post hatch turkeys are characterized by fast-growth rate and high satellite cell mitotic activity [24, 25]. However, after 9-weeks of age the growth significantly slows down, satellite cell mitotic activity begins to diminish, and muscle growth occurs mainly through and increase of cytoplasmic to nuclear ratio [25]. Current data substantially contributes to the available knowledge base regarding transcriptional regulation of molecular pathways governing pure fast-glycolytic and pure

slow-oxidative muscle phenotype in turkeys at 1 and 19 weeks of age. Among the differentially expressed genes, a number of candidate genes were uncovered that could potentially be related to phenotypic variations among functionally different muscles.

Materials and Methods

Sample Collection

All experiments involving animals were in compliance with the North Carolina State University Institutional Animal Care and Use Committee. Six 1-week-old and six 19-week-old Nicholas (85 sire x 700 dam) turkey males (Meleagris gallopavo) were randomly selected from a single flock and immediately killed by intra-venous injection of Euthasol® (Delmarva Laboratories, Midlothian, VA, USA) at a dose of 0.25mL/kg body weight. Right anterior latissimus dorsi (ALD), posterior latissimus dorsi (PLD), and biceps femoris (BF) muscles were excised immediately post-mortem from each bird, and immersed in RNA-Later (Applied Biosystems-Ambion, Foster City, CA).

RNA Isolation

A modified guanidinium thiocyanate-phenol-chlorophorm extraction method [26] was utilized to isolate total RNA from each muscle sample. Six RNA isolations were performed per muscle sample. The six RNA samples from each muscle were later pooled, resulting in one sample per muscle per bird (6 birds total). In brief, 100mg of sample was placed in 1ml of Trizol reagent (Invitrogen, Carlsbad, CA) and homogenized using a bead beater (Cole-Parmer, Vernon Hills, IL).

Subsequently, 0.2 ml chloroform was added, followed by centrifugation at 12,000*g*, which yielded upper phase containing total RNA. The RNA was precipitated by addition of 0.5 ml of isopropyl alcohol, and the samples were incubated at 22 ºC for 10 minutes followed by centrifugation at 12,000*g*. The resulting RNA pellet was washed with 75% ethyl alcohol, centrifuged at 7,500*g*, and resuspended in diethylpyrocarbonate-treated water. The amount and quality of the isolated RNA was determined by measuring its absorbance at 260 nm with Nanodrop spectrophotometer (NanoDrop Technologies, Wilmington, DE), and RNA integrity was further evaluated using agarose gel electrophoresis. Samples with A260:280>1.8 were considered suitable for generating cDNA.

Microarray Platform

The Turkey Skeletal Muscle Long Oligo (TSKMLO) microarrays utilized in this study were printed at Michigan State University Research Technology Support Facility (East Lansing, MI). The oligonucleotide probes were synthesized based on cDNA libraries constructed from Pectoralis major from 18-day turkey embryo, 1-day post-hatch poult, and 16 week-old bird from two genetic lines: RBC2 and F [27]. Each oligonucleotide probe was a 70-mer spotted in duplicate and 'blank' spots containing spotting solution only were included on each printed array. Detailed information pertaining to microarrays utilized in this study can be found at National Center for Biotechnology Information (NCBI)'s Gene Expression Omnibus database (www.ncbi.nlm.nih.gov/projects/geo/, platform accession: GPL9788) and in Sporer et al., (2010) [28].

Microarray Procedure

Each analyzed cDNA sample was derived from six pooled RNA samples. The amount of cDNA was determined with Nanodrop spectrophotometer (NanoDrop Technologies, Wilmington, DE). cDNA samples with concentration of at least 18 ng/µL were considered suitable for microarray analysis. The goal was to compare functionally unique muscles within the same age group, and functionally identical muscles between two time points. The experimental setup is represented by Figure 1.

Muscle RNA samples were reverse-transcribed to amino-allyl-cDNA using the ChipShot Indirect Labeling and Clean-up System kit (Promega, Madison, WI). Subsequently, the amino-allyl-cDNA was labeled either with Cy3 or Cy5 fluorescent dye (Amersham Biosciences Corp., Piscataway, NJ). To minimize dye bias, the cDNA samples from six analyzed turkeys were labeled either with Cy3 or Cy5. The microarray slides were pre-hybridized and hybridized using Pronto Plus Microarray Hybridization Kit (Corning Inc., Corning, NY). The Cy3- and Cy5-labeled cDNA samples were applied to pre-hybridized array slides and covered with a pre-cleaned glass cover slip (Lifterslip, Portsmouth, NH). The slides were hybridized for 18 hours at 42°C, washed, and air-dried by centrifugation in a slide centrifuge for 2 minutes. A total of 17 arrays were labeled with representative muscle cDNAs (Figure 1). The hybridized microarray slides were scanned using a ScanArray Gx PLUS Microarray Scanner (PerkinElmer Life and Analytical Sciences, Shelton, CT) with laser intensity adjusted to 65%.

Quantitative Real-Time PCR

Quantitative Real-Time PCR analysis was performed to confirm the microarray results. The selected genes analyzed were as follows: Bat2d, Clu2, Egfr, and Leprot. The genes selected for Real-Time PCR analysis were selected based on their differential expression levels (fold change≥1.5) in analyzed muscles and the uniqueness of molecular pathways. The total RNA (6 samples per muscle from 6 birds at each age group) was isolated by modified guanidinium thiocyanate-phenol-chlorophorm extraction method [26] and was reverse-transcribed to generate cDNA. The reverse transcription reaction was performed with a High Capacity cDNA Reverse Transcription Kit (Applied Biosystems Inc., Foster City, CA) in a 20μL volume containing 1μg of total RNA. The cDNA samples were diluted 1:20 and analyzed by quantitative real-time PCR (qPCR) with a Bio-Rad iQ thermocycler. Each real-real time reaction contained 1 μL diluted cDNA, 1 μL primer, 10 μL Power SYBR Green PCR Master Mix (Applied Biosystems Inc., Foster City, CA), and 8 μL of diethylpyrocarbonate-treated water. Primers pertaining to genes of interest (Suppl. Table 1) were designed with Beacon Designer software (Premier Biosoft International, Palo Alto, CA) based on gene sequences available through National Center for Biotechnology information (www.ncbi.nlm.nih.gov).

The qPCR reaction was executed at the following thermocycler temperature settings: 95°C for 5min; 40 cycles of 95 °C for 30s, predetermined annealing temperature for 30s (Table 1), 72°C for 30s, 72°C for 5 minutes.. Each cDNA sample was amplified in duplicate and each gene was amplified on a single run.

The efficiency of each run was determined by standard curves generated for each gene. Standards were generated by diluting pooled cDNA at 1:5, 1:25, 1:125, and 1:625. Each standard dilution was amplified in triplicate. Fluorescence was measured at each extension step (72°C) and the cycle threshold (Ct) values were calculated for each cDNA according to the cycle at which the gene amplification was the highest. Gene expression was normalized against β-actin internal control (Table 2). The β-actin has been previously shown to be an appropriate internal control for muscle phenotype analysis [29, 19, 30, 20]. The fold change in gene expression level between samples was calculated using Pfaffl (2001) [31] method.

Data Processing and Statistical Analysis

Microarrays

The ScanAlyze Software (Stanford University, Stanford, CA) was utilized to extract the intensity of the scanned array spots for each dye combination on each array slide. The intensity of the data points was then analyzed with JMP Genomics software (SAS Institute Inc., Cary, NC). Data was first Log_2 transformed and then normalized by using locally weighed regression and smoothing within each array and across all arrays. The normalized data was evaluated by distribution analysis of the transformed data. Mixed model ANOVA [32] with Bonferroni correction of P=0.05 for multiple testing was performed to increase the sensitivity of detected differences in gene expression levels [33]. The following mixed model was utilized to identify differentially expressed genes:

$$Y = \mu+A+M+Dye+GS+e,$$

where age (A), muscle (M), and Dye were set as fixed effects, and grid x slide (GS) was considered as a random effect.

Real-Time

The statistical analysis was performed using JMP software (SAS Institute Inc., Cary, NC). A two-way analysis of variance was utilized for sample gene Ct: sample housekeeper gene Ct according to the following model:

$$Y = \mu+A+M+AM+e,$$

with age (A), muscle (M), and age x muscle (AM) as fixed effects.

Correlation analysis of Real Time PCR results and microarray results of expression levels of selected genes' (Bat2d, Clu2, Egfr, and Leprot) was performed for ALD1-PLD1, ALD19-PLD19, ALD1-BF1, and ALD19-BF19 comparisons.

Gene Network Analysis

Differentially expressed genes were identified based on their homology with previously reported nucleotide sequences available through National Center for Biotechnology information (www.ncbi.nlm.nih.gov).

Metacore database (GeneGo Inc., St. Joseph, MI) was utilized to identify biological processes and networks associated with differentially expressed genes. The list of genes with different expression level was uploaded to Metacore for biological pathway analysis. The software ranked differentially expressed genes according to their P-value and utilized the shortest path algorithm to generate the shortest path of interaction between genes of interest.

Results

Microarray Analysis

Of the 6,000 gene EST sequences analyzed, 170 genes were differentially expressed in ALD, PLD, and BF muscles across all comparisons. The largest differences were observed between ALD and PLD muscles, where 32 genes were over-expressed and 82 genes were under-expressed in ALD1-PLD1 comparison; and 70 genes were over-expressed and 70 under-expressed in ALD19-PLD19 comparison.

The differential gene expression pattern is represented by volcano plots (Figure 2). Expression values presented in all tables have been determined as significant by Bonferroni correction at P=0.05. Age-related differences were observed only in ALD muscles, where four genes (Col3a1, Ctnna1, Sfrs3, Atp2a1) were over-expressed in 1-week old ALD (ALD1) as compared 19-week old ALD muscles (ALD19) (Table 1). Among these four genes, two code for proteins involved in calcium metabolism (Ctnna1 and Atp2a1) [34, 35], one is an important component of extracellular matrix (Col3a1) [36], and the last one (Sfrs3) is a splicing factor involved in pre-mRNA processing [37].

Metabolic Pathways and Gene Networks

Biological processes and gene networks involving differentially expressed genes generated from the microarray analysis were built using GeneGo software of MetaCore database. Among all muscle types, the largest number of notably different genes was involved in metabolic process of anaerobic glycolysis, endoplasmic reticulum calcium ion homeostasis, and protein translation.

The most discernable differences in gene expression levels were observed between ALD and PLD muscles, where 32 genes were over-expressed and 82 genes were under-expressed in ALD1-PLD1 comparison; and 70 genes were over-expressed and 70 under-expressed in ALD19-PLD19 comparison. As expected, several genes coding for proteins responsible for muscle contraction and cellular calcium homeostasis were differentially expressed in ALD, PLD, and BF muscles (Tables 2 and 3).

The largest number of genes over-expressed in ALD muscles code for extracellular matrix proteins such as dystroglycan and collagen (Table 4, Figure 3). Moreover, large numbers of genes involved in glycolytic metabolism were under-expressed in ALD muscles as compared to BF and PLD muscles (Table 5, Figure 4). Interestingly, PLD and BF muscles were very similar on both regulatory and metabolic levels. The gene analysis revealed that BF muscles categorized as "red" based on their myoglobin expression have high expression of glycolytic genes usually associated with "white" muscle phenotype.

The microarray analysis also revealed that muscle phenotype is strictly regulated on transcriptional level, where 22 genes were differentially expressed between muscles (Table 6). An obvious muscle-related pattern of expression of these genes can be observed, with ALD muscles having opposite gene expression levels than PM and BF muscles.

The Gene-Go-derived results indicate that genes coding for proteins involved in proteosomal degradation are down-regulated in ALD muscles as compared to PLD muscles at both time points, and as compared to BF muscles at 19 weeks of age (Table 7).

Noteworthy muscle-dependent differences in gene expression levels were also observed in genes coding for heat shock proteins (Table 8).

Interestingly, some of the largest fold differences in the array data were detected in genes involved in G-protein coupled receptor signaling, where inositol monophosphate (ImpadI) and probable G-protein coupled receptor 20 (Gpr 20) were significantly under-expressed in ALD muscles as compared to PLD and BF muscles (Table 9).

Quantitative Real-Time PCR Analysis

Quantitative real-time PCR (qPCR) was performed on selected genes to assess the validity of the microarray approach. The following genes were evaluated using qPCR: Bat2d, Clu, Egfr, and Leprot (Suppl. Figure 1, Table 10). Each gene of interest was normalized to β-actin internal control. The genes selected for qPCR analysis participate in both newly established (Bat2d, Clu, Egfr) [38, 39, 40, 41] and already characterized (Leprot) muscle-fiber-specific molecular networks. Tissue-related variations in Bat2d gene expression levels have been associated with caloric restriction in mice [38]. Clusterin (Clu) belongs to family of genes coding for proteins involved in cell to cell adhesion, cell lysis, and apoptosis [39, 40], and the Egfr gene codes for proteins responsible for signal transduction cascades that regulate protein synthesis, cell proliferation, cell survival, and inhibition of apoptosis [41]. Therefore, further analysis of Bat2d, Clu, and Egfr gene may present insight on pathways regulating muscle-dependent insulin resistance, cell to cell interaction, and tissue turnover. Because function of Leprot-associated genes has already been studied in the muscle [42, 18], real time PCR analysis of Leprot was performed to further confirm the microarray results. Fold differences in the gene expression levels obtained from both

analyses may be related to differences in relative basal expression level of target gene and on varying sensitivities of both assays [43]. Although fold differences in the expression levels are not the same, the direction of change in the expression level is the same in every case, which validates the reliability of focused microarrays in this study. Additionally, correlation analysis of microarray and qPCR results revealed strong positive correlations between gene expression levels in each comparison (Table 10).

Discussion

Malleability of skeletal muscles is characterized by metabolic, mechanical, and neuronal adjustments to internal and external stimuli. A goal of this study was to advance the knowledge base about gene expression profiles that lead to fiber type-specific metabolic and contractile variations. Although the differences in expression levels of genes coding for contractile proteins and for proteins involved in glucose homeostasis were expected to be present in fast-glycolytic, slow-oxidative, and mixed-phenotype muscles; the results of the current study significantly extended the understanding of biochemical diversity of vertebrate skeletal muscles.

It appears that genes coding for proteins involved in mRNA processing and translation regulation (e.g. ribosomal proteins, Table 6), as well as factors involved in proteosomal degradation (e.g. ubiquitin, Table 7), apoptosis (e.g. clusterin, Table 10), insulin resistance (e.g. Bat2d, Table 10), and protein synthesis (e.g. EGFR, Table 10), may be utilized as markers of skeletal muscle phenotype and provide deeper understanding of metabolic processes governing muscle differentiation and plasticity.

Age-related Differences in Gene Expression Levels within a Muscle Type

The age groups selected for this analysis were based on muscle growth data [24, 25]. Prior researches demonstrated significant differences in growth rate and hyperplastic activity between young (1 week of age) and mature (19-weeks of age) turkey Pectoralis major muscles. Mozdziak et al., 1994 [25] demonstrated that satellite cell mitotic activity is elevated in early post-hatch birds. However, at 9 weeks of age, satellite cell mitotic activity begins to diminish and muscle growth occurs primarily through an increase of cytoplasmic to nuclear ratio. Additionally, performance data generated by Anthony et al. (1990) [24] revealed that turkeys grow rapidly before 10 weeks of age and the difference in weight gain plateaus shortly thereafter [24]. Consequently, it was expected that the microarray data would reveal significant differences in expression levels of genes regulating growth (e.g., genes regulating extracellular matrix components) and protein synthesis (e.g., genes coding for proteins involved in translation regulation) between muscles derived from turkeys at 1 and 19 weeks of age. Surprisingly, there were no significant differences between means in gene expression intensities between PLD1 and PLD19 muscle groups. The absence of significant differences between PLD1 and PLD19 muscles may be related to strict statistical testing utilized in this study. Based on the Bonferroni correction for multiple testing, only Myh1 (myosin heavy chain 1) gene was different between BF1 and BF19 muscle groups with a decrease in expression equal to 4.0. The Myh1 gene codes for myosin heavy chain protein present in high amount in fast-twitch (type II) muscle fibers [44]. The age related-decrease in expression of Myh1 in BF muscles indicates possible shift towards oxidative phenotype.

The highest age-related differences in gene expression levels were observed in ALD muscles, where four genes (Col3a1: collagen type III, alpha 1; Ctnna: catenin, alpha 1; Sfrs3: splicing factor, arginine/serine-rich 3; and Atp2a1**:** sarcoplasmic/endoplasmic reticulum calcium ATPase 2a1) were over-expressed in ALD1 muscles as compared to ALD19. Of these four genes two code for proteins involved in calcium metabolism (Ctnna1 and Atp2a1), one is an important component of extracellular matrix (Col3a1), and the last one (Sfrs3) is a splicing factor involved in pre-mRNA processing. Lower expression levels of aforementioned genes in BF19 and ALD19 muscles are likely related to age-related change in functional demands such as an increased load on the muscle with aging and resulting difference in collagen turnover and synthesis [45, 46, 11, 12]. Additionally, a small number of differentially-expressed genes in ALD1-ALD19 comparison may be related to hyperplastic muscle growth in post-hatch fast-growing turkey strains [21]. Satellite cell mitotic activity in the ALD is also associated with expression of embryonic myosin in ALD muscles of adult birds, which may provide an explanation for small number of differentially expressed genes between ages [47].

Metabolic and Contractile Muscle-related Difference in Gene Expression

The microarray analysis revealed that the highest number of differentially expressed genes was between ALD and PLD muscles. As expected, the largest differences were observed in expression levels of genes coding for contractile proteins and proteins involved in glucose metabolism.

Calcium ion plays a principal signaling and regulatory function in skeletal muscle [48]. Genes coding for proteins involved in calcium homeostasis, such as Atp2a1, calmodulin, and calponin had very similar expression levels in ALD-PLD and ALD-BF comparisons. In both comparisons, the Atp2a1 and calmodulin were under-expressed and calreticulin was over-expressed in ALD muscle. The calcium ATPase coded by Atp2a1 gene is an ion pump involved in calcium transport and reuptake from cytosol to sarcoplasmic reticulum [49]. Calcium ion sequestration by calcium ATPases is associated with muscular excitation and contraction [49]. Calreticulin is a calcium ion buffering protein and molecular chaperone in the lumen of endoplasmic and sarcoplasmic reticula [50]. Studies demonstrated that calreticulin modulates calcium storage capacity in sarcoplasmic and endoplasmic reticula and alters activity of calcium ATPases [49, 51, 52]. Therefore, opposite expression patterns of calreticulin and Atpa2a1 can be justified by antagonistic interaction of these molecules. It is surprising that the calmodulin coding gene is down-regulated in oxidative muscles because calmodulin is positively associated with calcineurin, which is up-regulated in oxidative muscles [53]. Microarray results generated by Campbell et al. (2001) [18] have indicated that calcineurin mRNA is under-expressed in oxidative muscles as compared to glycolytic muscles despite calcineurin over-expression in vivo. Therefore, measurements of calcineurin and calmodulin protein levels are necessary to confirm their fiber-specific function.

In contrast to ALD-PLD comparison, PLD and BF muscle groups were observed to be very similar on both regulatory and metabolic levels. Interestingly, major similarities between PLD and BF muscles were observed in genes coding for proteins involved in glycolytic metabolism. These results indicate that the “red” appearance of the BF muscle

does not necessarily correlate with its metabolic function. The microarray results correspond to data generated by Wiskus et al. (1976) [22] who demonstrated that fast-white and slow-red classification of muscle fibers is not accurate and that BF muscles appear red due to high myoglobin content, but have enzymatic characteristics of white fibers.

Although the microarray analysis confirmed that various muscles can be distinguished based on expression of genes coding for contractile and energy metabolism-associated proteins, the present data further indicates that there are many other potential markers of muscle phenotype. Some of the additional genes that were differentially expressed in ALD-PLD and ALD-BF comparisons code for extracellular matrix proteins, proteins involved in physical and oxidative stress, and cell membrane receptor proteins.

Extracellular Matrix

Some of the major differences between muscle groups were observed between genes coding for proteins associated with extracellular matrix. Formation of extracellular matrix is crucial for skeletal muscle differentiation during embryogenesis [54]. ALD muscles were characterized by over-expression of several proteins that belong to collagen family. It was observed that smaller number of genes coding for collagen proteins were over-expressed in ALD19-BF19 and ALD19-PLD19 than in ALD1-PLD1 and ALD1-BF1 comparisons. An over-expression of Col3a1 gene was observed in younger ALD muscles. Therefore, aside from muscle-type related differences in genes coding for collagen proteins, there is an age-related decrease in genes coding for collagen proteins in ALD muscles. An age-related decrease in collagen proteins in ALD muscles can be a result of a “dilution effect” of collagen during a period of rapid hypertrophy of the muscle [55]. It has been demonstrated

that age-related fold increase in muscle fiber diameter is much greater than increase in size of connective tissues associated with the muscle [56]. Consequently, an age-related increase in muscle to connective tissue growth may be related to morphological abnormalities and muscle damage [6, 57]. However, there were no age-related changes in genes coding for PLD and BF collagen proteins, which may occur as a result of a slower rate of collagen synthesis. It has been reported that in rodent species, the collagen content is higher in slow/oxidative muscle types than fast/glycolytic muscles [58, 59]. The ALD depends on oxidative metabolism for energy and is under more tonic tension than glycolytic muscle types [10]. Muscles subjected to chronic load have increased synthesis of enzymes regulating collagen turnover [45, 46]. These extracellular matrix modifications cause changes in elasticity of the tissue and decrease load-induced stress. In contrast, inactivity causes decrease in collagen protein turnover and synthesis [45, 46].

Connective tissue cross-linking is dependent on enzymatic reaction between collagen proteins and various glycoproteins [36]. The microarray analysis demonstrated that gene DAG1 that codes for dystroglycan glycoprotein was strongly over-expressed in one-week-old and 19-weeks-old ALD muscles in relation to both BF and PLD. High expression of dystroglycan in ALD muscles may also be related to higher requirements for synthesis of connective tissue components in muscles subjected to chronic load [11,12, 60].

Although mature muscle fibers comprise the majority of muscle tissue, satellite cells, fibroblasts, smooth muscle cells, endothelial cells, and neurons are closely associated with the muscle fibers and allow muscle tissue to fully serve its function. Therefore, large differences in gene expression levels coding for extracellular matrix proteins are likely

associated with muscle fiber- and age-related changes in connective tissue associated with the muscle.

Cell Death and Stress

One of the genes that were determined to be under-expressed in ALD muscles as compared to both PLD and BF muscles codes for a glycoprotein, clusterin. Aside from its function in cell to cell adhesion, clusterin is involved in clearance of cellular debris, cell lysis, and apoptosis [39, 40]. It was demonstrated that clusterin inhibits apoptosis in human cancer cells by interfering with activation of a pro-apoptotic Bax protein [61]. Recent studies performed by Anderson and Neufer (2005) [62] have demonstrated that the amount of free radical release from mitochondria is dependent on muscle fiber type. Many myopathies and age-related muscle atrophy have been associated with a loss of type IIB (fast-twitch, glycolytic) muscle fibers, which make up fatigue-prone muscles such as PLD and Pectoralis. Fast-glycolytic muscle fibers have been shown to have unique mechanisms that stimulate mitochondrial superoxide generation [62]. Consequently, it is likely that over-expression of clusterin in predominantly glycolytic BF and glycolytic PLD may indicate that there is a protective mechanism against free radical damage in fast-glycolytic fibers and this mechanism is compromised under stress or in aging PLD muscle.

Another gene that may be associated with oxidative muscle damage and was identified to be under-expressed in ALD muscles as compared to BF and PLD muscles, codes for BAT2 domain-containing protein 1. Studies identifying genes associated with caloric restriction and aging indicated that BAT2d gene is associated with age-at onset of

insulin-dependent (type II) diabetes mellitus in mammals [55]. Poultry species were characterized by relative insulin resistance and high blood glucose levels [63, 3], which makes them a good model for studying diabetes-associated genes. Individuals suffering from type II diabetes mellitus exhibit an array of defects in complex I and complex IV of electron transport chain in skeletal muscle. Furthermore, increased production of reactive oxygen species and decreased ATP synthase activity has been observed in skeletal muscle mitochondria of patients suffering from type II diabetes mellitus [64]. Insulin-resistance may be related to muscle fiber type, because there is an increased number of glycolytic (IIB) muscle fibers in type II diabetes mellitus patients [13]. Therefore, further evaluation of biological networks associated with BAT2d protein in skeletal muscle may present useful information regarding insulin metabolism.

Furthermore, the microarray analysis revealed that gene coding for ubiquitin is under-expressed in ALD as compared to BF and PLD. Ubiquitin is involved in proteosomal degradation and controls the stability and intracellular localization of a wide range of proteins [65]. It is likely that glycolytic fiber types are more prone to protein degradation than oxidative fiber types, hence the under-expression of the ubiquitin gene in ALD muscles.

The microarray analysis also revealed a strong relationship between muscles exposed to constant load and genes coding for heat shock proteins. Because heat shock or stress proteins protect muscle from exercise-induced stress, it is not surprising that the heat shock protein coding genes, HSPa and HSPb, are over-expressed in ALD muscles [66].

Additionally, it has been established that leptin down-regulates highly stress-inducible heat shock protein-70 (HSP-70) in chicken organs [67]. Leptin receptor (Leprot) is

an integral membrane protein widely distributed throughout the body [68]. Leptin is an adipocyte-derived hormone that plays an essential role in energy homeostasis, thermoregulation, inflammatory processes, and modulation of oxidative stress [69, 70, 71, 72, 73]. Oxidative muscles are associated with higher amount of intracellular fat then glycolytic muscles [42, 18]. Because leptin is derived from adipocytes, over-expression of leptin receptor gene in ALD muscles is likely related to previously reported high expression of adipocyte specific PPAR-α gene in oxidative muscles [18, 42]. It has also been demonstrated that skeletal muscle has an ability to transform from glycolytic/fast-twitch to oxidative/slow-twitch as a result of thermal stress [23]. Therefore, observed increased expression of adipocyte-specific genes in oxidative muscles and resulting increase in intramuscular fat, may serve as a protective mechanism against physical and environmental stresses.

Cell Membrane Receptors

Genes coding for major cell membrane receptors, EGFR and GPR20, were identified to be under-expressed in ALD muscles as compared to BF and PLD at 1-week and 19 weeks of age. Epidermal Growth Factor Receptor (EGFR) regulates down-stream molecular cascades involving proteins such as MAPK, Akt, and JNK. The EGFR signaling cascades lead to transcription of genes that regulate protein synthesis, cell proliferation, cell survival, and inhibition of apoptosis [41]. Genes coding for EGFR and Clusterin are involved in processes that inhibit apoptosis, and both of these genes are down-regulated in ALD muscles.

The G-protein Coupled Receptor (GPR) regulates cAMP and phosphotidylinositol signaling cascades that are responsible for glycogen, carbohydrate, and lipid metabolism [74]. Because, ALD muscle relies primarily on oxidative metabolism to satisfy its energy needs, it is expected that signaling pathways leading to glycogen and carbohydrate synthesis will be down-regulated in this muscle.

Validity of Microarray Analysis and qPCR

Based on previously documented studies [10, 21], it was expected that genes involved in glycolysis (Fig 4, Table 5) and muscle-twitch determination (Table 2) would be differentially expressed in oxidative ALD muscles as compared to glycolytic PLD muscles. Microarray-detected differences in expression levels of genes associated with glucose metabolism and muscle contraction confirm the reliability of focused microarray analysis. The microarray results were further confirmed by qPCR analysis. The genes selected for qPCR analysis participate in both newly established (Bat2d, Clu, Egfr) and previously characterized (Leprot) muscle-fiber-specific molecular networks. It has been demonstrated that adipogenic genes are over-expressed in oxidative muscles [18, 42], therefore over-expression of Leprot in ALD as compared to PLD further confirms the microarray results. Although there are limitations to qPCR as a validation tool [75, 76], the same direction of change and strong positive correlation (Table 10) were observed between qPCR and microarray-derived gene expression levels proving that TSKMLO microarrays utilized in this study are a reliable tool for analyzing muscle gene expression levels.

Conclusions

Collectively, it can be concluded that there is a complex gene-dependent regulation of muscle fiber phenotype. The microarray analysis revealed potential new markers delineating specific muscle characteristics. Although the versatile functions of fast-glycolytic and slow-oxidative muscles are reflected in differential expression of genes coding for glycolytic and contractile proteins, the studied in the current experiment muscles can also be distinguished based on expression of genes coding for transcription factors, structural proteins, proteins involved in apoptosis and proteosomal degradation, and signaling molecules. Interestingly, the data indicate strong similarities in the direction of expression and in expression levels of the large majority of genes involved in the aforementioned pathways in PLD and BF muscles as compared to ALD muscles, suggesting that color (phenotype) of the muscle does not necessarily correspond to its functional metabolic biochemistry.

The results of the current study significantly extend knowledge base regarding pathways characterizing skeletal muscle phenotype and illustrate that turkey skeletal muscle is a great model for studying muscle fiber plasticity *in vivo*. Present findings can have large implications in muscle-type related disorders and improvement of muscle quality in agricultural species.

Acknowledgements

The authors express their appreciation to Goldsboro Milling Company, Goldsboro, NC for the animals employed in this study. The authors also express thanks to Shelly Nolin for technical assistance.

Support provided in part by funds under multi-state project number NC1131.

Supported in part by National Research Initiative. This project was supported by National Research Initiative Competitive Grant no. 2005-35206-15241 (PEM) from the USDA Cooperative State Research, Education, and Extension Service. Support also provided in part by the North Carolina Agricultural Foundation (PEM).

References

1. Tikkanen HO., Harkonen M, Naveri H, Hamalainen E, Elovainio R, Sarna S, Frick MH: **Relationship of skeletal muscle fiber type to serum high density lipoprotein cholesterol and apolipoprotein A-I levels.** *Atherosclerosis* 1991, **90:**49-57.

2. Hickey MS, Weidner MD, Gavigan KE, Zheng D, Tyndall GL, Houmard JA: **The insulin action-fiber type relationship in humans is fiber type specific.** *Am J Physiol Endocrinol Metab* 1995, **269:**150-154.

3. Taouis M , Chen J-W, Daviaud C, Dupont J, Derouet M, Simon J: **Cloning the chicken leptin gene.** *Gene* 1998**, 208:**239-242.

4. Richards MP, Poch SM: **Molecular cloning and expression of the turkey leptin receptor gene.** *Comp Biochem Physiol B* 2003, **136:**833-847.

5. Hocquette JF, Ortigues-Marty I, Pethick D, Herpin P, Fernandez X: **Nutritional and hormonal regulation of energy metabolism in skeletal muscles of meat-producing animals.** *Livestock Prod Sci* 1998**, 56:**115-143.

6. Dransfield E, Sosnicki AA: **Relationship between muscle growth and poultry meat quality.** *Poult Sci* 1999**, 78:**743-746.

7. Schiaffino S, Reggiani C: **Molecular diversity of myofibrillar proteins: Gene regulation and functional significance.** *Physiol Rev* 1996, **76:**371-423.

8. Pette D, Staron RR: **Cellular and molecular diversities of mammalian skeletal fibers.** *Rev Physiol Biochem Pharmacol* 1990, **116:**2-76

9. Shear CR, Goldspik G: **Structural and physiological changes associated with the growth of avian fast and slow muscle**. *J Morph* 1971, **135:**351-372.

10. Gardahaut MF, Rouaud T, Renaud D, Ledouarin G: **Developmental changes in myosin isoforms from slow and fast latissimus dorsi muscles in the chicken.** *Differentiation* 1988**, 37:**81-85.

11. Kasper CE, McNulty AL, Otto AJ, Thomas DP: **Alterations in skeletal muscle related to impaired physical mobility: An empirical model.** *Res Nurs Health* 1993, **16:**265-273.

12. Mozdziak PE, Greaser ML, Schultz E: **Myogenin, MyoD, and myosin expression after pharmacologically and surgically induced hypertrophy.** *J Appl Physiol* 1998, **84:**1359-1364.

13. Nyholm B, Qu Z, Kaal A, Pedersen SB, Grayholt CH, Andersen JL, Saltin B, Schmitz O: **Evidence of an increased number of type IIb muscle fibers in insulin-resistant first-degree relatives of patients with NIDDM.** *Diabetes* 1997**, 46:**1822-1828.

14. Helge JW, Fraser AM, Kriketos AD, Jenkins AB, Calvert GD, Ayre KJ, Storlien LH: **Interrelationships between muscle fibre type, substrate oxidation and body fat.** *Int J Obes Relat Metab Disord* 1999, **23:**986-991.

15. Sosnicki AA, Cassens RG, Vimini RJ, Greaser ML: **Histopathological and ultrastructural alterations in turkey skeletal muscle.** *Poult Sci* 1991**, 70:**349-357.

16. Owens CM, Hirshler EM, McKee SR, Martinez-Dawson R, Sams AR: **The characterization and incidence of pale, soft, oxidative turkey meat in a commercial plant.** *Poult Sci* 2000, **79:**553-558.

17. Velleman SG, Anderson JW, Coy CS, Nestor KE: **Effect of selection for growth rate on muscle damage during turkey breast muscle development.** *Poult Sci* 2003, **82:**1069-1074.

18. Campbell WG, Gordon SE, Carlson CJ, Pattison JS, Hamilton MT, Booth FW: **Differential global gene expression in red and white skeletal muscle.** *Am J Physiol Cell Physiol* 2001**, 280:**763-768.

19. Bai Q, McGillivray C, da Costa N, Dornan S, Evans G, Stear M.J, Chang K-C: **Development of a porcine skeletal muscle cDNA microarray: analysis of differential transcript expression in phenotypically distinct muscles**. *BMC Genomics* 2003, **4:**8.

20. Kang PB, Kho AT, Sanoudou D, Haslett JH, Dow CP, Han M, Blasko JM., Lidov HGW, Beggs AH, Kunkel LM: **Variations in gene expression among different types of human skeletal muscle.** *Muscle Nerve* 2005**, 32:**483-491.

21. Cherel L, Hurtrel M, Gardahaut MF, Merly F, Magrasresch C, Font Aineperus J, Wyers M: **Comparison of postnatal development of anterior latissimus-dorsi (ALD) muscle in heavy-weight and light-weight strains of turkey (Meleagris-Gallopavo).** *Growth Dev Aging* 1994**, 58**157-165.

22. Wiskus KJ, Addis PB, Ma RT-I: **Distribution of βR, αR and αW fibers in turkey muscles**. *Poult Sci* 1976**, 55:**562-572.

23. Hirabayashi M, Ijiri D, Kamei Y, Tajima A, Kanai Y: **Transformation of skeletal muscle from fast- to slow-twitch during acquisition of cold tolerance in the chick.** *Endocrinol* 2005**, 146:**399-405.

24. Anthony NB, Emmerson DA, Nestor KE, Bacon WL: **Comparison of growth curves of weight selected populations of turkeys, quail, and chickens.** *Poult Sci* 1990, **70:**13-19.

25. Mozdziak PE, Schultz E, Cassens RG: **Satellite cell mitotic activity in post hatch turkey skeletal muscle growth.** *Poult Sci* 1994**, 73:**547-555.

26. Chomczynski P, Sacchi N: **Single-step method of RNA isolation by acid guanidinium thiocyanate-phenol chloroform extraction**. *Anal Biochem* 1987**, 162:**156-159.

27. Reed KM, Mendoza KM, Juneja B, Fahrenkrug SC, Velleman S, Chiang W, Strasburg GM: **Characterization of expressed sequence tags from turkey skeletal muscle.** *Animal Genet* 2008, **39:**635-644.

28. Murphy RM., Watt KKO, Cameron-Smith D, Gibbons CJ, Snow RJ: **Effects of creatine supplementation on housekeeping genes in human skeletal muscle using real-time RT-PCR.** *Physiol Genomics* 2002**, 12:**163-174.

28. Sporer KRB, Chiang W, Tempelman RJ, Ernst CW, Reed KM, Velleman SG, Strasburg GM: **Characterization of a 6K oligonucleotide turkey skeletal muscle microarray.** *Anim Gen* 2010**,** DOI: 10.1111/j.1365-2052.2010.02085.x

30. Kim N-K, Joh J-H, Park H-R, Kim O-H, Park B-Y, Lee C-S: **Differential expression profiling of the proteomes and their mRNAs in porcine white and red skeletal muscles.** *Proteomics* 2004**, 4:**3422-3428.

31. Pfaffl MW: **A new mathematical model for relative quantification in real-time PCR.** Nucleic *Acid Res* 2001**, 29:**2002-2007.

32. Wolfinger RD, Gibson G, Wolfinger ED, Bennett L, Hamadeh H, Bushel P, Afshari C, Paules RS: **Assessing gene significance from cDNA microarray expression data via mixed models.** *J Comput Biol* 2001**, 8:**625-637.

33. Hochberg Y: **A sharper Bonferroni procedure for multiple tests of significance.** *Biometrika* 1988, **75:**800-803.

34. Brandl CJ, Green NM, Korczak B, MacLennan DH: **Two Ca2+ ATPase genes: homologies and mechanistic implications of deduced amino acid sequences.** *Cell* 1986, **44:**597–607.

35. Chitaev NA, Troyanovsky SM: **Adhesive but not lateral E-cadherin complexes require calcium and catenins for their formation.** *J Cell Biol* 1998, **1142:**837-46.

36. Hulmes DJ: **The collagen-superfamily- diverse structures and assemblies.** *Essays Biochem* 1992, **27:**49-67.

37. Gui JF, Lane W., Fu XD: **A serine kinase regulates intracellular localization of splicing factors in the cell cycle.** *Nature* 1994**, 369:**678–82.

38. Swindell WR: **Genes and gene expression modules associated with caloric restriction and aging in the laboratory mouse.** *BMC Genomics* 2009, **10:**585.

39. Fritz IB, Burdzy K, Setchell B, Blaschuk O: **Ram rete testis fluid contains a protein (clusterin) which influences cell-cell interactions in vitro.** *Biol Repro* 1983**, 28:**1173-1188.

40. Harold D, Abraham R, Hollingworth P, Sims R, Gerrish A, Hamshere ML, Pahwa JS, Moskvina V, Dowzel K, Williams A, et al.: **Genome-wide association study identifies variants at CLU and PICALM associated with Alzheimer's disease**. *Nature Gen* 2009, **41:**1088-1093.

41. Oda K, Matsouka Y, Funahashi A, Ktano H: **A comprehensive pathway map of epidermal growth factor receptor signaling.** *Mol Syst Biol* 2005, **1:**10.

42. Horowitz JF, Leone TC, Feng W, Kelly DP, Klein S: **Effect of endurance training on lipid metabolism in women: a potential role for PPAR-α in the metabolic response to training.** *Am J Physiol Endocrinol Metab* 2000**, 279:**348-355.

43. Wang Y, Barbacioru C, Hyland F, Xiao W, Hunkapiller KL, Blake J, Chan F, Gonzalez C, Zhang ., Samaha LL: **Large scale real-time PCR validation on gene expression measurements from two commercial long-oligonucleotide microarrays.** *BMC Genomics* 2006, **21:**59.

44. de Wilde J, Hulshof MFM, Boekschoten MV, de Groot P, Smit E, Mariman ECM **The embryonic genes Dkk3, Hoxd8, HOxd9 and Tbx1 identify muscle types in a diet-independent and fiber-type unrelated way.** *BMC Genomics* 2010, **11:**176.

45. Vihko V, Salminen A, Rantamaki J: **Acid hydrolase activity in red and white skeletal muscle of mice during a 2-week period following exhausting exercise.** *Pflugers Archiv-Europ J Physiol* 1978, **378:**99-106.

46. Myllyla R, Salminen A, Peltonen L, Takala T, Vihko V: **Collagen metabolism of mouse skeletal muscle during the repair of exercise injuries.** *Pflugers Archiv-Europ J Physiol* 1986, **407:**64-70.

47. McCormick KM, Schultz E: **Role of satellite cells in altering myosin expression during avian skeletal muscle hypertrophy**. *Dev Dyn* 1994**, 199:**52-63.

48. Berchtold MW, Brinkmeier H, Müntener M: **Calcium ion in skeletal muscle: Its crucial role for muscle function, plasticity, and disease.** *Physiol Rev 2000,* **80:**1215-1265.

49. Vangheluwe P, Raeymaekers L, Dode L, Wuytack F: **Modulating sacro(endo)plasmic reticulum Ca^{2+} ATPase 2 (SERCA2) activity: Cell biological implications.** *Cell Calcium 2005*, **38**: 291-302.

50. Baksh S, Michalak M: **Expression of calreticulin in Escherichia coli and identification of its Ca^{2+} binding domains.** *J Biol Chem 1991,* **266:** 21458-21465.

51. Camacho P, Lechleiter JD: **Calreticulin inhibits repetitive intracellular Ca^{2+} waves:** *Cell 1995*, **82:**765-771.

52. John LM, Lechleiter JD, Camacho P: **Differential modulation of SERCA2 isoforms by calreticulin.** *J Cell Biol 1998,* **142:** 963-973.

53. Naya FJ, Mercer B, Shelton J, Richardson JA, Williams RS, Olson EN: **Stimulation of slow skeletal muscle fiber gene expression in vivo.** *J Biol Chem* 2000, **275:**4545-4548.

54. Osses N, Brandan N: **ECM is required for skeletal muscle differentiation independently of muscle regulatory factor expression.** *Am J Physiol Cell Physiol* 2002, **282:**383-394.

55. Kovanen V, Suominen H: **Age- and training- related changes in the collagen metabolism of skeletal muscle.** *Eur J Appl Physiol Occup Physiol* 1989, **56:**765-771.

56. Swatland HJ: **A note on the growth of connective tissues binding turkey muscle fibers together.** *Can Inst Food Sci Technol J* 1990, **23:**239-241.

57. Wilson BW: **Developmental and maturational aspects of inherited avian myopathies.** *Proc Soc Exp Biol Med* 1990, **194:**87-96.

58. Kovanen V, Suominen H, Heikkinen E: **Collagen of slow-twitch and fast-twitch muscle fibers in different types of rat skeletal muscles.** *Eur J Appl Physiol Occup Physiol* 1984, **52:**235-242.

59. Kovanen V: **Effects of aging and physical training on rat skeletal muscle. An experimental study on properties of collagen, laminin, and fiber types in muscles serving different functions**. *Acta Physiol Scand* 1989, **577:**1-56.

60. Ayalon G, Davis JQ, Scotland PB, Bennett V: **An ankyrin-based mechanism for functional organization of dystrophin and dystroglycan.** *Cell* 2008, **135:**1189-1200.

61. Zhang HL, Kim JK, Edwards CA., Xu ZH, Taichman R, Wang CY: **Clusterin inhibits apoptosis by interacting with activated Bax.** *Nature Cell Bio* 2005, **7:**909-915.

62. Anderson EJ, Neufer PD: **Mitochondrial superoxide production varies in different skeletal muscle fiber types.** *FASEB J* 2005, **19:**A566.

63. Simon J, Taouis M: **The insulin receptor in chicken tissues.** In *Avian Endocrinology*. Edited by Sharp J. Bristol UK J Endocrinology; 1993:177-188.

64. Anderson CM: **Mitochondrial dysfunction in diabetes mellitus**. *Drug Dev Res* 1999**, 46:**67-79.

65. Thrower JS, Hoffman L, Rechsteiner M, Pickart CM: **Recognition of the polyubiquitin proteolytic signal**. *EMBO J* 2000, **19:**94-102.

66. Hernando R, Manso R: **Muscle fibre stress in response to exercise. Synthesis, accumulation and isoform transitions of 70-kDa heat-shock proteins.** *Eur J Biochem* 1997, **243:**460-467.

67. Figuiredo D, Gertler A, Cabello G, Decuypere D, Buyse J, Dridi S: **Leptin downregulates heat shock protein-70 in chicken liver and hypothalamus.** *Cell Tissue Res* 2007, **329:**91-101.

68. Huang Y, Ying K, Xie Y, Zhou Z, Wang W, Tang R, Zhao W, Zhao S, Wu H, Gu S, Mao Y: **Cloning and characterization of a novel human leptin receptor overlapping transcript-lie I gene (LEPROTLI).** *Biochem Biophys Acta* 2001, **15:** 327-321.

69. Zhang Y, Proenca R, Maffei M, Barone M, Leopold L, Friedman JM: **Positional cloning of the mouse obese gene and its human homologue.** *Nature* 1994, **372:**425-432.

70. Bouloumie A, Marumo T, Lafontan M, Busse R: **Leptin induces oxidative stress in human endothelial cells.** *FASEB J* 1999, **13:**1231-1238.

71. Lappas M, Permezed M, Rice GE:. **Leptin and adiponectin stimulate the release of proinflamatory cytokines and prostaglandins from human placenta and maternal adipose tissue via nuclear receptor-gamma and extracellularly regulated kinase 1/2.** *Endocrinology* 2005, **146:**3334-3342.

72. Dridi S, Temim S, Derouet M, Tesseraud S, Taouis M: **Acute cold- and chronic heat-exposure upregulate hepatic leptin and muscle uncoupling protein (UCP) gene expression in broiler chickens.** *J Exp Zoo* 2008**, 3009:**381-388.

73. Eguchi M, Liu YT, Shin EJ, Sweeney G: **Leptin protects H9c2 rat cardiomyocytes from H202-induced apoptosis.** *FEBS J* 2008, **275:**3136-3144.

74. Gilman AG: **G proteins: Transducers of receptor-generated signals.** An Rev Biochem 1987**, 56:**615-649.

75. Morey JS, Ryan JC, Van Dolah FM: **Microarray validation: factors influencing correlation between oligonucleotide microarrays and real-time PCR**. *Biol Proced Online* 2006**, 8:**175-193.

76. Chuaqui RF, Bonner RF, Best CJM, Gillespie JW, Flaig MJ, Hewitt SM, Philips JL, Krizman DB, Tangrea MA, Ahram M, Linehan WM, Knezevic V, Emmert-Buck MR: **Post-analysis follow-up and validation of microarray experiments.** *Nature* 2002**, 32:** doi:10.1038/ng1034

Figures

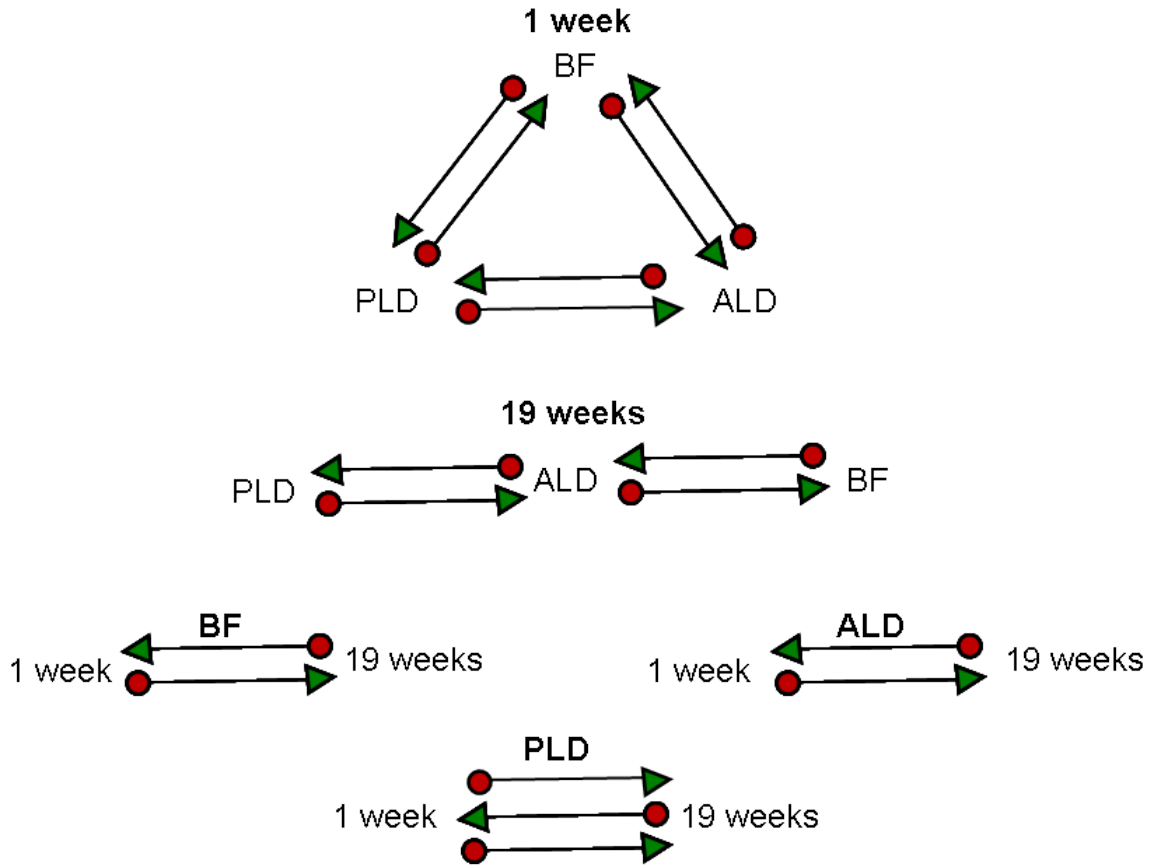

Fig 1. Microarray hybridization experimental setup for Cy3 and Cy5 dye labeling. A total of 17 arrays (represented by arrows) were hybridized with cDNA samples derived from PLD, ALD, and BF at either 1- or 19-weeks of age. Samples at the tail end (red circle) of the arrow were labeled with Cy3 and samples and the arrowhead (green) were labeled with Cy5.

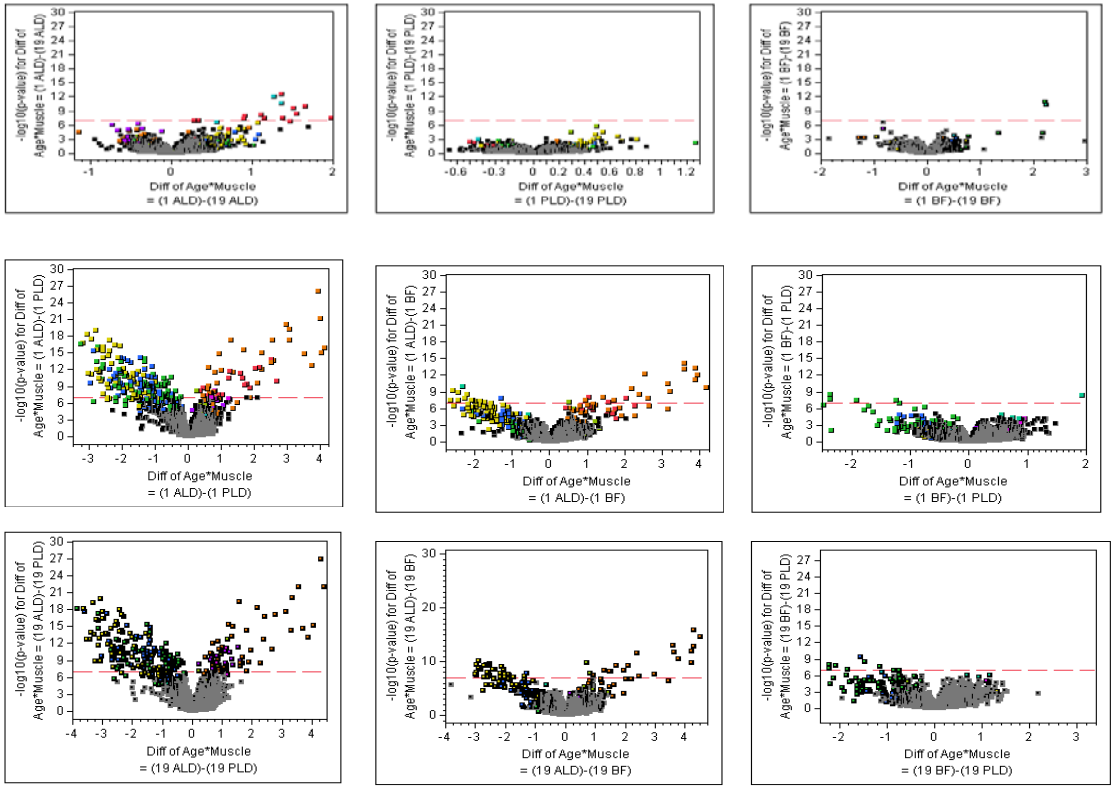

Fig 2. Volcano plots of P-value versus Log_2-transformed difference in gene expression level. Each dot represents one of 170 differentially expressed genes. The dashed line represents the significance threshold of P=0.05.

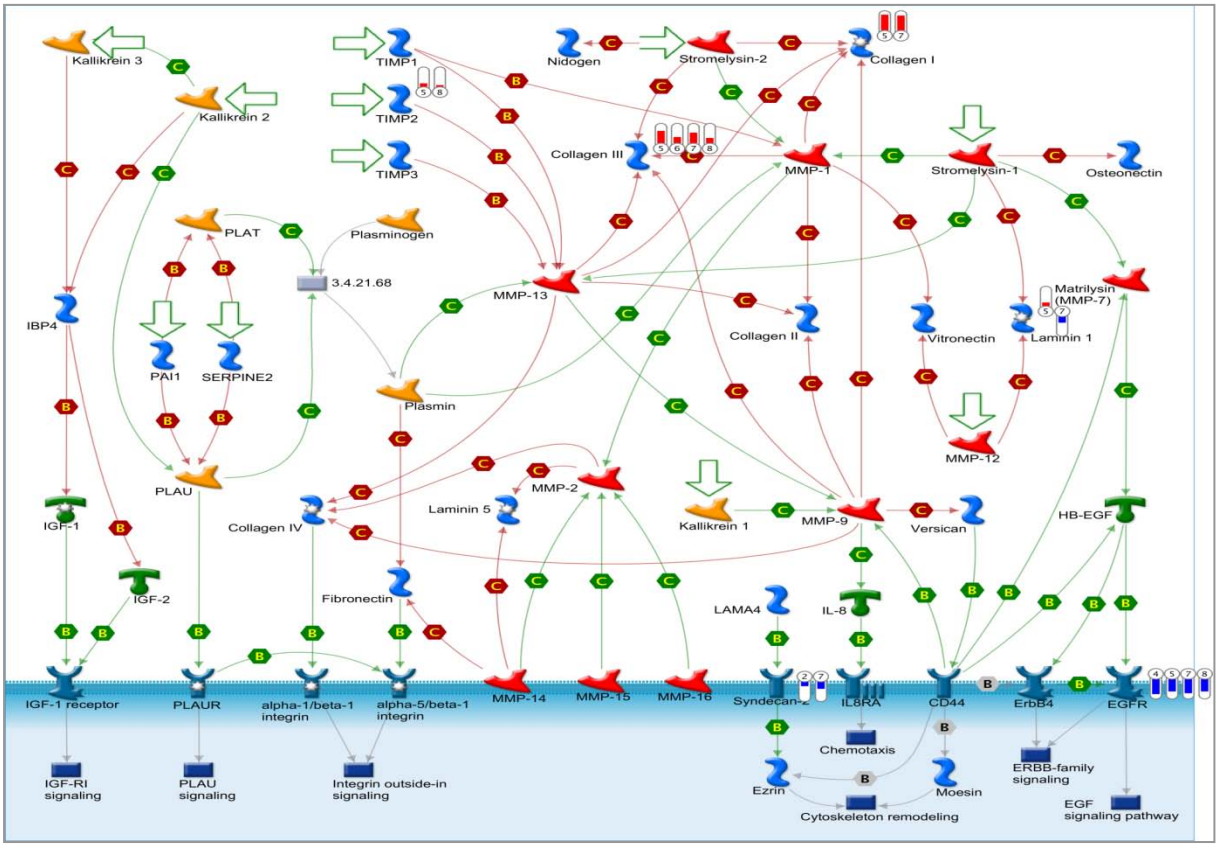

Fig 3. GeneGo-generated extracellular matrix components' pathway showing differentially expressed genes from multiple experimental comparisons (1. ALD19-BF19; 2. ALD19-PLD19; 4. ALD1-BF1; 5. ALD1-PLD1; 6. BF19-PLD19; 7. BF1-BF19; 8. BF1-PLD1). Blue indicates under-expressed genes and red indicates over-expressed genes in each comparison.

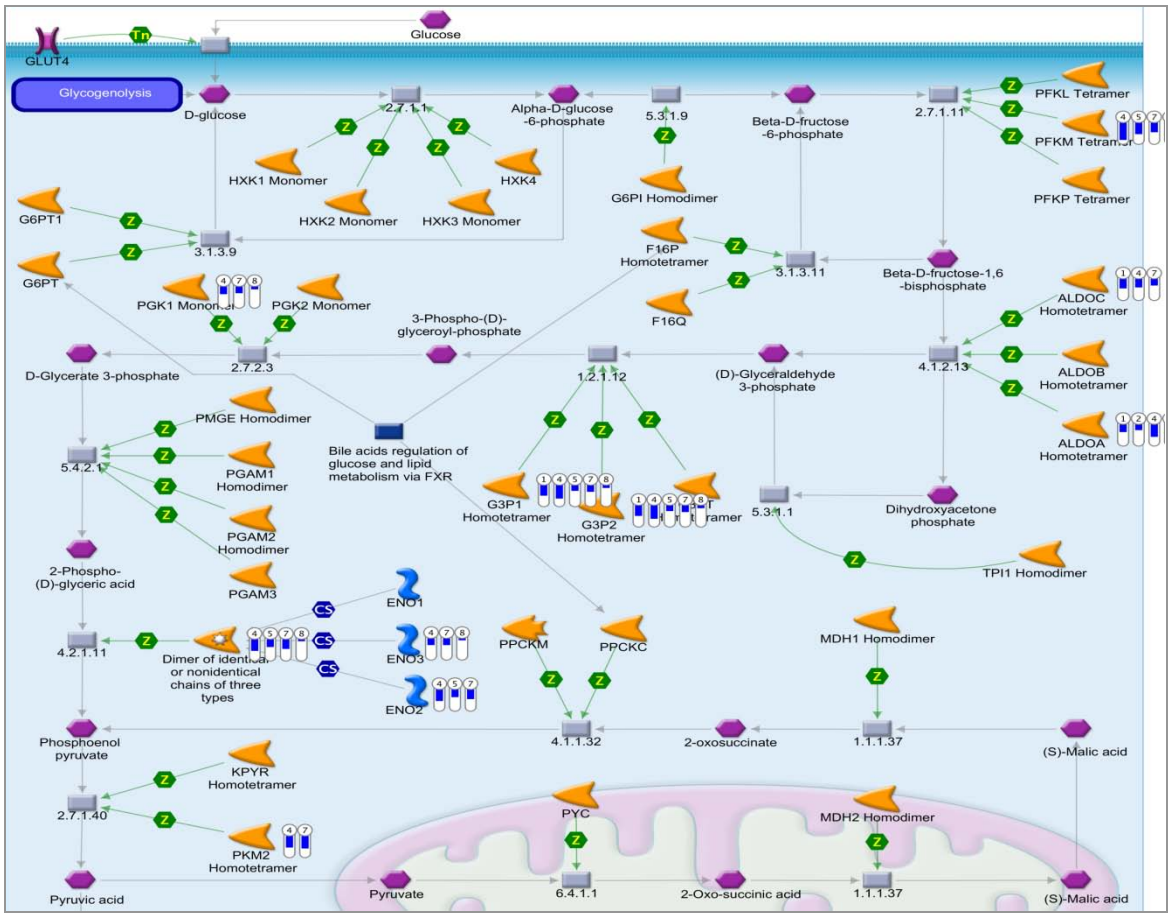

Fig 4. GeneGo-generated glucose homeostasis pathway showing differentially expressed genes from multiple experimental comparisons (1. ALD19-BF19; 2. ALD19-PLD19; 4. ALD1-BF1; 5. ALD1-PLD1; 6. BF19-PLD19; 7. BF1-BF19; 8. BF1-PLD1). Blue indicates under-expressed genes and red indicates over-expressed genes in each comparison.

Tables

Table 1. Differentially expressed genes represented by differences in fluorescence intensities between 1-week-old (ALD1) and 19-week-old (ALD19) turkey muscles. All genes listed are over-expressed in ALD1 as compared to ALD19. The threshold of significance was determined by Bonferroni correction at P=0.05.

Gene Symbol	Protein name	ALD1-ALD19
Col3a1	Collagen alpha-1(III) chain	1.88
Ctnna1	Catenin alpha-1	2.37
Sfrs3	Splicing factor, arginine/serine-rich 3	3.14
Atp2a1	Sarcoplasmic/endoplasmic reticulum calcium ATPase 1	2.27

Table 2. Differentially expressed genes coding for muscle contractile proteins. Gene expression levels are represented by differences in fluorescence intensities between 1-week-old (ALD1, PLD1, BF1) and 19-week-old (ALD19, PLD19, BF19) turkey muscles. Blue indicates under-expressed genes and red indicates over-expressed genes in each comparison. The threshold of significance was determined by Bonferroni correction at P=0.05.

Gene Symbol	Protein name	ALD1-ALD19	ALD19-PLD19	ALD19-BF19	BF19-PLD19	ALD1-BF1	ALD1-PLD1	BF1-PLD1	BF1-BF19
Cfl2	Cofilin-2			2.62		2.45			
Ctnna1	Catenin alpha-1	2.37	-2.49	-1.11					
Des	Desmin		2.54	1.6		1.68			
Dnm1l	Dynamin-1-like protein		-1.61	-1.55		-1.51	-1.59		
Fscn1	Fascin		-1.52	-1.31			-1.45		
Gm5915	Similar to myosin, light polypeptide 6, alkali, smooth muscle and non-muscle					1.58	1.36		
Igfn1	Immunoglobulin-like and fibronectin type III domain-containing protein 1		-2.52				-2.29		
Mprip	Myosin phosphatase Rho-interacting protein			1.48		1.55			
Mybpc1	RIKEN cDNA 8030451F13 gene		3.07	4.28		2.34	2.14		
Mybpc2	Myosin-binding protein C, fast-type		-2.49	-1.56		-2.31	-2.61		
Myh1	Myosin-1		-1.65	-1.9	4.38	-2.16	-1.55	5	4.19

Table 2 Continued

Myh15	Similar to Myosin heavy chain, cardiac muscle alpha isoform (MyHC-alpha)		3.12	3.01					
Myh2	Myosin, heavy polypeptide 2, skeletal muscle, adult		-7.49	-1.9	8.1	-4.62	-5.89		
Myh7	Myosin-7		14.66	7.69		17.45	14.82		
Myh7b	Myosin-7B		18.07			33.99	18.65		
Myh8	Myosin-8					-6.21	-1.99		
Myl1	Myosin light chain 1, skeletal muscle isoform		-4.78	-1.33		-2.41	-2.96		
Myl10	Myosin regulatory light chain 10		13.08			28.78	17.01		
Myl3	Myosin light chain 3		19.04	4.74		21.78	17.36		
Myl6	Myosin light polypeptide 6					1.58	1.36		
Mylpf	Myosin regulatory light chain 2, skeletal muscle isoform		-1.98			-1.98	-1.72		
Myom1	Myomesin-1			1.76		1.67			
Myom2	Myomesin 2		-1.79	-1.46		-1.59	-1.64		
Myoz1	Myozenin-1		-4.31			-3.06	-3.88		
Myoz2	Myozenin-2					1.56	1.43		

Table 2 Continued

Nap1l1	Nucleosome assembly protein 1-like 1		-5.34	-5.2		-4.97	-5.73		
Svil	Supervillin		1.9	1.69		1.66			
Tekt1	Tektin-1					-1.62		1.44	
Tmod1	Tropomodulin-1			1.44		1.63	1.77		
Tnnc1	Troponin C, slow skeletal and cardiac muscles		12.17	-1.88		20.1	11.21		
Tnnc2	Troponin C, skeletal muscle		-2.53	-1.63		-2.24	-2.62		
Tnni1	Troponin I, slow skeletal muscle		6.26	10.59		12.03	7.82		
Tnni3	Troponin I, cardiac muscle		12.17	-1.88		20.1	11.21		
Tnnt1	Troponin T, slow skeletal muscle		12.71			33.91	20.03		
Tnnt3	Troponin T, fast skeletal muscle		-3.91	-1.54	-2.96	-3.09	-1.86	-2.17	
Tpm1	Tropomyosin alpha-1 chain		-5.05			-3.69	-4.86		
Tpm3	Tropomyosin alpha-3 chain		-5.08	-3.35		2.75	-4.48		
Tuba4a	Tubulin alpha-4A chain		-2.59	-1.61			-2.29		
Tuba4a	Tubulin alpha-4A chain	-1.37	-0.6			-1.19			

Table 3. Differentially expressed genes coding for proteins involved in calcium signaling. Gene expression levels are represented by differences in fluorescence intensities between 1-week-old (ALD1, PLD1, BF1) and 19-week-old (ALD19, PLD19, BF19) turkey muscles. Blue indicates under-expressed genes and red indicates over-expressed genes in each comparison. The threshold of significance was determined by Bonferroni correction at P=0.05

Gene Symbol	Protein name	ALD1-ALD19	ALD19-PLD19	ALD19-BF19	BF19-PLD19	ALD1-BF1	ALD1-PLD1
Atp2a1	Sarcoplasmic/ endoplasmic reticulum calcium ATPase 1	2.27	-1.91	-2.26		-2.44	-2.84
Calm1	Calmodulin		-3.57	-3.04		-2.67	-3.45
Calr	Calreticulin			1.23	-1.47	1.34	
Cnn1	Calponin-1					2.61	2.31

Table 4. Differentially expressed genes coding for extracellular matrix components. Gene expression levels are represented by differences in fluorescence intensities between 1-week-old (ALD1, PLD1, BF1) and 19-week-old (ALD19, PLD19, BF19) turkey muscles. Blue indicates under-expressed genes and red indicates over-expressed genes in each comparison. The threshold of significance was determined by Bonferroni correction at P=0.05.

Gene Symbol	Protein name	ALD1-ALD19	ALD19-PLD19	ALD19-BF19	ALD1-BF1	ALD1-PLD1	BF1-PLD1
Clu	Clusterin		-4.66	-2.06	-2.32	-3.73	
Col1a1	Collagen alpha-1(I) chain				5.29	5.22	
Col1a2	Collagen alpha-2(I) chain				5.56	4.16	
Col3a1	Collagen alpha-1(III) chain	1.88		1.67	3.80	3.32	
Col5a1	Collagen alpha-1(V) chain				1.67	1.41	
Col6a1	Collagen alpha-1(VI) chain			1.50	2.40		
Col6a2	Collagen alpha-2(VI) chain			1.53	1.98		
Col6a3	procollagen, type VI, alpha 3				1.75		
Dag1	Dystroglycan		16.21	18.89	15.92	14.40	
Efemp1	EGF-containing fibulin-like extracellular matrix protein 1		1.82	1.83			
Fap	Seprase		1.72	1.95	2.18	-1.84	1.80
Fras1	Extracellular matrix protein FRAS1				2.16	2.20	
Gsn	Gelsolin		2.16	2.57	1.96		
Jph1	Junctophilin-1		-1.59	-1.51		-1.62	
Krt42	Keratin, type I cytoskeletal 42		-1.80		-1.82	-1.83	
Ldb2	LIM domain-binding protein 2		1.94	1.74	2.14	1.66	
Mfap4	Microfibril-associated glycoprotein 4		-1.83			-1.74	
Mgp	Matrix Gla protein			1.60		2.15	
Sdc2	Syndecan-2					-2.06	-1.61
Sdc3	Syndecan-3			-1.29		-2.32	
Tuba1b	Tubulin alpha-1B chain				1.69		

Table 5. Differentially expressed genes coding for proteins involved in glucose metabolism. Gene expression levels are represented by differences in fluorescence intensities between 1-week-old (ALD1, PLD1, BF1) and 19-week-old (ALD19, PLD19, BF19) turkey muscles. Blue indicates under-expressed genes and red indicates over-expressed genes in each comparison. The threshold of significance was determined by Bonferroni correction at P=0.05.

Gene Symbol	Protein name	ALD19-PLD19	ALD19-BF19	BF19-PLD19	ALD1-BF1	ALD1-PLD1	BF1-PLD1
Ak1	Adenylate kinase isoenzyme 1	-3.69			-2.32	-2.94	
Aldoa	Fructose-bisphosphate aldolase A	-3.55	-1.66	-2.24	-1.86	-3.18	-1.83
Aldoc	Fructose-bisphosphate aldolase C	-2.26		-2.53		-1.89	
Car3	Carbonic anhydrase 3	7.89			7.87	4.25	
Ckb	Creatine kinase B-type	-2.28			-3.71	-2.57	
Ckm	Creatine kinase M-type		-1.78			-2.28	
Eno2	Gamma-enolase	-3.14			-2.08	-2.74	
Eno3	Beta-enolase	-1.94	-1.15			-1.88	
Gapdh	Glyceraldehyde-3-phosphate dehydrogenase	-4.11	-1.33	-3.02	-1.80	-2.02	
Ldha	L-lactate dehydrogenase A chain	-4.17	-1.57			-4.38	
Pfkm	6-phosphofructokinase, muscle type	-5.62	-1.38		-3.33	-2.64	
Pgk1	Phosphoglycerate kinase 1	-2.06	-1.23			-2.03	
Pgm1	Phosphoglucomutase-2	-2.79	-1.59		-1.79	-2.46	-1.72
Pkm2	Pyruvate kinase isozymes M1/M2	-3.37				-3.39	
Pygm	Glycogen phosphorylase, muscle form	-4.11	-1.62		-1.72	-2.43	
Sds	L-serine dehydratase					-2.08	-1.69
Slc37a3	Sugar phosphate exchanger 3	-2.69				-2.56	

Table 6. Differentially expressed genes coding for transcription and translation regulatory proteins. Gene expression levels are represented by differences in fluorescence intensities between 1-week-old (ALD1, PLD1, BF1) and 19-week-old (ALD19, PLD19, BF19) turkey muscles. Blue indicates under-expressed genes and red indicates over-expressed genes in each comparison. The threshold of significance was determined by Bonferroni correction at P=0.05.

Gene Symbol	Protein name	ALD1-ALD19	ALD19-PLD19	ALD19-BF19	ALD1-BF1	ALD1-PLD1
Bzw2	Basic leucine zipper and W2 domain-containing protein 2		-1.99			-1.82
C78339	RNA binding motif protein 24		1.95	2.23		
Chordc1	Cysteine and histidine-rich domain-containing protein 1				-2.62	-2.24
Csrp3	Cysteine and glycine-rich protein 3		4.67	4.99	4.17	3.66
Ddx46	Probable ATP-dependent RNA helicase DDX46		-2.00	-2.24	-1.92	-1.94
Eef1a1	Elongation factor 1-alpha 1			1.65	1.88	1.86
Eif4b	Eukaryotic translation initiation factor 4B		-1.25	-1.08		
Fhl1	Four and a half LIM domains protein 1			1.25	2.62	
Gm16468	similar to ribosomal protein L3 isoform b			1.58		1.52
Klf2	Krueppel-like factor 2		1.72	1.07		
Med7	Mediator of RNA polymerase II transcription subunit 7		-2.55	-2.56	-2.28	-2.78
Phf10	PHD finger protein 10		1.77	1.66	1.82	2.04
Phf17	Protein Jade-1		1.95		1.56	1.46
Prkdc	DNA-dependent protein kinase catalytic subunit			-1.28		-1.29
Rbm24	similar to RNA binding motif protein 24		1.95	2.23		
Rfc4	Replication factor C subunit 4		-2.19	-1.83	-1.92	-2.17
Rpl3	60S ribosomal protein L3			1.58		1.52
Rpl4	60S ribosomal protein L4			1.37	1.62	
Rps23	40S ribosomal protein S23				1.70	
Rps27	40S ribosomal protein S27					
Rps3	40S ribosomal protein S3		-3.24			-2.49
Sfrs3	Splicing factor, arginine/serine-rich 3	3.14			4.40	4.21

Table 7. Differentially expressed genes coding for proteins involved in proteosomal degradation Gene expression levels are represented by differences in fluorescence intensities between 1-week-old (ALD1, PLD1, BF1) and 19-week-old (ALD19, PLD19, BF19) turkey muscles. Blue indicates under-expressed genes and red indicates over-expressed genes in each comparison. The threshold of significance was determined by Bonferroni correction at P=0.05

Gene Symbol	Protein name	ALD19-PLD19	ALD19-BF19	ALD1-BF1	ALD1-PLD1
Rnf128	E3 ubiquitin-protein ligase RNF128		-1.71		-1.98
Ubb	Ubiquitin	-2.86	-2.49	2.83	
Usp14	Ubiquitin carboxyl-terminal hydrolase 14		-1.31		-1.59
Usp8	Ubiquitin carboxyl-terminal hydrolase 8	-1.91	-1.85		-2.49

Table 8. Differentially expressed genes coding for Heat shock proteins. Gene expression levels are represented by differences in fluorescence intensities between 1-week-old (ALD1, PLD1, BF1) and 19-week-old (ALD19, PLD19, BF19) turkey muscles. Blue indicates under-expressed genes and red indicates over-expressed genes in each comparison. The threshold of significance was determined by Bonferroni correction at P=0.05.

Gene Symbol	Protein name	ALD19-PLD19	ALD19-BF19	ALD1-BF1	ALD1-PLD1
Cdc37l1	Hsp90 co-chaperone Cdc37-like 1	-1.76			-1.53
Hsp90aa1	Heat shock protein HSP 90-alpha		1.27	1.47	1.51
Hspb1	Heat shock protein beta-1	5.12	2.89	6.39	3.84

Table 9. Differentially expressed genes coding proteins involved in G-protein coupled receptor signaling pathway. Gene expression levels are represented by differences in fluorescence intensities between 1-week-old (ALD1, PLD1, BF1) and 19-week-old (ALD19, PLD19, BF19) turkey muscles. Blue indicates under-expressed genes and red indicates over-expressed genes in each comparison. The threshold of significance was determined by Bonferroni correction at P=0.05.

Gene Symbol	Protein name	ALD19-PLD19	ALD1-BF1	ALD1-PLD1
Impad1	Inositol monophosphatase 3	-2.80	-1.89	-2.42
Gpr20	Probable G-protein coupled receptor 20	-11.24	-4.34	-6.50

Table 10. Comparison of gene expression profiles analyzed using focused microarrays and qPCR. The n-fold change was calculated by comparing the intensities of the arrays or using ΔΔCt method of Pfaffl (2001) [31]. The "-"sign preceding the fold change value indicates that the experimental gene is under-expressed as compared to the control gene. The direction of expression was calculated by subtracting (muscle 2 gene/muscle 2 β-actin)-(muscle 1 gene/muscle 1 β-actin). NS indicates that values were not significantly different (P>0.05). The last row indicates the correlation between microarray and qPCR results in each comparison.

	ALD1-BF1		**ALD1-PLD1**		**ALD19-BF19**		**ALD19-PLD19**	
Gene	Microarray	qPCR	Microarray	qPCR	Microarray	qPCR	Microarray	qPCR
Bat2d	-1.98	-6.39	-1.82	-1.22	-2.11	-3.86	-1.67	-5.77
Clu	-3.73	-6.20	-2.32	-2.43	-4.66	-3.24	-2.06	-14.13
Egfr	-4.76	-3.72	-4.03	-3.76	-5.30	-4.68	-3.91	-16.35
Leprot	2.22	3.25	2.09	3.32	2.06	4.23	NS	13.42
Correlation Coefficient	0.81		0.99		0.92		0.77	

CHAPTER 6

Summary

Research presented in this dissertation provides insight onto molecular mechanisms that govern skeletal muscle growth and function. Manipulation of skeletal muscle fiber phenotype and energy utilization through nutritional and physical perturbations can improve muscle growth, health, and meat quality. Data presented in Chapter 2 revealed significant increase in apoptosis and presence of inflammatory cells (macrophages) in Pectoralis major (PM) muscles of feed deprived birds and birds fed below NRC requirement (0.88NRC) diet provided early post-hatch. PM muscle fibers rely predominately on glycolysis as their main energy source and have been proven to be more prone to sarcopenia than any other muscle fiber types. Muscle fiber type is directly associated with incidence of mitochondrial respiratory dysfunction, diabetes, and a number of myopathies (Anderson, 1999; Whittaker et al., 2007). Mitochondrial free radical generation is the highest in glycolytic (IIB) muscle fibers and the age-related muscular abnormalities take place primarily in these fiber types (Sosnicki at al., 1991; Dransfield and Sosnicki, 1999). Direct targeting of skeletal muscle mitochondrial free radical sources with CoQ_{10} may prevent or decrease the damage caused due to physical stress and potential malnutrition. Studies described in Chapter 3 reveal that functionally diverse muscles are characterized by significantly different mitochondrial and whole muscle CoQ_{10} content. Therefore, it can be concluded that skeletal muscle energy utilization and metabolism may be altered through regulation of factors participating in

electron transport chain. Data presented in Chapter 4 demonstrates that CoQ_{10} analog ($MitoQ_{10}$) administration increases oxidative potential and adipogenesis in myotubes derived from glycolytic PM muscles. Therefore, it seems that energy metabolism can be altered by controlling the intermediate steps of oxidative phosphorylation process. It is expected, that improvement in oxygen utilization will result in decreased production of free radicals and decreased apoptosis in *in vivo* systems.

Final study utilized microarray analysis to determine differentially expressed genes in phenotypically and functionally diverse muscles. Data generated from microarray analysis revealed several candidate genes that would provide basis for in depth analysis of factors regulating muscle phenotype and function.

Profound evaluation and nutritional manipulation of molecular mechanisms that govern muscle fiber metabolism, phenotype, and molecular energy sources is essential to improve muscle quality and quantity, and hence is of fundamental medical and agricultural importance. The results of the present research provide essential tools that could aid in understanding the pathways responsible for phenotypic changes in the muscle and associated with them muscle quantity and health.

References

Anderson, C.M., 1999. Mitochondrial dysfunction in diabetes mellitus. Drug Dev. Res. 46, 67-79.

Dransfield, E., Sosnicki, A.A., 1999. Relationship between muscle growth and poultry meat quality. Poult. Sci. 78, 743-746.

Sosnicki, A.A., Cassens, R.G., Vimini, R.J., Greaser, M.L., 1991. Histopathological and ultrastructural alterations in turkey skeletal muscle. Poult. Sci. 70, 349-357.

Whittaker, R.G., Schaefer, A.M., McFarland, R., Taylor, R.W., Walker, M., Turnbull, D.M., 2007. Prevalence and progression of diabetes in mitochondrial disease. Diabetologia 50, 2085-2089.